Evaluation of Xanthine Oxidase Inhibitory and Antioxidant Activities of Compounds from Natural Sources

Lam Rosanna Yen Yen

A Thesis Submitted in Partial Fulfillment
of the Requirements for the Degree of
Master of Philosophy
in
Chinese Medicine

September 2004

Abstract

Hyperuricemia could be caused by the overproduction or the underexcretion of urate. Urate is a product of an enzyme, xanthine oxidase (XOD). XOD participates in the purine degradation pathway, converting xanthine or hypoxanthine to urate, and urate is then excreted through the kidney. Medical treatments now available to treat hyperuricemia include the use of urate oxidase, uricosuric agents and XOD inhibitors. These methods of treatments may sometimes produce adverse side effects. Therefore, development of new and safer methods for the treatment of hyperuricemia is needed. Chinese medicinal materials (CMM) constitute a rich source of potential drugs, as they have demonstrated clinical efficacy and less side effects. The objective of this project is to search for XOD inhibitory compounds from the CMM: aloe, ginger and rhubarb. The chemical components of these herbs studied in the present investigation include 6-gingerol, aloe-emodin, barbaloin, chrysophanol, deoxyrhapontin, rhapontin and rhein. Deoxyrhapontin was found to possess reversible XOD inhibitory effect, with a mixed type mode of inhibition. The other compounds were found to be without positive effects. Moreover, compounds with XOD inhibitory effects could reduce the blood level of urate and alleviate hyperuricemia. If the compounds also possess antioxidant abilities, they might be able to alleviate atherosclerosis by lowering the susceptibility of blood components towards oxidative stress. A number of antioxidative assays on red blood cell (RBC) and RBC membrane were thus performed. They include AAPH-induced hemolysis inhibition assay, RBC membrane lipid peroxidation inhibition assay, RBC membrane Ca^{2+}-ATPase and Na^{+}/K^{+}-ATPase protection assays, and RBC membrane sulfhydryl group protection assay. Among the test compounds, 6-gingerol was demonstrated to possess positive effect in the AAPH-

induced hemolysis inhibition assay and RBC membrane lipid peroxidation inhibition assay. Rhapontin was demonstrated to possess positive effect in the AAPH-induced hemolysis inhibition assay, RBC membrane lipid peroxidation inhibition assay and RBC membrane Na^+/K^+-ATPase protection assay. Barbaloin was demonstrated to exhibit efficient protection in all of the assays except Na^+/K^+-ATPase assay. Apart from RBC, low-density lipoprotein (LDL) is another target of oxidants. Engulfment of oxidized LDL by macrophages would lead to accumulation of plaques in arteries, resulting in atherosclerosis. Lipid peroxidation inhibition assays of LDL were performed to evaluate the antioxidative abilities of the compounds towards LDL. 6-Gingerol, barbaloin and rhapontin were demonstrated to exhibit positive effects in these assays. The significance of these biologically active compounds from CMM is discussed in this thesis.

論文摘要

高尿酸血症是由於尿酸製造過多或尿酸排泄過少所引起的。尿酸是由黃嘌呤氧化酶所製造。黃嘌呤氧化酶參與嘌呤解體過程，它負責把黃嘌呤轉化爲尿酸，尿酸繼而通過腎臟排出體外。現時，用以治療高尿酸血症的方法包括使用重組尿酸氧化酶、促進尿酸排泄劑及黃嘌呤氧化酶抑制劑。由於以上方法偶而會引起副作用，所以有關專家正在積極發展治療高尿酸血症較安全的新方法。中藥中蘊含大量有效藥品，不但在臨床應用中表現成效，也顯示出引起副作用的機會較少。是次研究的宗旨就是要在中藥中找出對黃嘌呤氧化酶有抑制作用的有效成份，涉及的中草藥包括蘆薈、生薑及大黃，這些中草藥的提取物中含有的有效成份在是次研究進行測試，它們包括 6-薑辣醇，蘆薈大黃素，蘆薈大黃素甙，大黃酚，去氧食用大黃甙，食用大黃甙及大黃酸。研究結果顯示去氧食用大黃甙對黃嘌呤氧化酶有抑制作用，抑制方式呈混合式。其餘接受測試的有效成份都呈陰性反應。黃嘌呤氧化酶抑制劑能降低血液中尿酸含量，這樣便可緩解高尿酸血症。如果受測試的有效成份同時擁有降尿酸及抗氧化能力，那些有效成份便可減低血液內的細胞受氧化攻擊的機會，緩解動脈粥樣硬化症。對紅血細胞及紅血細胞膜的抗氧化測試包括抗溶血測試，抑制酯質過氧化測試，鈣 ATP 酶及鈉鉀 ATP 酶保護測試，及巯基保護測試。在接受測試的有效成份當中，6-薑辣醇在抗溶血及抑制酯質過氧化測試中均呈陽性反應。食用大黃甙在抗溶血測試、鈉鉀 ATP 酶保護測試及抑制酯質過氧化測試中呈陽性反應。蘆薈大黃素甙在所有測試中都呈陽性反應，只有鈉鉀 ATP 酶保護測試除外。除了紅血細胞，低密度酯蛋白是另一會受氧化攻擊的目標，氧化了的低密度酯蛋白會

被巨噬細胞吞食，它們的生成物會在血管壁聚集而導致動脈粥樣硬化症。抑制低密度酯蛋白的酯質過氧化測試是要試驗有效成份對低密度酯蛋白的抗氧化功能。6-薑辣醇, 蘆薈大黃素甙及食用大黃甙在該測試中都呈陽性反應。中藥有效成份的重要性將會在這論文中討論。

Acknowledgement

I would like to express my sincere gratitude towards my supervisors, Prof. C.H.K. Cheng from the Department of Biochemistry and Prof. C.T. Che from the School of Chinese Medicine, for their professional guidance throughout my study and their valuable advice in my thesis. I would also like to thank them for providing me the chance to work in their lab.

Special thanks to Dr. Anthony Y.H. Woo for his helps and instructions. Moreover, I am grateful to my colleagues for their assistance and encouragement, as my work would not be able to run smoothly without their concern.

Furthermore, I would like to express my appreciation to the technicians of Department of Biochemistry and Multiple Discipline Laboratory in Basic Medical Sciences Building for their help and friendliness. Thanks are also extended to the technicians of Laboratory Animal Service Center for their assistance in providing animal-related materials.

Finally, I would like to express my deepest thanks to my parents, my brothers and sister for their love and encouragement. I would not be able to endure the hard times in my study without their support.

Table of Contents

List of Abbreviations

$^{\bullet}OH$	hydroxyl radical
$^{1}O_2$	singlet oxygen
5'-ND	5'-nucleotidase
AAPH	2,2'-azobis (2-amidinopropane) dihydrochloride
ADA	adenosine deaminase
AK	adenosine kinase
AMP	adenosine monophosphate
AMP-S	adenoyl-succinate
APRT	adenine phosphoribosyltransferase
Ar	aromatic
ATase	amidophosphoribosyl-transferase
ATP	adenosine triphosphate
CMM	Chinese medicinal materials
DMSO	dimethylsulphoxide
DNA	deoxyribonucleic acid
DTNB	5,5'-dithiobis(2-nitrobenzoic acid)
DW	distilled water
EDTA	ethylene diamine tetraacetic acid
EGTA	ethylene glycol-bis(beta-aminoethyl-ether)-N,N,N',N'-tetraacetic acid
ETC	electron transport chain
FAD	flavin adenine dinucleotide
G6PD	glucose-6-phosphate dehydrogenase
GMP	guanosine monophosphate

GSH	reduced glutathione
GSH-Px	glutathione peroxidase
GSSG	oxidized glutathione
GSSG-Rd	glutathione reductase
HGPRT	hypoxanthine-guanine phosphoribosyl transferase
HO	heme oxygenase
IC_{50}	50% inhibitory concentration
IMP	inosine monophosphate
$L^{\bullet}$	lipid radical
LDL	low-density lipoprotein
LH	polyunsaturated lipid
$LOO^{\bullet}$	lipid peroxyl radical
LOOH	lipid peroxide
MDA	malondialdehyde
MG	malachite green
NAD^{+}	oxidized nicotinamide adenine dinucleotide
NADH	reduced nicotinamide adenine dinucleotide
$NADP^{+}$	oxidized nicotinamide adenine dinucleotide phosphate
NADPH	reduced nicotinamide adenine dinucleotide phosphate
NBT	nitroblue tetrazolium
$O_2^{\bullet -}$	superoxide anion radical
O_2^{2-}	peroxide ion
PBS	phosphate buffered saline
PHG	phenolic hydroxyl groups
PMS	phenazine methosulfate

PNP	purine nucleoside phosphorylase
PRPP	phosphoribosyl pyrophosphate
PVA	polyvinyl alcohol
$R^{\bullet}$	carbon-centered radicals
R-5-P	ribose-5-phosphate
RBC	red blood cell
$ROO^{\bullet}$	peroxyl radical
ROS	reactive oxygen species
SDS	sodium dodecyl sulfate
SH	sulfhydryl group
SOD	superoxide dismutase
TBA	thiobarbituric acid
TBARS	TBA reactive substance
*t*BHP	*tert*-butylhydroperoxide
TCA	trichloroacetic acid
TCM	Traditional Chinese Medicine
v/v	volume/volume
Vit $E^{\bullet}$	tocopheryl radical
Vit E_{ox}	tocopheryl quinone
w/v	weight/volume
WBC	white blood cell
XDH	xanthine dehydrogenase
XMP	xanthosine monophosphate
XOD	xanthine oxidase

List of Figures

List of Tables

Chapter 1 Introduction

1.1 Reactive oxygen species

Stable chemical molecules consist of paired electrons. However, there are other molecules that hold one or more unpaired electrons. They are the free radicals which are chemically very reactive. They may possess electropositive, neutral or electronegative charge, depending on the reaction conditions (Olinescu and Smith, 2002). Free radicals are produced during metabolic reactions, and many of them are important reaction intermediates. Oxygen is essential to life due to its key role in energy metabolism, but it is also harmful to biological molecules owing to its tendency to generate reactive oxygen species (ROS). In human, ROS can be produced intracellularly and extracellularly.

1.1.1 Intracellular sources of ROS

ROS including superoxide radicals, hydrogen peroxide and hydroxyl radicals are by-products of respiration in aerobes. Intracellular ROS are mainly produced in mitochondria. The amount of ROS produced differs among tissues due to the differences in metabolic processes taking place (Olinescu and Smith, 2002). For the complete reduction of molecular oxygen into water, four electrons are being added to the ROS intermediates one at a time (Olinescu and Smith, 2002). Although the mitochondrial electron transport chain (ETC) is highly efficient in reducing molecular

oxygen, 2-3% of the electrons leak out daily causing the release of ROS from the mitochondria (Rice-Evans *et al.*, 1995).

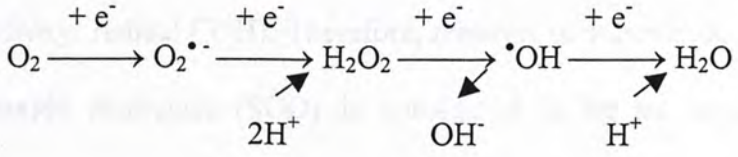

In the membrane-bound peroxisomes, hydrogen peroxide is produced for fatty acid oxidation in mitochondria (Olinescu and Smith, 2002). Sometimes, hydrogen peroxide may leak out from mitochondria or peroxisomes as it is lipid soluble (Marks *et al.*, 1996).

1.1.2 Extracellular sources of ROS

Extracellular ROS are produced by macrophages, neutrophils and eosinophils as a response to bacterial invasion (Marks *et al.*, 1996). The ROS produced by these cells include superoxide anion radicals, hydrogen peroxide, hydroxyl radicals and hypochlorous acid. These ROS constitute a major part in the bodies' defence against invading bacteria by their abilities to kill the engulfed bacteria through oxidizing their membranes and other cellular components (Marks *et al.*, 1996).

1.1.3 Superoxide anion radicals

Superoxide anion radicals ($O_2^{\bullet -}$) are believed to be the first ROS produced in the ETC as molecular oxygen accepts an electron.

$$O_2 + e^- \longrightarrow O_2^{\bullet -}$$

They are also produced in some enzyme-catalyzed reactions, e.g. xanthine oxidase (XOD). Superoxide anion radical is an anion and is a mild reducing agent (Rice-

Evans *et al.*, 1995). It is not particularly reactive compared to other ROS, but it is the precursor of other ROS such as hydroperoxyl radical ($HOO^{\bullet}$), hydrogen peroxide (H_2O_2) and hydroxyl radical ($^{\bullet}OH$). Therefore, removal of superoxide radicals by the enzyme superoxide dismutase (SOD) is considered to be an important primary antioxidant defence against ROS damage by virtually all aerobes from bacteria to multicellular organisms (Marks *et al.*, 1996).

1.1.4 Hydrogen peroxide

Peroxide ion (O_2^{2-}) is produced during the second step of the reduction of molecular oxygen in the ETC when a second electron is added to superoxide radicals (Olinescu and Smith, 2002).

$$O_2^{\bullet -} + e^- \longrightarrow O_2^{2-}$$

Under physiological conditions, the ion normally forms a stable compound, H_2O_2, which is a non-free radical form of oxygen since all of its electrons are paired (Olinescu and Smith, 2002).

$$O_2^{2-} + 2H^+ \longrightarrow H_2O_2$$

H_2O_2 is lipid soluble, so it is able to diffuse through cell membrane (Marks *et al.*, 1996). It is also produced by the SOD-catalyzed dismutation of superoxide radicals. The equation is mentioned in section 1.2.2.

1.1.5 Hydroxyl radicals

Hydroxyl radicals ($^{\bullet}OH$) are the most powerful ROS. They can be produced from superoxide radicals by the Haber-Weiss reaction (Olinescu and Smith, 2002):

$$O_2^{\bullet -} + H_2O_2 \longrightarrow O_2 + OH^- + {}^{\bullet}OH$$

They can also be produced by disintegration of hydrogen peroxide through the Fenton reaction (Olinescu and Smith, 2002):

$$Fe^{2+} + H_2O_2 \longrightarrow Fe^{3+} + OH^- + {}^{\bullet}OH$$

They form peroxides on reacting with organic substances such as proteins and lipids.

1.1.6 Singlet oxygen

Singlet oxygen ($^1O_2$) is another powerful ROS which is a non-free radical (Olinescu and Smith, 2002). It is believed to be produced by photosensitization reactions in the eyes and may also be produced by neutrophils. It is able to react with organic substances such as polyunsaturated fatty acids to form peroxides (Olinescu and Smith, 2002).

1.1.7 Peroxyl radicals and peroxides

Peroxyl radicals and peroxides are formed during a series of chain reactions in compounds with unsaturated carbon backbones. The process of formation includes initiation, propagation and termination. Initiation of free radical production can be achieved by homolysis, metabolism, enzymatic reactions, photolysis, radiolysis, redox reactions and free radicals in nature (Roberfroid and Calderon, 1995). In these reactions, an electron is lost from a compound to form a free radical. The chain reaction is then propagated by the reaction of the free radicals with the substrates present. The substrates can be carbohydrates, protein or lipids in living organisms. During propagation, atom transfer, electron transfer and addition reaction can take

place. The chain reaction is terminated when there is linking of radicals, radical scavenging by antioxidants or when radicals are depleted (Larson, 1997).

1.1.8 Damage of cellular structures by ROS

As ROS are reactive, they can target on biological molecules and cause damage on cellular structures. When lipid becomes the target of ROS, lipid peroxidation results. Chain reaction can be initiated in the presence of metal ions such as copper and iron, as they can enhance the production of hydroxyl radicals. Lipid radical ($L^{\bullet}$) is formed due to free radical attack of polyunsaturated lipid (LH) (Marks *et al.*, 1996):

$$LH + {}^{\bullet}OH \longrightarrow L^{\bullet} + H_2O$$

Lipid peroxyl radicals ($LOO^{\bullet}$) and lipid peroxide (LOOH) are formed due to propagation of the chain reaction (Marks *et al.*, 1996):

$$L^{\bullet} + O_2 \longrightarrow LOO^{\bullet}$$

$$LOO^{\bullet} + LH \longrightarrow LOOH + L^{\bullet}$$

Malondialdehyde (MDA) is produced as a result of lipid degradation. MDA in blood or urine can be determined to indicate the degree of free radical injury during oxidative stress. The chain reaction continues until terminated by a termination reaction (Marks *et al.*, 1996):

$$LOO^{\bullet} + L^{\bullet} \longrightarrow LOOH + LH$$

When proteins become the target of ROS, a series of reactions occur which finally lead to protein degradation. These include protein carbonyl formation, scission or cross-linking of polypeptides, oxidation of sulfhydryl group, and dysfunction and denaturation of proteins. When DNA becomes the target, DNA mutation and DNA breakage occurs. Degradation of DNA bases into purines and pyrimidines may result.

1.2 Antioxidative defence in the body

Human body is equipped with a series of antioxidant defence mechanisms to counteract the destructive effects of ROS. These defence mechanisms could be in the form of proteins, enzymes or compounds.

1.2.1 Antioxidant proteins

Certain plasma proteins can be regarded as antioxidant proteins. Some of them such as albumin react with ROS by sacrificing themselves to spare other blood components (Miller *et al.*, 1995). Other antioxidant proteins such as serum transferrin and cytosolic ferritin chelate transition metal ions (Fe^{2+}) which take part in the Fenton reaction (Camejo *et al.*, 1998). Plasma also contains haptoglobin which binds hemoglobin and hemopexin which binds hemin (Miller *et al.*, 1996).

1.2.2 Antioxidant enzymes

Antioxidant enzymes remove ROS or convert them into less toxic forms. They include SOD, catalase and glutathione peroxidase (GSH-Px) (Knight, 2000). Superoxide radicals synthesized in the mitochondria are removed by mitochondrial Mn-SOD (Marks *et al.*, 1996). Cytosolic Cu,Zn-SOD removes superoxide radicals in the cytosol and extracellular Cu,Zn-SOD helps to attenuate oxidative damage of brain and lung (Bowler *et al.*, 2002). Universal occurrence of SOD in the body reflects the importance of superoxide radicals as the primary ROS.

$$2O_2^{\bullet-} + 2H^+ \xrightarrow{\text{SOD}} H_2O_2 + O_2$$

GSH-Px and catalase are present inside the cell to remove H_2O_2, as H_2O_2 is the precursor of the highly reactive hydroxyl radicals (Marks *et al.*, 1996). Catalase is mainly associated with peroxisomes where a large amount of H_2O_2 is produced. GSH-Px is found in the cytosol, on membranes and other cellular compartments. It has been suggested that GSH-Px is capable of removing very low level of H_2O_2 , but it has low capacity due to the requirement of reduced nicotinamide adenine dinucleotide phosphate (NADPH) to regenerate reduced glutathione (GSH). In contrast, catalase has high capacity in removing H_2O_2 produced by drug oxidation or fatty acid oxidation, but it is insensitive to low H_2O_2 concentrations (Rice-Evans *et al.*, 1995).

$$2H_2O_2 \xrightarrow{\text{Catalase}} 2H_2O + O_2$$

$$2GSH + H_2O_2 \xrightarrow{\text{GSH-Px}} GSSG + 2H_2O$$

Intracellular GSH level is maintained by glutathione reductase (GSSG-Rd) for the normal activity of GSH-Px. The reduction of oxidized glutathione (GSSG) by GSSG-Rd requires reducing equivalents from NADPH:

$$GSSG + NADPH + H^+ \xrightarrow{\text{GSSG-Rd}} 2GSH + NADP^+$$

1.2.3 Antioxidant compounds

Vitamin E, vitamin C and carotenoids are low-molecular-weight antioxidant compounds with *in vivo* effects, and dietary supplementation is required. Urate, bilirubin, GSH and ubiquinol can be produced *in vivo* (Knight, 2000). Among the antioxidants, vitamin E, vitamin C, GSH and urate will be described.

1.2.3.1 Vitamin E

The lipid soluble vitamin E (Vit E or tocopherols) serves as the main antioxidant to protect against lipid peroxidation in which α-tocopherol is the most biologically active form in animals. Its ability to form stable tocopheryl radical (Vit E$^{\bullet}$) enables it to scavenge free radicals and to stop propagation of chain reactions. Tocopheryl quinone (Vit E_{ox}) is formed eventually by further oxidation (Marks *et al.*, 1996). Its water soluble form, trolox, is used as positive control in most assays.

$$L^{\bullet} + \text{Vit E} \longrightarrow LH + \text{Vit E}^{\bullet}$$

$$\text{Vit E}^{\bullet} + L^{\bullet} \longrightarrow LH + \text{Vit } E_{ox}$$

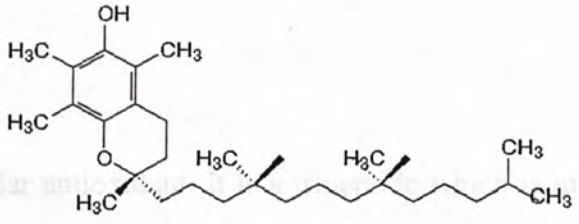

Figure 1.1 Chemical structure of vitamin E.

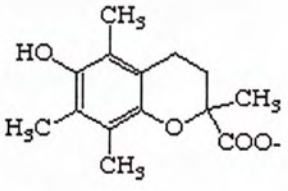

Figure 1.2 Chemical structure of trolox.

1.2.3.2 Vitamin C

Vitamin C (or L-ascorbic acid) is hydrophilic in nature. It is able to react with superoxide and hydroxyl radicals to form ascorbyl radical and eventually becomes dehydro-L-ascorbic acid upon complete oxidation (Marks *et al.*, 1996). It can regenerate vitamin E from its oxidized forms (Marks *et al.*, 1996).

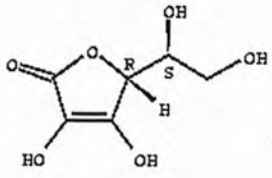

Figure 1.3 Chemical structure of vitamin C.

1.2.3.3 Glutathione

GSH is an intracellular antioxidant. It is a tripeptide which is made up of glutamate, cysteine and glycine (γ-Glu-Cys-Gly). The GSH pool is compartmentalized in different organelles. Detailed antioxidant mechanism of GSH will be described in the RBC section.

1.2.3.4 Urate

Urate is the reaction product of XOD in the purine degradation pathway. It possesses antioxidative ability as it accepts electrons readily from ROS. It scavenges hydroxyl radicals and peroxynitrite and reacts with nitric oxide (Kirschbaum, 2001). It also has transition metal ion chelating ability as it inhibits metal-induced oxidative destruction by binding with them without being oxidized itself (Rice-Evans *et al.*, 1995). Urate can protect red blood cell (RBC) membrane against lipid peroxidation and inhibit

hemolysis (Ames *et al.*, 1981). Therefore, urate may have the ability to defend against aging, a condition hypothesized to be caused by the accumulation of free radical-induced damage. In fact, a high serum urate level is believed to contribute to the longevity of human as compared to other mammals (Knight, 2000). As urate is the product of purine degradation, therefore the purine metabolic pathway can be considered as one of the defence mechanisms against ROS attack.

1.2.3.4.1 Purine metabolism

Purine metabolism consists of two major pathways: *de novo* purine synthesis and the purine salvage pathway (Moriwaki *et al.*, 1999). For the *de novo* pathway, 5'-phosphoribosyl-1-pyrophosphate (PRPP) is produced from ATP and ribose-5-phophate (R-5-P) in the initial step. R-5-P is the product of the pentose phosphate pathway which is essential to the antioxidation mechanism of RBC. Phosphoribosylamine is formed from PRPP and L-glutamine. Consequently, inosine monophosphate(IMP) is produced for purine ring formation. Adenosine monophosphate(AMP), IMP, xanthosine monophosphate(XMP) and guanosine monophosphate(GMP) are dephosphorylated into adenosine, inosine, xanthosine and guanosine, respectively. Inosine and guanosine are then cleaved into hypoxanthine and guanine, respectively. Hypoxanthine is oxidized into xanthine and subsequently to urate by XOD. Urate is the end product of purine *de novo* pathway in human and primates. In other mammals and lower vertebrates, urate is further degraded into allantoin by urate oxidase, an enzyme that is defective in human. For the purine salvage pathway, hypoxanthine and guanine are recycled to IMP and GMP respectively, and adenine is recycled to AMP (Figure 1.4).

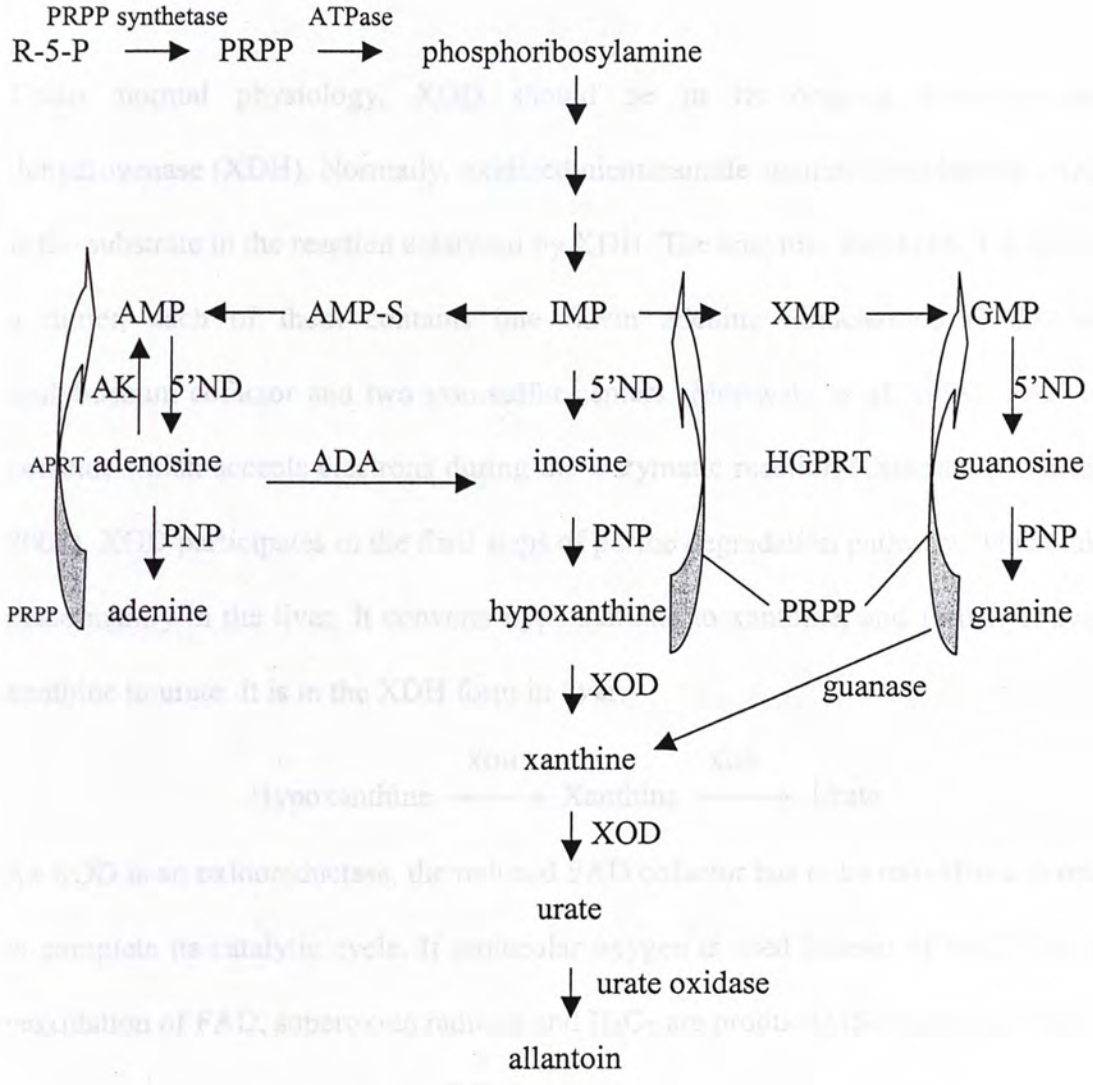

Figure 1.4 Purine ribonucleotide biosynthesis, interconversion and degradation pathways. Abbreviations: AK, adenosine kinase; APRT, adenine phosphoribosyltransferase; HGPRT, hypoxanthine-guanine phosphoribosyltransferase; 5'-ND, 5'-nucleotidase; ADA, adenosine deaminase; PNP, purine nucleoside phosphorylase; XOD, xanthine oxidase; IMP, inosine monophosphate; AMP, adenosine monophosphate; AMP-S, adenoyl-succinate; XMP, xanthosine monophosphate; GMP, guanosine monophosphate (Moriwaki *et al.*, 1999).

1.2.3.4.2 Xanthine oxidase

Under normal physiology, XOD should be in its original form: xanthine dehydrogenase (XDH). Normally, oxidized nicotinamide adenine dinucleotide (NAD^+) is the substrate in the reaction catalyzed by XDH. The enzyme, XOD (EC 1.1.3.22), is a dimer, each of them contains one flavin adenine dinucleotide (FAD), one molybdenum cofactor and two iron-sulfur centers (Moriwaki *et al*, 1999). FAD is a cofactor which accepts electrons during the enzymatic reaction (Olinescu and Smith, 2002). XOD participates in the final steps of purine degradation pathway, which takes place mainly in the liver. It converts hypoxanthine to xanthine, and further converts xanthine to urate. It is in the XDH form in liver.

$$\text{Hypoxanthine} \xrightarrow{\text{XDH}} \text{Xanthine} \xrightarrow{\text{XDH}} \text{Urate}$$

As XOD is an oxidoreductase, the reduced FAD cofactor has to be reoxidized in order to complete its catalytic cycle. If molecular oxygen is used instead of NAD^+ for the reoxidation of FAD, superoxide radicals and H_2O_2 are produced (Silverman, 2000).

$$\text{Hypoxanthine} + H_2O + 2O_2 \xrightarrow{\text{XOD}} \text{Xanthine} + \underline{2O_2^{\bullet-} + 2H^+} \longrightarrow H_2O_2 + O_2$$

$$\text{Xanthine} + H_2O + 2O_2 \xrightarrow{\text{XOD}} \text{Urate} + \underline{2O_2^{\bullet-} + 2H^+} \longrightarrow H_2O_2 + O_2$$

1.2.4 Oxidative stress and antioxidant defence mechanisms in RBC

RBC are highly differentiated cells which do not have any nuclei, mitochondria and other cellular organelles (Surgenor, 1974). They carry respiratory gases between the lungs and other tissues in the body. Since protein synthesis is virtually absent in mature RBC, replacement of damaged structures is impossible. This renders RBC

vulnerable to attack by endogenous and exogenous ROS. One of the endogenous ROS sources for RBC comes from the hemoglobin they carry. About 2-3% of hemoglobin is constantly converted into methemoglobin by molecular oxygen and superoxide radicals are produced during the process:

$$Hb(Fe\text{-}II) + O_2 \longrightarrow O_2^{\bullet -} + Hb(Fe\text{-}III)$$

In addition, the heme group in hemoglobin also contributes to ROS generation. Heme is composed of a porphyrin ring which is associated with an iron atom. The porphyrin ring is made up of four pyrrole rings linked with methenyl bondings (Marks *et al.*, 1996). During the degradation of RBC under oxidative stress (Takahashi *et al.*, 2004), heme is released from hemoglobin which is then oxidized to become hemin.

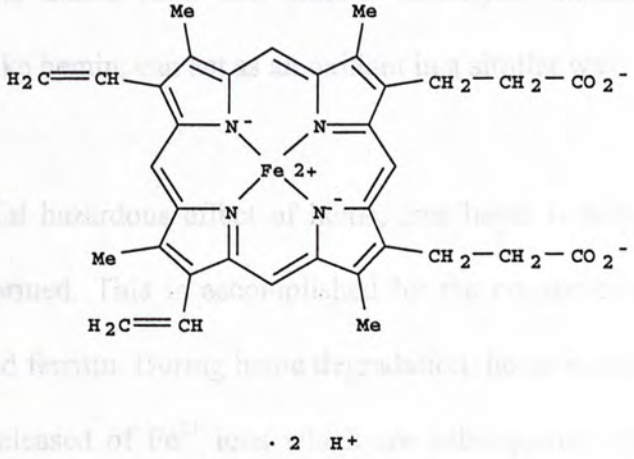

Figure 1.5 Chemical structure of heme.

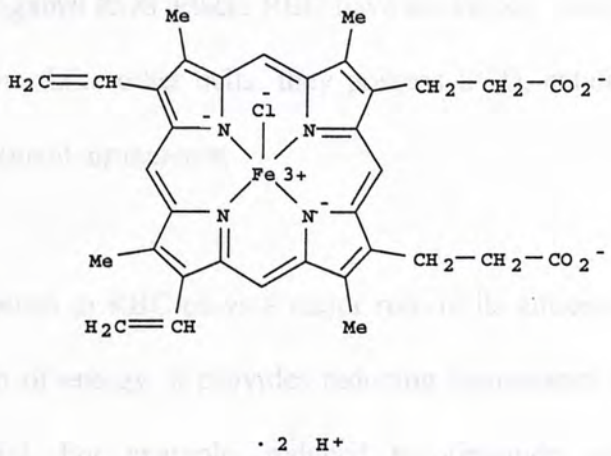

Figure 1.6 Chemical structure of hemin.

Hemin is an oxidant. It enhances peroxyl radical formation and propagates chain reaction in lipid peroxidation. Hemin also generates hydroxyl radicals in the presence of H_2O_2 in a Fenton-type reaction. When excess heme is present under oxidative stress, it is able to attack RBC and induces hemolysis. Methemoglobin, with a trivalent iron ion like hemin, can act as an oxidant in a similar way.

Due to the potential hazardous effect of heme, free heme is being removed by the body once it is formed. This is accomplished by the consecutive actions of heme oxygenase(HO) and ferritin. During heme degradation, heme is oxidized to biliverdin by HO with the released of Fe^{2+} ions which are subsequently chelated by ferritin. Biliverdin is further converted into bilirubin and excreted (Marks *et al.*, 1996). Bilirubin is an antioxidant *in vivo*. It associates with albumin and produces antioxidant effect at low concentrations (Mireles *et al.*, 1999).

In order to defend against ROS attack, RBC have developed some special antioxidant defence mechanisms. Like other cells, they possess SOD, catalase and GSH-Px as their primary antioxidant armaments.

The energy metabolism in RBC plays a major role in its antioxidant defence. Apart from the generation of energy, it provides reducing equivalents to maintain cellular antioxidant potential. For example, reduced nicotinamide adenine dinucleotide (NADH) produced from glycolysis is essential to reduce methemoglobin to hemoglobin by the action of methemoglobin reductase. NADPH produced from the pentose phosphate pathway is essential to complete the GSH antioxidant mechanism by keeping GSH in the reduced form through the action of GSSG-Rd (Marks *et al.*, 1996).

The GSH antioxidant mechanism is particularly important to RBC. RBC have GSH-Px which removes hydrogen peroxide and lipid peroxides (Marks *et al.*, 1996). Coupling of GSSG reduction is performed by GSSG-Rd. The thiol group in GSH also serves as a ligand for the heme-associated iron ion (Shviro and Shaklai, 1987). GSH competes for hemin with the membrane, thus lowering the damaging effect of hemin towards RBC (Shviro and Shaklai, 1987).

RBC membrane is a phospholipid bilayer with proteins embedded. Among the membrane proteins, ATPases help to keep the cell intact by maintaining ion homeostasis. Two of the ATPases are the Na^+/K^+-ATPase and the Ca^{2+}-ATPase. Their 3-dimentional structures have been compared (Jorgensen *et al.*, 2003), and is found to be similar.

1.2.5 Oxidative stress and antioxidant defence mechanisms in LDL

Low density lipoprotein (LDL) is a class of serum lipoprotein with a phospholipid monolayer and an apoprotein B100 (Alberts *et al.*, 1994). It is responsible for the transport of cholesterol, cholesterylesters and triglycerides to tissues and regulates *de novo* cholesterol synthesis. The transported substances are the main constituents of cellular membrane and they enter target cells by receptor-mediated endocytosis (Stryer, 1995). LDL in the circulation are susceptible to oxidation by molecular oxygen and other pro-oxidants. Each LDL contains several molecules of vitamin E and some LDL also contain ubiquinol for antioxidation purpose (Stocker, 1993). Ubiquinol can be considered as an antioxidant in human (Knight, 2000). When LDL is attacked by free radicals, vitamin E on LDL scavenges the radicals and is in turn converted to α-tocopheroxyl radical. In order to protect LDL from peroxidation, vitamin E has to be regenerated. This is done by the presence of ubiquinol in LDL and vitamin C in human plasma (Stocker, 1993).

1.3 Human diseases originated from pro-oxidant conditions

ROS can be generated massively if there are defects in the metabolism or under pathological conditions. When the amount of ROS exceeds the antioxidant capacity of the body, cells and tissues will become vulnerable to free radical attack, a condition known as oxidative stress.

1.3.1 Atherosclerosis

Blood LDL undergoes continual oxidation. If it remains in the circulation for an extended period of time due to insufficient LDL uptake, the oxidized form of LDL will accumulate and injure cells on the vessel lumen. This condition attracts monocytes. The monocytes may become foam cells if they engulf too much oxidized LDL (Marks *et al.*, 1996). These foam cells together could form plaques on arterial walls, thus narrowing the vessels' diameter and minimizing the vessels' flexibility. This eventually causes atherosclerosis (Marks *et al.*, 1996). If the event happens in coronary arteries, cardiovascular disease and heart attack may result.

1.3.2 Ischemia / reperfusion injury

XOD has been suggested to be involved in the pathogenesis of post-ischemic reperfusion injury such as during organ transplantation. This is due to the generation of ROS (Moriwaki *et al.*, 1999). XOD usually exists in cells in the form of XDH. XDH is converted into XOD by the proteolytic action of cytosolic calcium-dependent protease which is probably activated due to the increase in intracellular calcium ion concentration during ischemia (Engerson *et al.*, 1987; Fernandez *et al.*, 2004). In addition, release of adenosine also increases due to extensive hydrolysis of ATP. The adenosine is converted into inosine then into hypoxanthine. Therefore, XOD constitutes an important source of ROS during reperfusion since the oxidation of xanthine and hypoxanthine by XOD leads to the generation of massive amount of superoxide radicals (Engerson *et al.*, 1987). The organs that may be injured by

ischemia/reperfusion include brain, heart, gastrointestinal tract and kidney (Canas, 1999).

1.3.3 Glucose-6-phosphate dehydrogenase deficiency

Glucose-6-phosphate dehydrogenase (G6PD) deficiency is an inborn disease in which NADPH is unavailable for GSSG-Rd's action. GSSG formed by GSH-Px cannot be reduced back to GSH in the absence of NADPH. The RBC become vulnerable to oxidative stress. Cross-linking of hemoglobin results in the formation of Heinz bodies on RBC membrane. Heinz body is an aggregate of cross-linked hemoglobin. This results in the decrease in deformability of RBC. The shear stress exerted on the RBC during passage through the capillaries renders the RBC to undergo hemolysis (Marks *et al.*, 1996).

1.3.4 DNA mutation

Transition metal ions such as Fe^{2+} and Cu^{2+} may bind to DNA non-specifically. The highly reactive hydroxyl radicals will be produced by the Fenton reaction in the presence of H_2O_2 (Marks *et al.*, 1996). The hydroxyl radicals in turn cause DNA strand breakage or mutation. ROS may also interact with transcription factors and influence their normal function. If mutation occurs in mitochondrial DNA, the components of ETC may become defective. The output of energy may decline and electron leakage may increase which would result in the release of more ROS. This mechanism has been hypothesized to be involved in the process of aging (Knight,

2000). If DNA mutation happens in somatic cells, the ordinary cellular function and regulation will be affected. This will lead to cancer.

1.3.5 Other pro-oxidant state related diseases

Other diseases that are associated with oxidative stress include diabetes, asthma, cystic fibrosis, cataract, hematologic disorders, acute renal failure, stroke, Parkinson's disease, cerebrovascular disorder, Alzheimer's dementia and psoriasis (Rice-Evans *et al.*,1995; Marks *et al.*, 1996; Olinescu and Smith, 2002).

1.4 Hyperuricemia and gout: diseases originated from an extreme antioxidant condition

Hyperuricemia is a hallmark of gout which is caused by elevation in urate synthesis or reduction in urate excretion, or both. Prolonged hyperuricemic condition enhances accumulation of urate, leading to the formation of sodium urate crystals. When the urate deposits in joints and kidneys, gout results. The disease can be classified into primary gout and secondary gout. The former is a congenital disease, whereas the latter is non-congenital and is common in male. Symptoms of gout include swelling and inflammation of joints, malfunctioning of kidneys, chills and fever. Primary gout is caused by disorder in purine metabolism, which is contributed by genetic abnormality which leads to functional deficiency of one or more enzymes in the purine pathway (Lehninger, 2000).

There are several conditions for primary gout. Some patients may have a partial deficiency of hypoxanthine-guanine phosphoribosyltransferase (HGPRT). This is an enzyme catalyzing the synthesis of IMP and GMP in the salvage pathway from hypoxanthine and guanine respectively.

$$\text{Hypoxanthine} + \text{PRPP} \xrightarrow{\text{HGPRT}} \text{IMP} + \text{PPi}$$

$$\text{Guanine} + \text{PRPP} \xrightarrow{\text{HGPRT}} \text{GMP} + \text{PPi}$$

In the case of complete HGPRT deficiency, Lesch-Nyhan Syndrome results. Deficiency of HGPRT reduces GMP and IMP synthesis and elevates PRPP level. This enhances purine biosynthesis by the *de novo* pathway, thus the formation of 5-phosphoribosyl-1-amine increases. Another condition is that some patients may have hyperactive PRPP synthetase with impaired allosteric regulation. This will lead to excess PRPP production. Similar problem arises which finally lead to hyperuricemia.

Regarding secondary gout, it can be caused by different non-congenital factors. The reasons for elevated urate production may include rich purine meal, obesity and hypertriglyceridemia (Harris *et al.*, 1999). The reasons for reduced urate excretion may include the use of diuretic drugs, renal dysfunction and hypothyroidism (Harris *et al.*, 1999). Prevalence of gout from 1983 to 1985 according to the National Health Survey in USA is 1.36% in men and 0.64% in women. The incident rate has increased three folds since 1969 (Harris *et al.*, 1999).

1.4.1 Inhibition of XOD as a treatment method for hyperuricemia

One of the treatment methods for gout is to inhibit XOD. By inhibiting the enzyme, xanthine and hypoxanthine become the products of the purine metabolic pathway.

They are more soluble in water compared to urate, and therefore they do not form crystals and can be excreted more easily (Lehninger, 2000).

Allopurinol has been used to treat gout extensively. It is an analog of hypoxanthine. When compared to hypoxanthine, the position of one of the N atoms is exchanged with one of the C atoms of allopurinol.

Hypoxanthine *Allopurinol*

Figure 1.7 Chemical structures of hypoxanthine and allopurinol.

However, there are a number of adverse side effects associated with allopurinol administration. Allopurinol is a very powerful irreversible inhibitor of XOD. Urate production is inhibited, and hypoxanthine and xanthine levels rise. On the one hand, this leaves out an important antioxidant. The reduction in serum urate level would reduce the antioxidant capacity of the body (Waring *et al.*, 1991; Nieto *et al.*, 2000). On the other hand, xanthinuria may result. The dramatic increase in hypoxanthine and xanthine levels may lead to xanthine precipitation and results in the development of kidney stones (Kenney, 1991; Stryer, 1995). Moreover, there are a number of adverse side effects associated with allopurinol. Symptoms including rashes, fever, vomiting, eosinophilia, nausea, diarrhea, toxic epidermal necrolysis, acute vasculitis, renal dysfunction and massive hepatic necrosis have been reported (Wortmann, 2002; Horiuchi *et al.*, 2000; Kong, Cai, *et al.*, 2000). In severe situations, some patient may

develop allopurinol hypersensitivity syndrome, which could be lethal (Kong, Zhang, *et al.*, 2000).

1.4.2 Relationship between ROS injury and hyperuricemia

XOD plays significant roles in purine metabolism and ischemia-reperfusion injury. This is due to its reaction products urate and superoxide radicals, which are antioxidant and ROS respectively. Normal serum urate levels for male and female are lower than 7mg/dL and lower than 6mg/dL respectively (Chang *et al.*, 2001), which are close to the solubility limit of urate in human blood (7mg/dL at 37°C) (Stryer, 1995). Although the high serum urate level in human increases the danger of hyperuricemia, it may contribute to the protection of blood components from ROS attack since urate is an antioxidant (Nieto *et al.*, 2000; Ames *et al.*, 1981). Epidemiological studies have shown a positive correlation between hyperuricemia and atherosclerosis (Lin *et al.*, 2004; Aucamp *et al.*, 1997). The reason for this phenomenon is still controversial. One of the studies suggested that urate level increases in atherosclerotic patients may be due to a compensatory antioxidant defence mechanism (Nieto *et al.*, 2000). The correlation between hyperuricemia and atherosclerosis leads to the research direction of finding potential drugs with XOD inhibitory and antioxidant effects (Aucamp *et al.*, 1997). If a compound is found to have both XOD inhibitory and antioxidative ability, it would be ideal (Shigematsu *et al.*, 2003; Tsutsumi *et al.*, 2004). Compounds with both effects might be able to inhibit urate production on the one hand, and replenishing the antioxidative ability on the other.

1.5 Antioxidants in human nutrition

Regarding the prevalence of ROS-derived diseases, supplementation with antioxidant vitamins is a possible preventive measure. However, human are exposed to higher oxidative stress due to new diseases and environmental pollution. Therefore, application of natural products contributes another possible alternative, since these products contain antioxidants with potency comparable to that of traditional vitamins, and they are abundantly available with fewer side effects. Examples of natural antioxidant sources include green tea, cruciferous vegetables and many herbs.

1.6 Chinese medicinal therapeutics

Numerous natural products have been evaluated for their effects towards different diseases. Supplementation with traditional antioxidants and vitamins which aids in the prevention of free radical derived diseases become insufficient to cope with many new diseases. Regarding the side effects generated by the current drugs, it is necessary to explore new drugs with higher efficacy and potential. Chinese medicinal material (CMM) has become a new source of such explorations (Lee, 2000). Among thousands of CMM, a number of them have been applied in prescriptions since ancient times for curing diseases which are currently identified to be caused by ROS and hyperuricemia.

Gout is classified as *bizheng* (痹症) in traditional Chinese medicine (TCM) where *bi* stands for obstruction. *Bizheng* results from the attack of wind, cold, dampness and heat in which the flow of *qi* and blood through channels and meridians is hindered.

This generates pain and numbness to muscles, bones, tendons and joints. *Bizheng* in chronic condition may cause blood stasis or phlegm-turbidity (Wu and Fisher, 1944). In *The Yellow Emperor's Canon of Internal Medicine* (黃帝內經), the cause of *bi* was described:

"*As wind, cold and dampness attack in turn or strike in alliance, bi will occur.*"

「*風寒濕三氣襲至，合而爲痹也。*」

In *The Synopsis of the Golden Chamber, Zhongfeng Lijie Chapter* (金匱要略，中風歷節篇), symptoms of gout including painful joints and swollen limbs have been reported. Gout is called *tongfeng* (痛風) (which means the pain spreads like a wind), *lijie* (歷節) (which means over the joint) or *lijie wind* (歷節風) (which means the pain spreads over the joint in an acute manner). In accordance to the TCM theory, the clinical symptoms of gout can be identified as follows. They include wind-cold-dampness obstruction which means acute arthritis, obstruction of meridians by phlegm-turbidity which means ankylosis and stranguria, kidney *qi* deficiency which means edema and dizziness, *qi* and *yin* deficiency which means kidney failure (Kong, Cai, *et al.*, 2000).

From previous research work carried out by my former labmates (Kong, Cai, *et al.*, 2000), 122 herbal extracts from ancient Chinese prescription for treatment of diseases related to gout were screened. Several extracts including an extract of rhubarb were found to possess positive effects on XOD inhibition. However, the chemical components which are responsible for the effect and the reaction mechanisms remain unclear. In the present study, the XOD inhibitory effects of selected chemical

compounds from rhubarb and structurally similar compound from aloe were investigated. A phenolic compound from ginger with phenolic structures similar to the stilbenes tested in the present investigation was also studied.

1.6.1 Rhubarb

Rhubarb is the common name for the *Rheum* species, which belongs to the family of Polygonaceae. Examples of *Rheum* species include *Rheum palmatum* L., *R. tanguticum* Maxim., *R. officinale* Baill., *R. coreanum* Nakai and *R. undulatum* L. (Matsuda *et al.*, 2001). Rhubarb is distributed in western and northwestern China, Korea, other parts of Asia and Europe. Its rhizomes and roots are applied for medicinal purposes (WHO, 1999). In *The Divine Farmer's Classic of Materia Medica* (神農本草經), the application of rhubarb was described:

"*It is bitter in taste and cold in nature. It is mainly used for the discharge of blood stasis in the cold-heat blood blockage condition.*"

「味苦寒。主下瘀血，血閉寒熱。」

It has been used for curing chronic renal failure and blood stagnation syndrome which are related to the clinical conditions of gout (Kong, Cai, *et al.*, 2000; Matsuda *et al.*, 2001). This herb has also been reported to possess antimicrobial, antitumor, anti-inflammatory, hemostatic and hypercholesterolemic lowering activities. Almost half of the *Rheum* species found possess drug value (Xiao *et al.*, 1984).

Anthraquinone derivatives and stilbenes are the major constituents isolated from the rhizomes and roots of *Rheum*. The anthraquinones aloe-emodin and rhein have been reported to be good scavengers of hydroxyl radicals (Yuan and Gao, 1997; Yen *et al.*,

2000). Rhapontin, a stilbene commonly found in *Rheum* species, has been suggested to be a good agent for decreasing cholesterol level and anti-allergy (Li and Ye, 1981; Kim *et al.*, 2000). In this study, several compounds from *Rheum* including aloe-emodin (1,8-dihydroxy-3-(hydroxymethyl)anthraquinone), chrysophanol (1,8-dihydroxy-3-methylanthraquinone), rhein (4,5-dihydroxyanthraquinone-2-carboxylic acid), deoxyrhapontin (deoxyrhaponticin or 3,5-dihydroxy-4'-methoxystilbene 3-β-D-glucoside) and rhapontin (rhaponticin or 3,3',5-trihydroxy-4'-methoxystilbene 3-β-D-glucoside) were tested in order to investigate their inhibitory effect on XOD and their antioxidative ability.

1.6.2 Aloe

Aloe belongs to the family of Liliaceae. Aloe is the common name and genus name of all *Aloe* species. There are about 300 *Aloe* species. Examples of medicinal aloe include *Aloe vera* (L.) Burm f., *A. ferox* Mill. and *A. vera* L. var. *chinensis* Berger. Most *Aloe* species are originated from Africa, they can also be found in Asia and America. Their leaves are applied for medicinal purposes. Aloe can be used to enhance wound healing, improve skin quality, decelerate skin aging, treat occasional constipation (WHO, 1999), increase urine production due to its uricosuric ability (Yagi *et al.*, 2002). Aloe contains anthraquinones and their derivatives. Barbaloin (1,8-dihydroxy-10-(β-D-glucopyranosyl)-3-(hydroxymethyl)-9(10H)-anthracenone or aloin A) is the major constituent (WHO, 1999).

1.6.3 Ginger

Zingiber officinale Roscoe belongs to the family of Zingiberaceae. Its common name is ginger. This herb is originated from south-east Asia and found in Africa, China and India. Its rhizomes are well-known for its spicy taste and have been used in different nations both as spices and medicines. Ginger has been used in TCM for thousands of years to induce perspiration and to calm nausea (WHO, 1999). It has also been used in several prescriptions of *bizheng* such as Fang-feng-tang, Gui-zhi-shao-yao-zhi-mu-tang, Yi-yi-ren-tang and Zhi-gan-cao-tang (Wu and Fisher, 1944). Other usages include enhancing flu healing and to treat cataract, bile stone formation, atherosclerosis, and rheumatoid arthritis (Aeschbach *et al.*, 1994). Ginger contains zingiberene, gingerols, shogoals and their derivatives as its major ingredients (WHO, 1999). 6-Gingerol is the major pungent constituent in ginger oils extracted from the rhizomes (Aeschbach *et al.*, 1994).

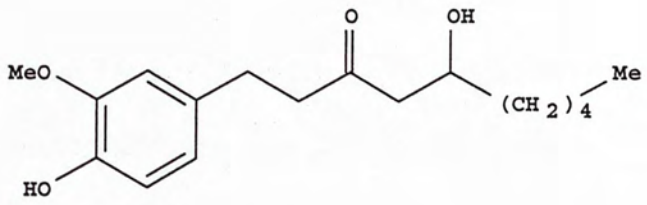

Figure 1.8 Chemical structure of 6-gingerol.

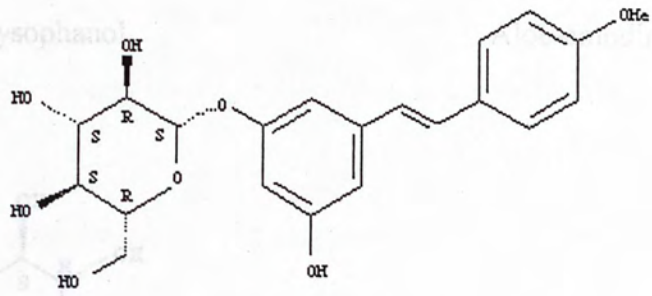

Deoxyrhapontin

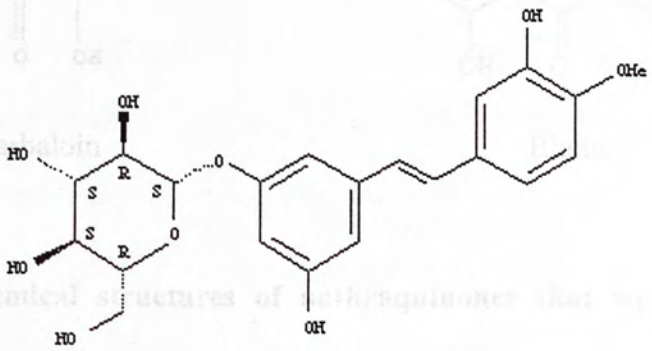

Rhapontin

Figure 1.9 Chemical structures of stilbenes that were tested in the present study.

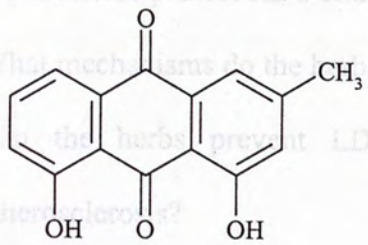

Chrysophanol

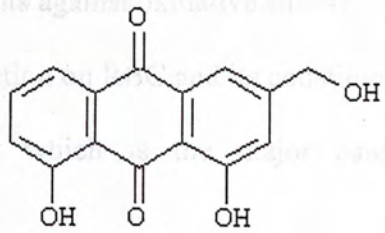

Aloe-emodin

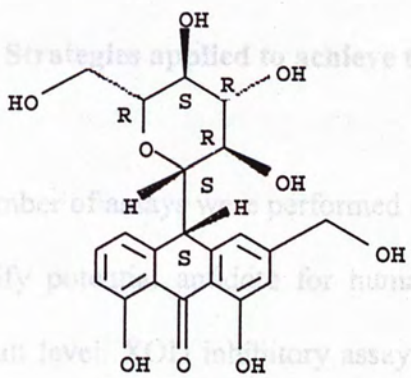

Barbaloin

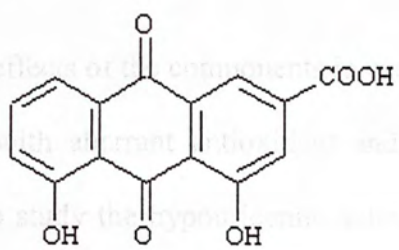

Rhein

Figure 1.10 Chemical structures of anthraquinones that were tested in the present study.

1.6.4 Objectives of the project

1. Do the herbs that have been applied for curing hyperuricemia and gout-related diesases in ancient China possess XOD inhibitory effects?
2. Do the herbs protect RBC and its constituents against oxidative stress?
3. What mechanisms do the herbs exert protection on RBC and its constituents?
4. Can the herbs prevent LDL oxidation which is the major cause of atherosclerosis?
5. Do the herbs possess both XOD inhibitory effect and antioxidative effect?
6. What is the structure-activity relationship of the active compounds?

1.6.5 Strategies applied to achieve the objectives of the present project

A number of assays were performed to study the effects of the components in order to identify potential antidote for human diseases with aberrant antioxidant and pro-oxidant level. XOD inhibitory assay was done to study the hypouricemic actions of the compounds. Antioxidant assays were also performed to evaluate the compounds' ability in alleviating pro-oxidant situations. RBC assays aim to reveal the compounds' protective ability on two important biomolecules, lipids and proteins, since RBC membrane possesses typical human cell membrane structure and is easy to obtain (Albert *et al.*, 1994). Activity assays for ATPases and protein sulfhydryl group protection assay are used to study the degree of protein damage by ROS, and thiobarbituric acid (TBA) assay is used for the determination of lipid peroxidation. Moreover, LDL assays were carried out to assess the compounds' potential in preventing atherosclerosis.

Chapter 2 Materials and methods

In this chapter, the methods of the assays are described in detail. The order that reagents were added into the assay mixture is the order that they are listed in the procedure. The listed concentrations of the reagents are the final concentrations. Reagents used were of analytical grade.

2.1 XOD inhibition assay

The enzyme XOD used in this study was purchased from Roche Diagnostics isolated from bovine milk. All other reagents used were of analytical grade. The assay was performed according to a standard method previously established in our laboratory (Kong, Zhang, *et al.*, 2000).

2.1.1 Assay development

Prior to the observation of compounds' inhibitory effect on the enzyme, the concentrations of enzyme and substrate were determined, so that their optimal concentrations were used. A fixed enzyme concentration was reacted with various substrate concentrations to determine the saturating substrate concentration. This is important as saturating substrate concentration indicates the maximum reaction rate at that particular enzyme concentration. A fixed substrate concentration was used with various enzyme concentrations to ensure linearity of the assay under the assay

conditions. After that, the optimal reaction condition was obtained, at which the potential inhibitors could be tested.

2.1.2 Dose-dependent study

The activity of XOD was assayed by reacting the enzyme with xanthine under aerobic condition (Kong, Zhang, *et al.*, 2000). The assay procedures for XOD are as follows. The assay was performed in a final volume of 1ml containing 80mM sodium pyrophosphate buffer (pH 7.5), the test compound dissolved in DMSO initially and 0.089U/ml XOD were mixed and incubated for 10 min in a quartz cuvette at 25°C. Then, the reaction was started by adding xanthine (final concentration = 0.12mM) and increase in absorbance due to urate production was monitored spectrophotometrically at 295nm. The final concentration of DMSO in the assay was 5% at which the assay was not affected. Allopurinol was used as a positive control in the assay.

2.1.3 Reversibility of the enzyme inhibition

There are two main types of enzyme inhibition, reversible and irreversible. For the former type, it is further divided into several different kinds. They are competitive, non-competitive, uncompetitive and mixed. In reversible inhibition, the inhibitory effect exerted on XOD by the compounds can be reversed, meaning that the activity of XOD can regain its original activity after the removal of the inhibitor. The mode of reversible enzyme inhibition could then be assessed by the Lineweaver-Burk plot. On the other hand, irreversible inhibitor differs from reversible inhibitor that the irreversible one forms covalent bond or very tight binding with the enzyme. This

renders the enzyme inactive, and the activity of the enzyme can no longer resume its original activity again.

The procedures were the same as in section 2.1.1, except that the enzyme was incubated with inhibitor at high concentration for 10 min. The mixture was then diluted with assay buffer just before the beginning of reaction, so that the final concentrations of the inhibitor, enzyme and substrate were the same as that in the dose-dependent experiment. The DMSO concentration in the assay was kept at 5% (before and after dilution).

2.1.4 Lineweaver-Burk plot

Lineweaver-Burk plot was conducted to find out the mode of inhibition of the test compound, whether it is competitive, non-competitive, uncompetitive or mixed type inhibitor. The procedures were the same as in section 2.1.1, except that the assays were carried out in the absence and presence of the test compound and the concentration of the substrate, xanthine, varied.

2.2 Lipid peroxidation inhibition assay of mouse liver microsomes

The lipid peroxidation of mouse liver microsome was produced using the Fe^{2+}-ascorbate system (Zheng and Zheng, 1992; Basaga *et al.*, 1997) with some modifications.

2.2.1 Preparation of mouse liver microsomes

BALB/c mice were sacrificed by decapitation. Livers were excised and rinsed twice with 0.9% saline at 4°C. All subsequent preparative procedures were carried out at 4°C unless otherwise specified. Livers were then homogenized in 0.15M KCl. The amount of KCl added to liver was 3ml/g. The homogenate was centrifuged at 10,000g for 20 min at 4°C. After that, the supernatant was retained and centrifuged at 100,000g for 1 h at 4°C. The supernatant was discarded. The pellet was resuspended with KCl. The stock was stored at -20°C after determination of protein concentration.

2.2.2 Basis of assay

This assay works on the principle that the Fe^{2+}-ascorbate system generates free radical-mediated lipid peroxidation of the liver microsomal preparation. Trichloroacetic acid (TCA) is added for protein precipitation after incubation to stop further reaction. MDA, the product of the lipid peroxidation, forms complexes with TBA. The absorbance of the pink color adduct could be monitored at 532nm.

2.2.3 Assay procedures

The assay was performed in a final volume of 1ml containing phosphate buffered saline (PBS) (pH 7.4), 50μl of the test compound, 0.4mg/ml mice liver microsomes, 0.01mM $FeSO_4$ and 0.1mM ascorbic acid. The mixture was incubated for 1 h at 30°C. When incubation was completed, 1ml of 20% TCA and 1.5ml of 0.8% TBA were added to each sample to terminate the reaction. The mixture was boiled for 20 min at 100°C. After that, it was centrifuged at 3000g for 5 min. The absorbance of the supernatant was measured at 532nm. Net absorbance was calculated by subtraction between the samples and their own blanks. The degree of lipid peroxidation for each sample was expressed in terms of a percentage of the drug-free control. Trolox was used as a positive control. The percentage of control was calculated according to the following formula:

$$\% \text{ of control} = A_{532} / A_{532}' \times 100\%$$

where:

A_{532} = net absorbance of sample

A_{532}' = net absorbance of control

2.3 AAPH-induced hemolysis inhibition assay

The assay was adopted from the AAPH-induced hemolysis system (Jimenez *et al.*, 2000) with some modifications.

2.3.1 Preparation of RBC

Blood samples from Sprague-Dawley rats were obtained from the Laboratory Animal Service Center of the Chinese University of Hong Kong. About 10ml of rat blood collected in heparinized tubes was centrifuged at 1500g for 10 min at 4°C. After the plasma with white blood cell (WBC) and platelets were removed, the RBC were then washed with 0.15M NaCl and centrifuged at 1500g for 10 min at 4°C. This procedure was repeated for two more times. In the last wash, the centrifugal speed was lowered to 1000g. After saline was removed, a 20% suspension of the RBC was prepared by adding PBS.

2.3.2 Basis of assay

This assay works on the principle that 2,2'-azobis (2-amidinopropane) dihydrochloride (AAPH) could generate peroxyl radicals which attack RBC *in vitro*. Antioxidant compounds could thus protect the red cells from this hemolytic action of AAPH.

2.3.3 Assay procedures

For each sample, the final volume is 1ml containing 500μl RBC preparation, 250μl of the test compound dissolved initially in DMSO then diluted with PBS, and 100mM AAPH. The final DMSO concentration in the 1ml mixture was 2.5% at which concentration there was minimal effect on the RBC. All samples were incubated at 37°C for 3 h with gentle agitation. When incubation was completed, 0.1ml of the reaction mixture was diluted with 0.9ml PBS, and another 0.1ml of the same reaction mixture was diluted with 0.9ml distilled water (DW). All the samples were mixed well and centrifuged at 1500g for 10 min at 4°C. From each sample, 200μl was transferred to a 96-well plate for measurement of absorbance at 540nm. Vitamin C and trolox were used as positive controls in the assay. Percentage of RBC lysed for each sample was calculated according to the following equation:

$$\% \text{ of RBC lysed} = A_{540} \text{ in PBS} / A_{540} \text{ in DW} \times 100\%$$

2.4 Lipid peroxidation inhibition assay of RBC membrane

The lipid peroxidation assay of RBC membrane was performed using the *tert*-butylhydroperoxide (*t*BHP)/hemin as the ROS generation system (Rice-Evans *et al.*, 1991; Yokode and Kita, 1988; Zuckerman and Bryan, 1996) with some modifications.

2.4.1 Preparation of RBC membrane

Blood collection

The RBC membrane was prepared according to a reported method (Matteucci *et al.*, 1995) with some modifications. Approximately 90ml rabbit blood was provided by the Laboratory Animal Service Center of the Chinese University of Hong Kong on each experimental day. The blood was collected in tubes with 60mM EDTA in saline as anticoagulant (blood:anticoagulant = 9:1 v/v).

RBC washing

Blood was centrifuged at 200g for 10 min at 20°C. The supernatant containing the plasma and WBC was removed. RBC was transferred from the Falcon tube to a 250ml Nalgene centrifuge bottle, and was then resuspended in Buffer 1 in a ratio of cell:buffer = 1:10 by volume. The mixture was centrifuged at 1320g for 5 min at 4°C, and the supernatant was removed. The above washing step was repeated twice. After the last washing, 175ml Buffer 2 was added after removing the supernatant. The mixture was shaken vigorously for 5 min, and kept on ice afterwards. It was centrifuged at 1320g for 5 min at 4°C. Hemolysate was transferred to a beaker, and the pellet discarded.

RBC membrane purification

The hemolysate was centrifuged at 25000g for 20 min at 4°C. The supernatant was removed and the pellet was resuspended with 175ml Buffer 2. It was centrifuged at 25000g for 20 min at 4°C and the pellet was resuspended with 175ml Buffer 3. The mixture was centrifuged at 25000g for 20 min at 4°C and its pellet was resuspended with 175 ml Buffer 3. It was centrifuged at 25000g for 20 min at 4°C and the pellet was resuspended with 175ml Buffer 4. The mixture was centrifuged at 25000g for 20 min at 4°C and its pellet was resuspended in Buffer 4. Finally, RBC membrane in all centrifuge bottle were combined and homogenized with a syringe several times on ice. The stock was pipetted into 1.5ml microfuge tubes and stored at -80°C.

Buffers

Buffer 1: 0.15M NaCl

Buffer 2: 0.01M Tris-HCl buffer with 1mM EDTA, pH 7.6

Buffer 3: 0.01M Hepes-NaOH buffer with 1mM EDTA, pH 7.6

Buffer 4: 0.01M Hepes-NaOH buffer, pH 7.6

2.4.2 Basis of assay

This assay works on the principle that hemin catalyses the formation of peroxyl radicals from *t*BHP. The peroxyl radicals then initiate lipid peroxidation of the RBC membrane. TCA is added for protein precipitation to stop further reaction. MDA, the product of lipid peroxidation, forms complexes with TBA. The fluorescence of TBA reactive substance (TBARS) is measured using a fluorometer with an excitation wavelength at 515nm and an emission wavelength at 553nm.

2.4.3 Assay procedures

The assay was performed in a final volume of 1ml containing PBS (pH 7.4), 50μl of the test compound, 0.05mg/ml RBC membrane, 0.5mM *t*BHP and 1.5μM hemin. The mixture was incubated at 37°C for 4 h. After incubation, 1ml of 20% TCA was added and mixed well. Then, 1ml of 0.8% TBA was added and mixed well. The mixture was heated for 1 h at 95°C. It was then centrifuged at 3000g for 5 min at 4°C. The supernatant was transferred to another test-tube. Then, 3ml of butan-1-ol was added and the mixture was vortexed vigorously for about 10 times. The mixture was centrifuged at 3000g for 5 min at 4°C and the top layer was removed for fluorescence measurement. The extent of RBC membrane oxidation was measured using an excitation wavelength of 515nm and an emission wavelength of 553nm. Net absorbance was calculated by subtraction between the samples and their own blanks. The degree of lipid peroxidation for each sample was expressed in terms of a percentage of the drug-free control. Trolox was used as the positive control. The percentage of control was calculated by the following formula:

$$\% \text{ of control} = F / F_1 \times 100\%$$

where:

F = net fluorescent unit of sample

F_1 = net fluorescent unit of control

2.5 ATPase protection assay

The ATPase protection assay was based on the *t*BHP / hemin inhibition system (Al-Jobore and Roufogalis, 1981; Kallner, 1975; Reinila *et al.*, 1982; Watanabe *et al.*, 1988) with some modifications.

2.5.1 Preparation of RBC membrane

The procedure was the same as described in section 2.4.1.

2.5.2 Preparation of malachite green (MG) reagent

A hundred and forty milliliter of 3.53% ammonium molybdate was added to 300ml DW. Sixty milliliter of concentrated HCl was then added with stirring. Malachite green base (0.1g) was dissolved in the mixture. After 1 h or above, when sedimentation of precipitate was completed, the solution was filtered through a glass fiber membrane and stored in the dark.

2.5.3 Basis of assay

Peroxyl radicals were generated through the *t*BHP/hemin system. The radicals would attack the ATPases and rendered them inactive. If the compound showed positive results in this assay, it might be able to inhibit the inactivation of ATPases. The active ATPases would be able to hydrolyse ATP to ADP, with the production of inorganic

phosphate (P_i). P_i reacts with MG to give a green-colored complex whose absorbance could be read spectrophotometrically at 650nm.

2.5.4 Assay procedure

The assay was performed in a final volume of 800μl containing 400μl of 50mM Hepes buffer (pH 7.4) and 100μl each of the test compound, RBC membrane, *t*BHP and hemin. The mixture was incubated in a 1.5ml microfuge tube for 4 h at 37°C with gentle agitation. The mixture was centrifuged at 20,000g for 5 min at 4°C. The supernatant was discarded and the pellet was kept on ice. RBC membrane was resuspended in 450μl of assay buffer with 0.01% Triton X-100 and incubated at 37°C on a dry bath. After 10 min, 50μl of 10mM ATP was added. A 50μl of sample was aliquoted for P_i determination. After 10 min, another 50μl sample was aliquoted from the same mixture again for P_i determination. The amounts of P_i in the samples were determined by absorbance measurement at 650nm after incubation for 30 min with 1ml of MG reagent and 450μl of 1% polyvinyl alcohol (PVA). The absorbance readings were compared against a preconstructed calibration curve using KH_2PO_4. The amount of P_i in the sample released by ATPase activity within a defined period was calculated by subtracting the aliquoted sample with zero-time incubation from the one with 10 min incubation for each assay. The activities of Ca^{2+}-ATPase and Na^+/K^+-ATPase expressed as nmole P_i/mg/min were calculated according to section 2.5.5 and 2.5.6.

2.5.5 Determination of ATPase activities

Determination of Ca^{2+}-ATPase activity

Assay conditions:

The final concentrations of RBC membrane, *t*BHP and hemin were 0.3mg/ml, 0.5mM and 2μM respectively.

Calculations:

Activity with Ca^{2+} or w/o Ca^{2+}

= ([P_i at 10 min] – [P_i at 0 min]) x 0.5 x 1000 x $(0.3 \times 0.8)^{-1}$ x 10^{-1}

Net activity = activity with Ca^{2+} – activity w/o Ca^{2+}

Determination of Na^+/K^+-ATPase activity

Assay conditions:

The final concentrations of RBC membrane, *t*BHP and hemin were 1mg/ml, 0.5mM and 1.5μM respectively.

Calculations:

Activity with K^+ or w/o K^+

= ([P_i at 10 min] – [P_i at 0 min]) x 0.5 x 1000 x $(1 \times 0.8)^{-1}$ x 10^{-1}

Net activity = activity with K^+ – activity w/o K^+

2.5.6 Assay buffers

- Buffer 1 (w/o K^+ and Ca^{2+}):
    - 30mM imidazole-HCl, pH 7.4
    - 0.1mM imidazole-EGTA
    - 6mM $MgCl_2$
    - 50mM NaCl

- Buffer 2 (with K^+):
    - 30mM imidazole-HCl, pH 7.4
    - 0.1mM imidazole-EGTA
    - 6mM $MgCl_2$
    - 50mM NaCl
    - 5mM KCl
- Buffer 3 (with Ca^{2+}):
    - 30mM imidazole-HCl, pH 7.4
    - 0.1mM imidazole-EGTA
    - 6mM $MgCl_2$
    - 50mM NaCl
    - 0.3mM $CaCl_2$

2.6 Sulfhydryl group protection assay

The sulfhydryl group protection assay of RBC membrane was performed using hemin/*t*BHP as the ROS generation system (Haest *et al.*, 1978; Liu *et al.*, 1992; Soszynski and Bartosz, 1997; Xia *et al.*, 1999) with some modifications.

2.6.1 Preparation of RBC membrane

The procedure was the same as described in section 2.4.1.

2.6.2 Basis of assay

Peroxyl radicals were generated through the *t*BHP/hemin system, oxidizing the sulfhydryl group in the membrane protein. If the test compound possessed protective effect, it would be able to inhibit the oxidation of protein sulfhydryl groups. The intact sulfhydryl groups react with 5,5'-dithiobis(2-nitrobenzoic acid) (DTNB) to yield a yellow-colored complex, which could be detected spectrophotometrically at 412nm.

2.6.3 Assay procedures

The assay was performed in a final volume of 800μl containing 400μl of 50mM Hepes buffer (pH 7.4), 100μl of the test compound, 0.3mg/ml RBC membrane, 0.5mM *t*BHP and 10μM hemin. The mixture was incubated in a 1.5ml microfuge tube for 4 h at 37°C with gentle agitation. The mixture was centrifuged at 20,000g for 5 min at 4°C. The supernatant was discarded and the pellet was kept on ice. Then, 300μl of 0.1M phosphate buffer (pH 7.4) and 100μl of 4mg/ml EDTA were added and vortexed. After that, 500μl of 10% w/v sodium dodecyl sulfate (SDS) was added and mixed well. Finally, 100μl of 1mM DTNB was added and mixed well. Color was allowed to develop for 15 min at 25°C and absorbance was measured at 412nm. Net absorbance was yielded by subtracting the absorbance of blank (containing an equivalent concentration of protein) from the absorbance of sample. The amount of free sulfhydryl groups in protein was determined from a standard curve constructed with known amounts of GSH.

2.7 Lipid peroxidation inhibition assay of LDL by the AAPH method

LDL used in this study was purchased from Calbiochem. All other reagents used were of analytical grade. Lipid peroxidation of LDL was produced by AAPH oxidation (Rice-Evans *et al.*, 1991; Yokode and Kita, 1988; Zuckerman and Bryan, 1996) with some modifications.

2.7.1 Basis of assay

This assay works on the principle that AAPH generates peroxyl radicals and induces lipid peroxidation of LDL. TCA is added for protein precipitation to stop further reaction. MDA, the product of lipid peroxidation, forms complexes with TBA. The fluorescence of TBARS is measured using a fluorometer with an excitation wavelength at 515nm and an emission wavelength at 553nm.

2.7.2 Assay procedures

The assay was performed in a final volume of 1ml containing PBS (pH 7.4), 0.5mM EDTA, 50μl of the test compound, 0.1mg/ml LDL and 20mM AAPH. The mixture was incubated at 37°C for 2 h. The procedures for the determination of lipid peroxidation products in the RBC membrane were performed as mentioned in section 2.4.3. Trolox was used as a positive control.

2.8 Lipid peroxidation inhibition assay of LDL by the hemin method

LDL used in this study was purchased from Calbiochem. All other reagents used were of analytical grade. Lipid peroxidation of LDL was produced in the presence of hemin (Rice-Evans *et al.*, 1991; Yokode and Kita, 1988; Zuckerman and Bryan, 1996) with some modifications.

2.8.1 Basis of assay

This assay works on the principle that hemin propagates lipid peroxidation with the aid of existing lipid peroxides. TCA is added for protein precipitation to stop further reaction. MDA, the product of lipid peroxidation, forms complexes with TBA. The fluorescence of TBARS is measured using a fluorometer with an excitation wavelength at 515nm and an emission wavelength at 553nm.

2.8.2 Assay procedures

The assay was performed in a final volume of 1ml containing PBS (pH 7.4), 50μl of the test compound, 0.1mg/ml LDL and 1μM hemin. The mixture was incubated at 37°C for 2 h. The procedures for the determination of lipid peroxidation products in the RBC membrane were performed as mentioned in section 2.4.3. Trolox was used as a positive control.

2.9 Protein assay

Protein assay was conducted according to the method of Lowry *et al.* (1951).

2.10 Statistical analysis

Statistical analyses of the results were performed using one-way ANOVA, followed by Dunnett's test. A p value < 0.05 would be considered significance. Calculations of IC_{50} were performed by using Sigma Plot 9.0.

2.11 Test compounds

The following compounds were studied in the present investigation. The compounds were obtained from Sigma-Aldrich (USA) except chrysophanol from Fluka (Germany) and 6-gingerol from Wako (Japan). The chemicals were supplied in the purities as shown below with certificates of analysis issued by the suppliers and were directly used in the present study without further purification.

- 6-Gingerol (>98%)
- Aloe-emodin (>95%)
- Barbaloin (>96%)
- Chrysophanol (>98%)
- Deoxyrhapontin (>99%)
- Rhapontin (>99%)
- Rhein (>85%)

The chemical structures of these compounds are shown in Chapter 1.

Chapter 3 Xanthine oxidase inhibition assay: results and discussion

3.1 Introduction

Enzymes are functional protein molecules with catalytic activities. They convert target substrates into products in chemical reactions. Enzyme works by lowering the energy of the transition-state, the formation of products can then be achieved much faster than the non-catalyzed reactions. In order to lower the activation energy, enzyme forms complex with substrate which results in an enzyme-substrate-complex. The fitting mechanism between enzyme and substrate depends on the "lock-and-key" hypothesis or the "induced fit" hypothesis. After that, suitable chemical groups on the substrate interact with the functional groups in the active site of enzyme and enhance alteration of structural conformation of the enzyme. As an enzyme is specific to its own substrate, unsuitable molecule is unable to fit. When the product is formed, its structure no longer fits the orientation of the active site, and is being expelt from the active site. At the active site, the presence of cofactors, which is either a metal ion or an organic molecule, may assist the function of the enzyme.

XOD is a key enzyme which participates in the purine degradation pathway. It has a molecular weight of 300,000. It is responsible for the conversion of xanthine into uric acid, with superoxide radicals produced at the same time. As a result, it plays a significant role in the pathophysiology of hyperuricemia and ischemia/reperfusion injury. XOD exists in two forms, the NAD^+-dependent dehydrogenase form and the

oxygen-dependent oxidase form (Moriwaki *et al.*, 1999). XOD can be converted from XDH under certain circumstances. They are located in the organs of many warm-blooded animals such as liver, heart, lung, intestine, skeletal muscles, kidney, etc. (Moriwaki *et al.*, 1999).

The reaction of enzyme depends on the concentration of substrate. When substrate is in excess, reaction rate is directly proportional to the concentration of enzyme. The Michaelis-Menten equation of enzyme kinetics is as follow (Silverman, 2000):

$$v = \frac{V_{max}[S]}{K_m+[S]}$$

where:

v = rate of reaction

V_{max} = maximum rate of reaction

[S] = concentration of substrate

K_m = Michaelis-Menten constant=dissociation constant of enzyme-substrate complex

In order to find out the values of V_{max} and K_m, the Michaelis-Menten equation is converted to the double reciprocal form (Silverman, 2000):

$$1 / v = K_m / V_{max} (1 / [S]) + 1 / V_{max}$$

In the Lineweaver-Burk plot, 1 / v is plotted against 1 / [S], with slope = K_m / V_{max}, y-intercept = $1 / V_{max}$ and x-intercept = $-1 / K_m$.

In competitive inhibition, the inhibitor competes with the substrate for the same active site of the enzyme such that the inhibitor prevents the substrate from binding to the active site of the enzyme. From the Michaelis-Menten equation, the equation for competitive inhibition is derived (Silverman, 2000):

$$v = \frac{V_{max}[S]}{K_m (1 + [I] / K_i) + [S]}$$

where:

[I] = concentration of inhibitor

K_i = dissociation constant of enzyme-inhibitor complex

K_m = Michaelis-Menten constant=dissociation constant of enzyme-substrate complex

In order to construct the Lineweaver-Burk plot for evaluating the mode of inhibition, this equation is converted into the double reciprocal (Silverman, 2000):

$$1 / v = K_m / V_{max} (1 / [S]) (1 + [I] / K_i) + 1 / V_{max}$$

When 1 / v is plotted against 1 / [S] in the Lineweaver-Burk plot, slope = K_m / V_{max} (1 + [I] / K_i), y-intercept = 1 / V_{max} and x-intercept = -1 / K_m (1 + [I] / K_i). The intersection of lines which varies in [I] should intersect on the y-axis.

In non-competitive inhibition, the inhibitor binds to the free enzyme at a site away from the active site. It can also bind to the enzyme-substrate complex to form the enzyme-substrate-inhibitor complex. It is assumed that the dissociation of substrate from the enzyme-substrate complex is the same as from the enzyme-substrate-inhibitor complex. From the Michaelis-Menten equation, the equation for non-competitive inhibition is represented by (Silverman, 2000):

$$v = \frac{V_{max}[S] / (1 + [I] / K_i)}{(K_m + [S])}$$

where:

[I] = concentration of inhibitor

K_i = dissociation constant of enzyme-inhibitor complex

K_m = Michaelis-Menten constant=dissociation constant of enzyme-substrate complex

In order to construct the Lineweaver-Burk plot for evaluating the mode of inhibition, this equation is converted into the double reciprocal form (Silverman, 2000):

$$1 / v = \{K_m / V_{max} (1 / [S]) + 1 / V_{max}\} (1 + [I] / K_i)$$

When 1 / v is plotted against 1 / [S] in the Lineweaver-Burk plot, slope = K_m / V_{max} (1 + [I] / K_i), y-intercept = 1 / V_{max} (1 + [I] / K_i) and x-intercept = -1 / K_m. The intersection of lines which varies in [I] should intersect on the x-axis.

In uncompetitive inhibition, inhibitor binds to the enzyme-substrate complex to form the enzyme-substrate-inhibitor complex, but it cannot bind to the free enzyme. It is assumed that the dissociation of substrate from the enzyme-substrate complex is the same as from the enzyme-substrate-inhibitor complex. From the Michaelis-Menten equation, the equation for uncompetitive inhibition is represented by (Silverman, 2000):

$$v = \frac{V_{max}[S] / (1 + [I] / K'_i)}{K_m / (1 + [I] / K'_i) + [S]}$$

where:

[I] = concentration of inhibitor

K'_i = dissociation constant of enzyme-substrate-inhibitor complex

K_m = Michaelis-Menten constant=dissociation constant of enzyme-substrate complex

In order to construct the Lineweaver-Burk plot for evaluating the mode of inhibition, this equation is converted into the double reciprocal form (Silverman, 2000):

$$1 / v = K_m / V_{max} (1 / [S]) + 1 / V_{max} (1 + [I] / K_i)$$

When 1 / v is plotted against 1 / [S] in the Lineweaver-Burk plot, slope = K_m / V_{max}, y-intercept = $1 / V_{max} (1 + [I] / K_i)$ and x-intercept = $-(1 + [I] / K_i) / K_m$. The lines of varying [I] are parallel to each other without any intersection.

In mixed inhibition, the inhibitor binds to the enzyme-substrate complex to form the enzyme-substrate-inhibitor complex, and it can also bind to the free enzyme. It possesses the characteristics of some non-competitive and some uncompetitive inhibition (Owen and Johns, 1999). In order to construct the Lineweaver-Burk plot for evaluating the mode of inhibition, the following equation is applied (Silverman, 2000):

$$1 / v = K_m / V_{max} (1 / [S]) (1 + [I] / K_i) + 1 / V_{max} (1 + [I] / K'_i)$$

where:

[I] = concentration of inhibitor

K_i = dissociation constant of enzyme-inhibitor complex

K'_i = dissociation constant of enzyme-substrate-inhibitor complex

K_m = Michaelis-Menten constant=dissociation constant of enzyme-substrate complex

When 1 / v is plotted against 1 / [S] in the Lineweaver-Burk plot, slope = $K_m / V_{max} (1 + [I] / K_i)$, y-intercept = $1 / V_{max} (1 + [I] / K'_i)$ and x-intercept = $-(1 + [I] / K'_i) / K_m (1 + [I] / K_i)$. The intersection of lines with varying [I] would not be exactly on the x-axis (Silverman, 2000). Also, the values of K_i and K'_i could be calculated accordingly.

In the present study, it was found that one of the test compounds possessed mixed type inhibition, so the equation for mixed inhibition was applied.

The XOD assay was carried out in order to evaluate the inhibitory potency of the test compounds towards XOD. The assay was performed according to the protocols as described in the Materials and methods chapter.

3.2 Results

Among the test compounds, deoxyrhapontin elicited inhibitory activity towards XOD in a dose-dependent manner. From figure 3.1, it was found that its IC_{50} value was about 114.7 μM. The IC_{50} of the positive control, allopurinol, was found to be 8.2 μM, which was similar to the value reported previously (Li *et al.*, 1999). Deoxyrhapontin was a reversible enzyme inhibitor, as shown in Figure 3.2. Moreover, the inhibitory mode of deoxyrhapontin is of the mixed type, as shown in Figure 3.3. On the other hand, other test compounds had no observable inhibitory effect at their maximum concentrations tested. The results are shown in Table 3.1. The K_i and K'_i values of deoxyrhapontin were calculated to be 72.2μM and 345.3μM respectively. The mode of inhibition of some structurally related compounds on XOD are shown in Table 3.2.

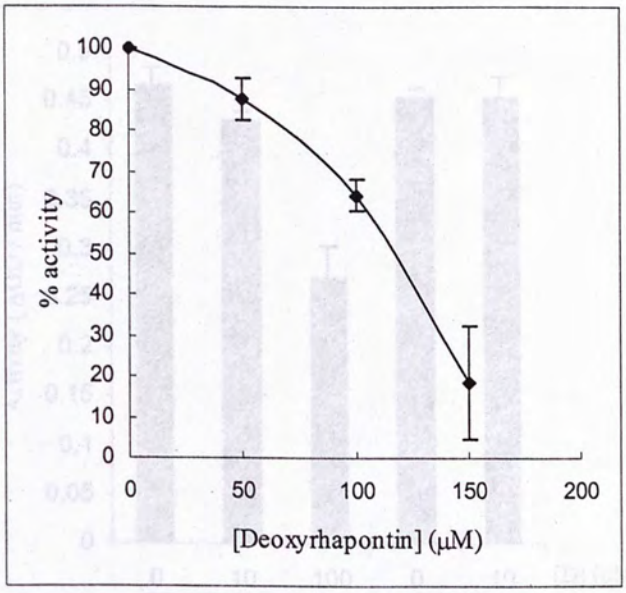

(A)

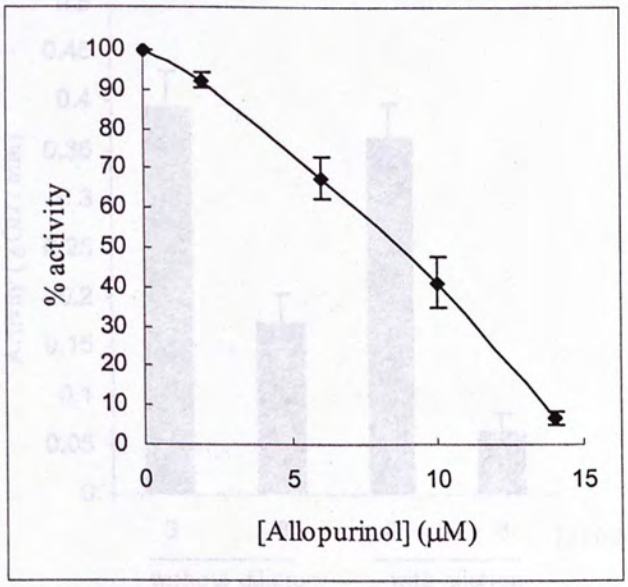

(B)

Figure 3.1 Dose-dependent inhibitory actions of deoxyrhapontin (Panel A) and allopurinol (Panel B) on XOD. The assay was conducted with 0.089U/ml XOD and 0.12mM xanthine. The extent of enzyme inhibition is expressed as percentage activity which is plotted against different concentrations of the inhibitor. Data were obtained from the average of three (for deoxyrhapontin) or four (for allopurinol) independent experiments with duplicated assays and the error bars indicate standard deviations.

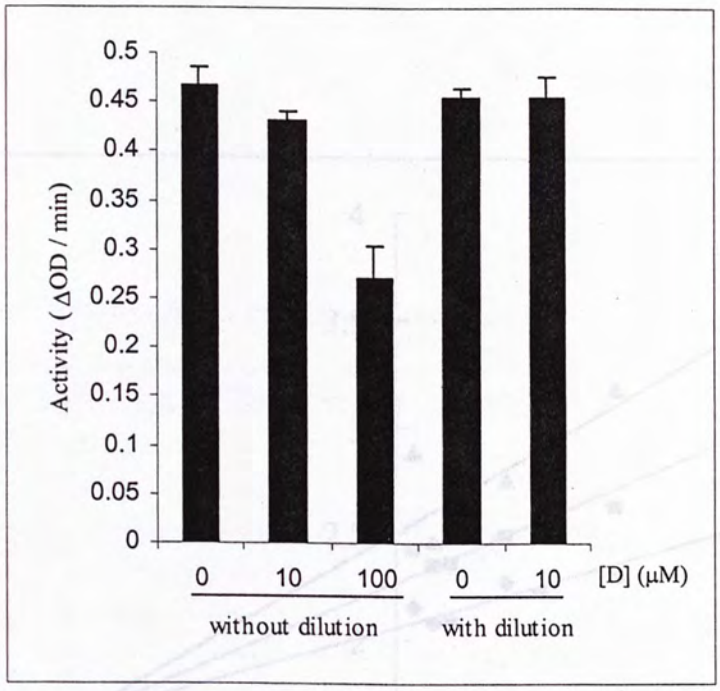

(A)

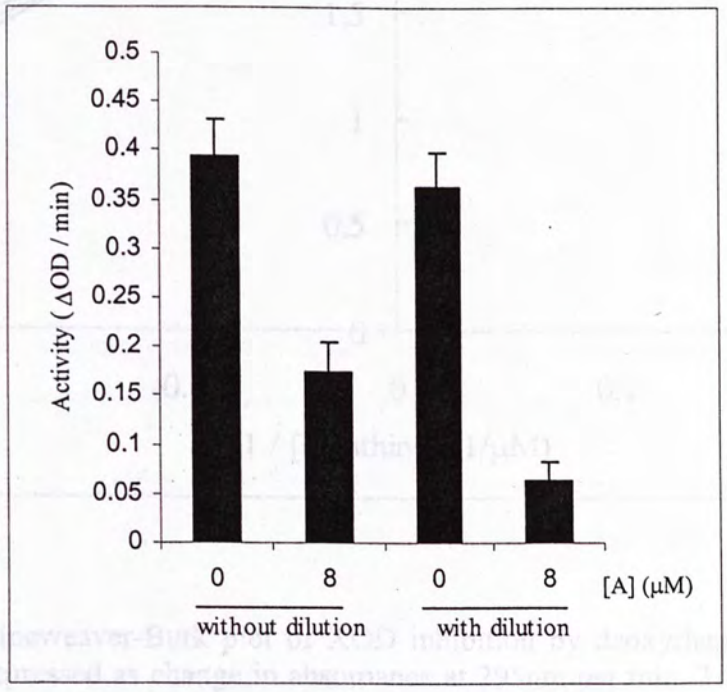

(B)

Figure 3.2 Reversibility studies of the inhibitory effects of deoxyrhapontin (Panel A) and allopurinol (Panel B) on XOD. Change in absorbance at 295nm is compared among two groups: the control and sample without dilution after incubation, the control and sample with dilution after incubation. Both groups contained same concentrations of enzyme and substrate during measurement of absorbance. Data were obtained from the average of three (for deoxyrhapontin) or four (for allopurinol) independent experiments and the error bars indicate standard deviations. D = Deoxyrhapontin, A = Allopurinol.

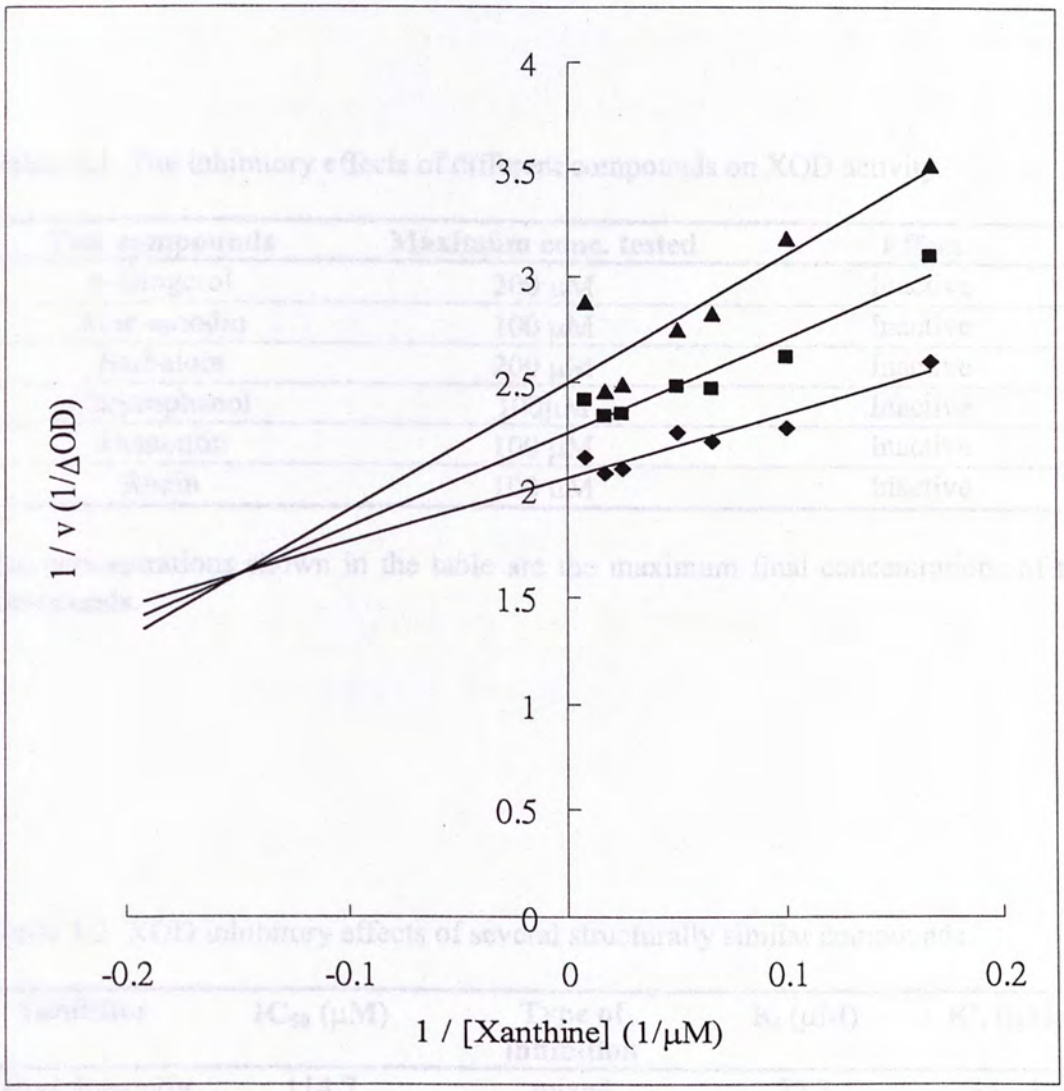

Figure 3.3 Lineweaver-Burk plot of XOD inhibition by deoxyrhapontin. Enzyme activity was expressed as change in absorbance at 295nm per min. The reciprocal of absorbance change is plotted against the reciprocal of substrate concentration. The concentrations of substrate used were 6μM, 10μM, 15μM, 20μM, 40μM, 60μM and 120μM. Each experiment consists of three conditions: control without any inhibitor (♦), in the presence of 50μM deoxyrhapontin (■), and in the presence of 70μM deoxyrhapontin (▲). The straight lines were generated by linear regression of the points. The values represent the average of duplicate experiments.

Table 3.1 The inhibitory effects of different compounds on XOD activity.

Test compounds	Maximum conc. tested	Effect
6-Gingerol	200 μM	Inactive
Aloe-emodin	100 μM	Inactive
Barbaloin	200 μM	Inactive
Chrysophanol	100μM	Inactive
Rhapontin	100 μM	Inactive
Rhein	100 μM	Inactive

The concentrations shown in the table are the maximum final concentrations of the compounds.

Table 3.2 XOD inhibitory effects of several structurally similar compounds.

Inhibitor	IC_{50} (μM)	Type of inhibition	K_i (μM)	K'_i (μM)
Deoxyrhapontin	114.7	mixed	72.2	345.3
Resveratrol	11.0	competitive	9.7	---
Piceid	66.1	competitive	14.3	---
Isorhapontin	70.0	competitive	19.1	---

Comparison of the XOD inhibitory effects of deoxyrhapontin, resveratrol, piceid and isorhapontin (Zhou *et al.*, 2001).

3.3 Discussion

As XOD plays an important role in hyperuricemia, compounds with inhibitory activities on this enzyme would be able to alleviate the pathologic conditions in hyperuricemic patients. Deoxyrhapontin elicited inhibitory activity on XOD, but rhapontin (which is structurally similar) as well as other test compounds did not. The IC_{50} value of deoxyrhapontin is larger than allopurinol, meaning that deoxyrhapontin is less potent than allopurinol. Moreover, a Lineweaver-Burk plot was drawn on the deoxyrhapontin inhibition to evaluate the mode of inhibition. Deoxyrhapontin was found to be a mixed inhibitor, since the Lineweaver-Burk plots of its inhibition on XOD intersect on the left of the 1/v axis and above the 1/[S] axis (Figure 3.3). Therefore, deoxyrhapontin belongs to the mixed type inhibition in which $K'_i > K_i$.

In the reversibility assay, the activity of XOD was restored after dilution in the presence of deoxyrhapontin. In the case of allopurinol, the enzyme activity was not restored. These results revealed that deoxyrhapontin is a reversible inhibitor, whereas allopurinol is not (Hotter *et al.*, 1994). In other words, the inhibitory effect of deoxyrhapontin can be eliminated when the inhibitor is removed, so the enzyme becomes active again. Nevertheless, the inhibitory effect of allopurinol remains upon dilution.

Structure-activity relationship was compared among deoxyrhapontin, rhapontin and other structurally-related compounds, in order to understand their difference in effects. Resveratrol and isorhapontin are two of the stilbenoids isolated from *Veratrum taliense* (Liliaceae). They are competitive inhibitors of XOD and they possess similar

structures with deoxyrhapontin and rhapontin (Zhou *et al.*, 2001). By comparing the potency of the compounds, it was found that the one with the highest inhibitory ability is resveratrol, followed by piceid, isorhapontin and deoxyrhapontin, whereas rhapontin has no effect at all. The IC_{50} values of resveratrol, piceid and isorhapontin have been reported to be 11μM, 66.1μM and 70μM respectively (Zhou *et al.*, 2001), which is lower than the determined value for deoxyrhapontin, 114.7μM, in the present study. Moreover, allopurinol was used as the positive control in the study of Zhou *et al.*, 2001 and the present study. The IC_{50} values of allopurinol obtained in both studies were similar. The structures of the compounds were inspected. The compounds differ in their inhibitory actions despite their high degree of structural similarity, possibly due to the presence of different functional groups and their positional variation on the benzene ring.

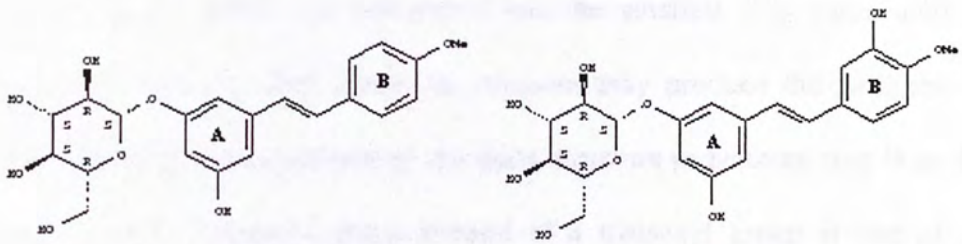

Deoxyrhapontin

Rhapontin

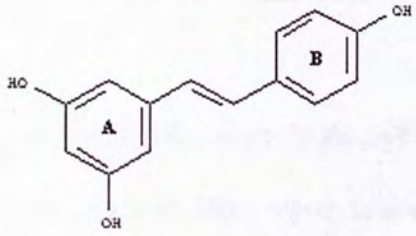

Resveratrol

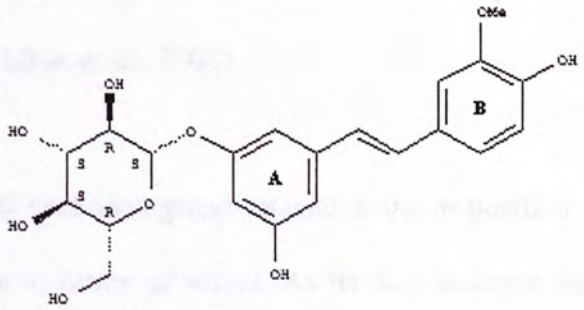

Isorhapontin

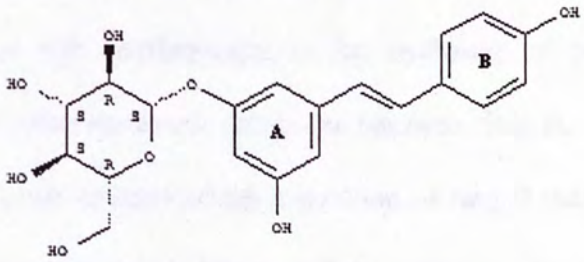

Piceid

Figure 3.4 Chemical structures of deoxyrhapontin, rhapontin and their analogs.

For resveratrol, its hydroxyl groups are located at the *para (p)* position in benzene ring B and the *meta (m)* positions in benzene ring A. Delocalization of electrons between the lone pair electrons of the phenoxyl oxygen and π electrons in the benzene ring occurs and the compound becomes electron-rich. This may enable the compound to interact with the molybdenum active center of the enzyme (Medvedev *et al.*, 1995;

Stupans and Ryan, 1984). As resveratrol has the smallest IC_{50} value among the compounds (Table 3.2), that means its structure may produce the strongest XOD inhibition. Although piceid possesses the same structure in benzene ring B as that in resveratrol, it has a glucosyl group instead of a hydroxyl group at one of the *m* position of benzene ring A. It is less potent than resveratrol. This shows that glycosylation may make the compound bulky and reduces its inhibitory ability (Chang *et al.*, 1994; Chan *et al.*, 1995; Zhou *et al.*, 2001).

For isorhapontin, there is an additional methoxyl group located at the *m* position of benzene ring B when compared to the structure of piceid. As its IC_{50} is larger than piceid, it implies that addition of methoxyl group may decrease the inhibition potency of the compound (Chang *et al.*, 1994; Chan *et al.*, 1995). For rhapontin, its only structural difference with isorhapontin is the exchange of position between the methoxyl group and the hydroxyl group on benzene ring B. The hydroxyl group located at the *m* position instead of the *p* position of ring B may decrease inhibitory effect. For deoxyrhapontin, it only has a methoxyl group on the *p* position of benzene ring B. It has a similar structure to rhapontin, the only difference is the absence of a hydroxyl group at the *m* position, but it has a higher inhibitory activity than rhapontin. Deoxyrhapontin and rhapontin possess lower inhibition potency than the other three compounds, showing that methylation of hydroxyl group at the *p* position may decrease inhibitory activity (Shin *et al.*, 1998; Kim *et al.*, 2002).

As shown in the IC_{50} values of resveratrol and other stilbenes, the numbers and position of hydroxyl groups are essential for the XOD inhibitory activities of the stilbenes. Hydroxyl group possesses a higher electron-donating property than

methoxyl group or glucosyl group. Stronger electron delocalization is achieved in resveratrol than in piceid, as the stronger electron-donating hydroxyl group is present at the *m* position of benzene ring A instead of a glucosyl group. Moreover, the presence of the *m*-hydroxyl group on benzene ring B of rhapontin instead of the *p*-hydroxyl group in isorhapontin may decrease its electron density, as delocalization of electrons between the lone pair electrons of oxygen and the π electrons of the benzene ring is weaker comparatively. This may be due to the spatial arrangement of oxygen atom at the *m* position which is unable to exert maximum electron delocalization as it is in the *p* position. A higher electron density may be present in deoxyrhapontin as compared to rhapontin. The additional hydroxyl group at the *m* position of benzene ring B of rhapontin may decrease the potency as it does not contribute to the increase of electron density. It reduces the electron density instead due to counteraction with the hydroxyl group at the *m* position of benzene ring A. As a result, rhapontin has the least inhibitory effect. Furthermore, the anthraquinones did not exhibit XOD inhibitory effects in the present study, this agrees with the results of a similar study in the past (Sheu and Chiang, 1997).

Further *in vivo* studies and clinical trials are required to evaluate the potential of deoxyrhapontin and other stilbenoids in treating hyperuricemia.

Chapter 4 Lipid peroxidation inhibition in mouse liver microsomes: results and discussion

4.1 Introduction

Lipid is an important component of cell membranes. Free radicals produced by either natural physiological reactions or unnatural chemical reactions such as radiation may cause lipid peroxidation of the membrane. This chapter aims at evaluating the effectiveness of the test compounds in the prevention of lipid peroxidation. The assay was performed according to the protocols described in the Materials and methods chapter.

4.2 Results

Figure 4.1 shows the results of trolox as the positive control. Its IC_{50} was determined to be 82.9μM. Among the test compounds, 6-gingerol and rhapontin possessed inhibitory effects towards lipid peroxidation in a dose-dependent manner. Figure 4.2 shows the effect of 6-gingerol. Its IC_{50} was found to be 66.3μM. Figure 4.3 shows the results of rhapontin. Its IC_{50} was determined to be 154.8μM. Other test compounds did not exhibit any positive effects at their maximum final concentrations used (Table 4.1). The relative potencies of the test compounds with positive effects in comparison to trolox are shown in Table 4.2.

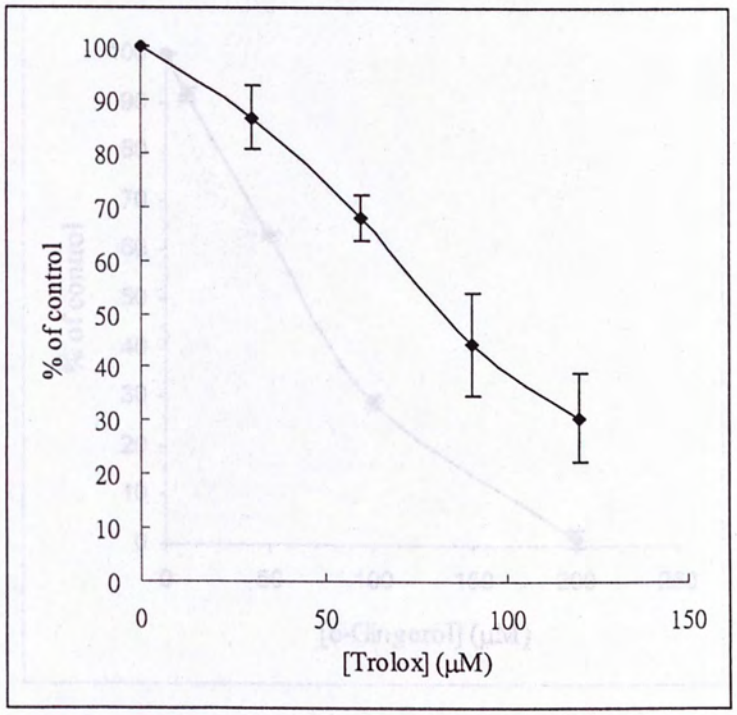

Figure 4.1 The inhibitory effect of trolox on mouse liver microsomal lipid peroxidation. In the assay, 0.01mM $FeSO_4$ and 0.1mM ascorbic acid were applied in the absence (control) or presence of various concentrations of trolox. Results are expressed as percentage of control. Data represent mean ± S.D. in two independent experiments.

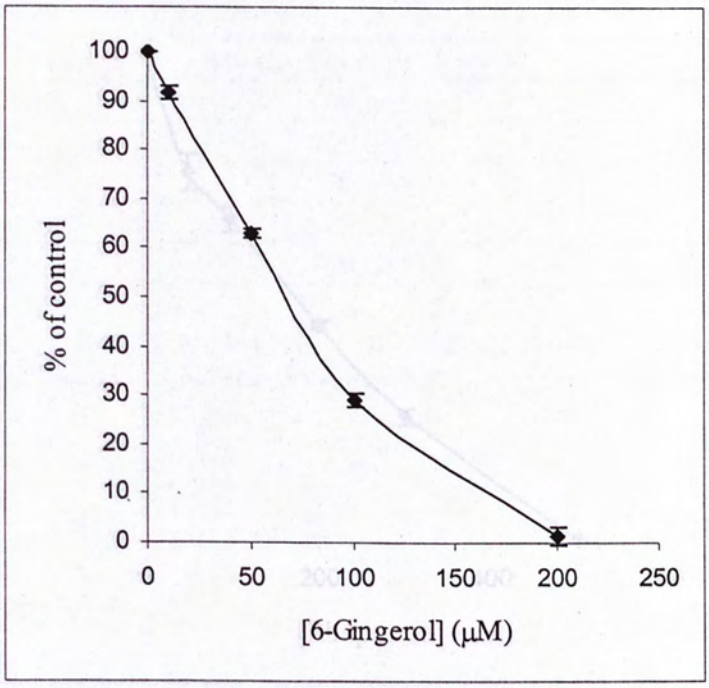

Figure 4.2 The inhibitory effect of 6-gingerol on mouse liver microsomal lipid peroxidation. In the assay, 0.01mM $FeSO_4$ and 0.1mM ascorbic acid were applied in the absence (control) or presence of various concentrations of 6-gingerol. Results are expressed as percentage of control. Data represent mean ± S.D. in four independent experiments.

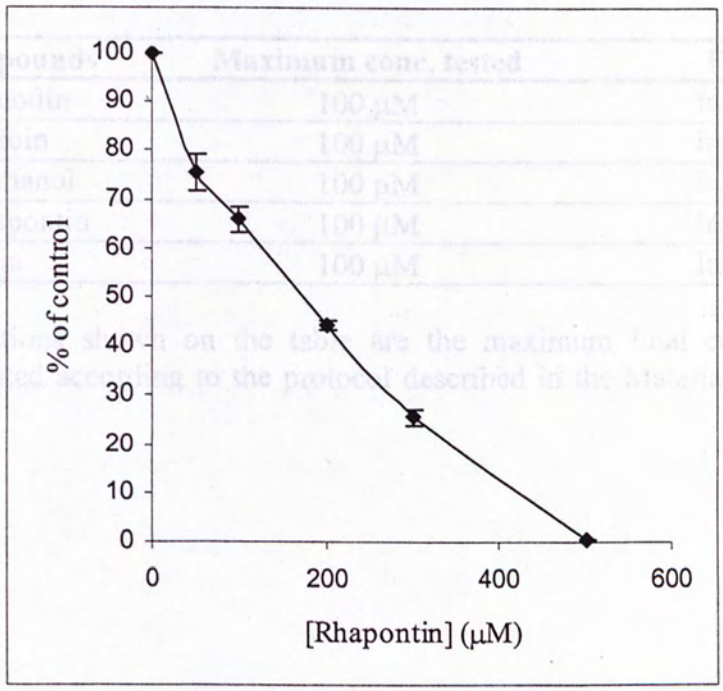

Figure 4.3 The inhibitory effect of rhapontin on mouse liver microsomal lipid peroxidation. In the assay, 0.01mM $FeSO_4$ and 0.1mM ascorbic acid were applied in the absence (control) or presence of various concentrations of rhapontin. Results are expressed as percentage of control. Data represent mean ± S.D. of four independent experiments.

Table 4.1 The inhibitory effects of different compounds on mouse liver microsomal lipid peroxidation.

Test compounds	Maximum conc. tested	Effect
Aloe-emodin	100 μM	Inactive
Barbaloin	100 μM	Inactive
Chrysophanol	100 μM	Inactive
Deoxyrhapontin	100 μM	Inactive
Rhein	100 μM	Inactive

The concentrations shown on the table are the maximum final concentration of compounds tested according to the protocol described in the Materials and methods chapter.

Table 4.2 The relative potencies of test compounds on the inhibition of mouse liver microsomal lipid peroxidation.

Test compounds	IC_{50}	Relative potency
Trolox	82.9 μM	1
6-Gingerol	66.3 μM	1.25
Rhapontin	154.8 μM	0.54

Their IC_{50} values are compared against trolox, which is the positive control. Relative potency = IC_{50} of trolox / IC_{50} of test compound.

4.3 Discussion

After examining the XOD inhibitory effects on the test compounds, we proceeded to study the compounds' ability to protect against lipid peroxidation. Mouse liver microsome acts as a lipid source in the assay. This assay investigates the ability of the compounds to protect the cell membrane from being oxidized. In the presence of Fe^{2+} which is a transition metal ion, ascorbic acid acts as a pro-oxidant (Higuchi *et al.*, 2003) and hydroxyl radicals would be formed in the presence of oxygen. This induces free radical-mediated lipid peroxidation of a liver microsomal preparation. As a result, lipid peroxides are produced due to free radical propagation (Messina *et al.*, 1991). MDA is produced as the final product of lipid peroxidation. MDA could be detected after reacting with TBA. The absorbance of the pink color adduct could be monitored colorimetrically at 532nm.

Among the test compounds, 6-gingerol and rhapontin exhibited inhibitory actions on lipid peroxidation of liver microsomes in a dose-dependent manner. Comparing the IC_{50} values of 6-gingerol and rhapontin to that of trolox, it is found that 6-gingerol is slightly more potent than trolox in inhibiting the formation of MDA whereas rhapontin appeared to be one-half as potent as trolox (Table 4.2). In other reports, 6-gingerol has been found to be four times more potent than α-tocopherol by using the ferric thiocyanate method for incubation (Kikuzaki *et al.*, 1993) and two times less potent than propyl gallate by using ox brain phospholipid liposomes as the lipid source (Aeschbach *et al.*, 1994). This assay confirms the antioxidant effect of 6-gingerol by using mouse liver microsomes as the lipid source which has never been applied before.

The antioxidative activities of 6-gingerol and rhapontin in lipid peroxidation might be related to the number and steric position of the functional groups on the compounds (Cao *et al.*, 2003). Rhapontin has a higher IC_{50} value than 6-gingerol. The presence of a bulky glucoside moiety may hinder its antioxidative activity (Matsuda *et al.*, 2000). Although 6-gingerol and rhapontin possess the same number of hydroxyl and methoxyl group at the benzene ring, the position of the constituent groups are exchanged. 6-Gingerol has a stronger effect as its hydroxyl group is located at the *p* position, enabling it to form a phenoxyl radical more readily due to a stronger resonance within the structure (Nakao *et al.*, 1998). Furthermore, the difference in the antioxidative effect of rhapontin and deoxyrhapontin may be due to the absence of a phenol group in benzene ring B for deoxyrhapontin. This renders it impossible to form a phenoxyl radical (Matsuda *et al.*, 2000). Rhapontin was able to form a stable phenoxyl radical, which might stop peroxide propagation reactions in lipids (Nakao *et al.*, 1998).

After screening the test compounds with lipid peroxidation inhibition assay of mouse liver microsomes, assays of RBC and LDL were performed to evaluate the antioxidative effect of the compounds in detail.

Chapter 5 Assays on protection of RBC from oxidative damage: results and discussion

5.1 Introduction

RBC constitute an important blood component as they contain hemoglobin and carry oxygen. Their life span lasts for about 120 days (Surgenor, 1974). Any abnormal hemolysis may cause serious diseases. No matter hemolysis is caused by congenital or noncongenital defects, protection of RBC from lysis would benefit the patients.

AAPH has been employed as a common free radical inducer in many oxidative stress systems. It is also applied for AAPH-induced hemolysis inhibition assay and LDL lipid peroxidation inhibition assay in the present investigation.

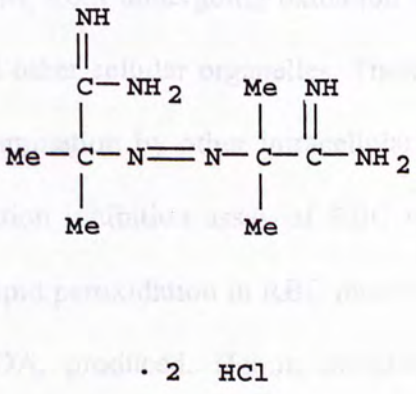

Chemical structure of AAPH.

The formation of AAPH peroxyl radical was responsible for inducing oxidative damage in biological systems. The AAPH-induced hemolysis inhibition assay is

performed to evaluate the protective abilities of the test compounds towards RBC lysis. In the assay, carbon-centered radicals ($R^{\bullet}$) derived from AAPH (R—N=N—R) attack RBC to induce hemolysis (Ou *et al.*, 2002).

$$R—N=N—R \longrightarrow 2R^{\bullet} + N_2$$

AAPH could produce peroxyl radicals ($ROO^{\bullet}$) to induce the formation of lipid radicals ($L^{\bullet}$ and $LOO^{\bullet}$) which are the lipid peroxidation intermediates on cell membranes. Lipid peroxides (LOOH) are formed from lipids (LH) (Ou *et al.*, 2002).

$$R^{\bullet} + O_2 \longrightarrow ROO^{\bullet}$$

$$ROO^{\bullet} + LH \longrightarrow ROOH + L^{\bullet}$$

$$L^{\bullet} + O_2 \longrightarrow LOO^{\bullet}$$

$$LOO^{\bullet} + LH \longrightarrow LOOH + L^{\bullet}$$

Apart from assessing the compounds' protective ability towards AAPH-induced hemolysis, it is essential to observe whether the test compounds prevent the major membrane component, lipid, from undergoing oxidation reaction. RBC do not have nucleus, mitochondria and other cellular organelles. Therefore, their membranes can be prepared without contamination by other intracellular organelles (Alberts *et al.*, 1994). The lipid peroxidation inhibition assay of RBC membrane was designed to investigate the degree of lipid peroxidation in RBC membrane by the amount of lipid peroxidation product, MDA, produced. Hemin initiates lipid peroxidation when organic peroxides such as *t*BHP are present.

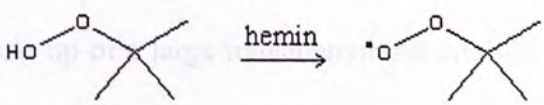

ATPase is another target apart from the membrane lipids. ATPase is a carrier protein that transports substances across the plasma membrane by reversible conformational change (Alberts *et al.*, 1994). Ion transport is done by exposing the binding site on both sides of the membrane alternatively. ATPase controls ion permeability across the membrane at the expense of energy. It plays an important role in cellular structure and function. By controlling cell volume and osmotic balance, ATPase is responsible for maintaining cell integrity (Alberts *et al.*, 1994). ATPase assay is applied to investigate whether the test compounds can protect ATPase from inactivation by ROS. The RBC ATPase is thus a good diagnostic indicator as blood can be obtained easily and ATPase assay can be easily performed. The ATPase assay was therefore used to evaluate the test compounds' protective abilities in maintaining the RBC ATPase activities.

Ca^{2+}-ATPase and Na^+/K^+-ATPase are found on RBC membrane. Ca^{2+} ion is transported by Ca^{2+}-ATPase for cell signaling and Na^+ and K^+ ions are transported by Na^+/K^+-ATPase to maintain cellular osmolarity and many other cellular functions. If the test compounds could protect these ATPases, they might contribute to the protection of cell membrane integrity. Ca^{2+}-ATPase pumps Ca^{2+} ions out of the cell against a steep concentration gradient. This active transport requires energy. This explains the influx of Ca^{2+} ions and the demand of active transport for homeostasis. Alteration of intracellular level of Ca^{2+} ions affects cell signaling.

Na^+/K^+-ATPase is made up of a large transmembrane catalytic subunit in association with a small glycoprotein (Alberts *et al.*, 1994). Na^+/K^+-ATPase pumps three Na^+ ions out of the cell and two K^+ ions into the cell for each ATP molecule hydrolyzed,

keeping the cell membrane negatively charged inside and positively charged outside (Alberts *et al.*, 1994). This active transport is against the steep concentration gradients of the two ions. This explains the entrance of Na^+ ion and the demand of active transport for homeostasis. The resulting Na^+ ion concentration gradient regulate cellular osmotic balance and facilitates the uptake of useful substances including glucose into the cell.

In order to further understand the protective mechanism of the test compounds on RBC, sulfhydryl group protection assay was also performed. As sulfhydryl groups present in proteins are prone to ROS attack, this assay would enable us to observe whether the test compounds could help preserve the protein structure of RBC membrane. In addition, the reduced state of some of the sulfhydryl groups in ATPase is important for their activities. The present study would also enable us to understand whether preservation of ATPase activities by the compounds are related to their sulfhydryl group-protecting effects. All the above assays were performed according to the protocols described in the Materials and methods chapter.

5.2 Results

5.2.1 AAPH-induced hemolysis inhibition assay

Figure 5.1 shows the effect of different concentrations of AAPH on AAPH-induced hemolysis. From the results, the optimal condition for the assay was determined. Figure 5.2 shows the putative effect of vitamin C. Its IC_{50} was determined to be 120.3μM. Figure 5.3 shows the protective effect of trolox. Its IC_{50} was found to be 59.2μM. Figures 5.4, 5.5 and 5.6 show the results of 6-gingerol, barbaloin and rhapontin respectively. The IC_{50} of 6-gingerol was determined to be 95.3μM, barbaloin 31.7μM, and rhapontin 31.9μM. Other test compounds did not exhibit any statistically significant protective effects towards RBC at their highest concentrations tested. The results are shown in Table 5.1. The relative potencies of the test compounds are shown in Table 5.2.

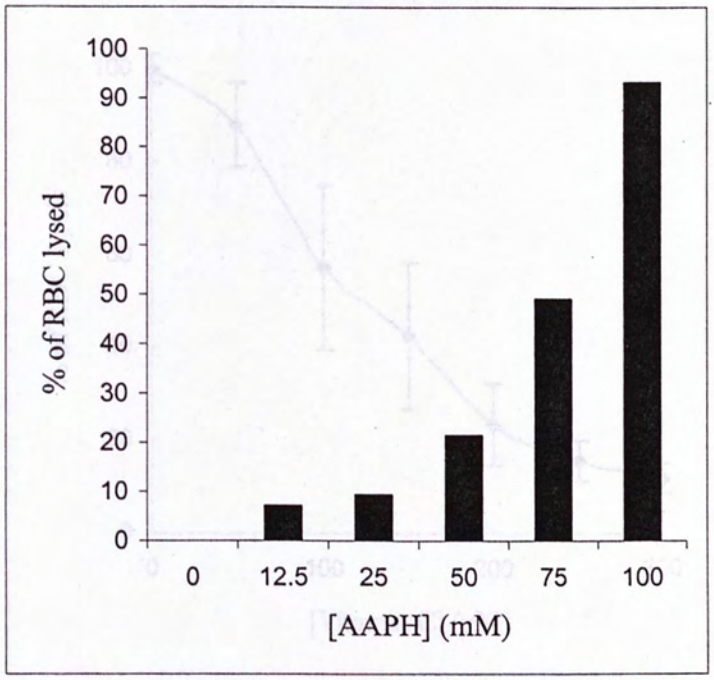

Figure 5.1 The dose-dependent AAPH-induced hemolysis. This is a preliminary experiment for obtaining the appropriate concentration of AAPH to be applied in subsequent assays. Results are expressed as the percentage of RBC lysed.

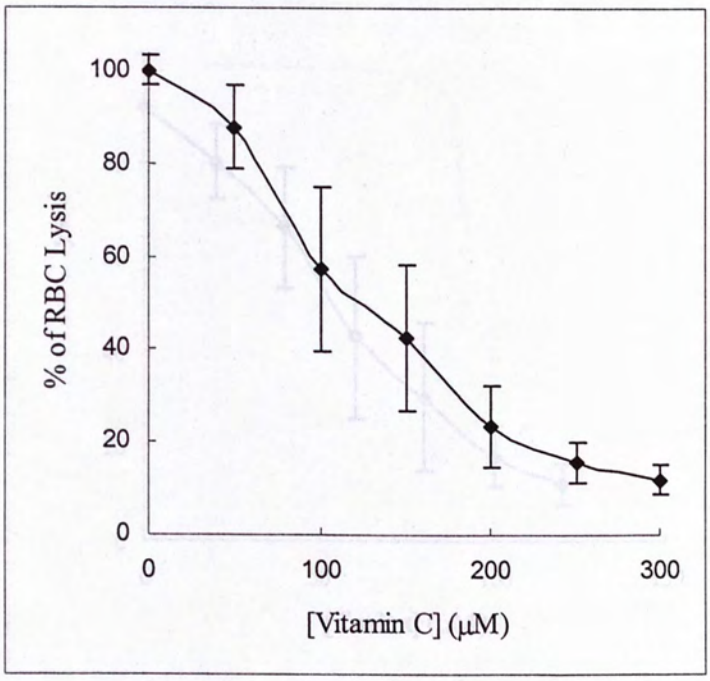

Figure 5.2 The inhibitory effect of vitamin C on AAPH-induced hemolysis. The assay was conducted with 100mM AAPH, in the absence (control) or presence of various concentrations of vitamin C. Results are expressed as the percentage of RBC lysed. Data represent mean ± S.D. of duplicate assays in four independent experiments.

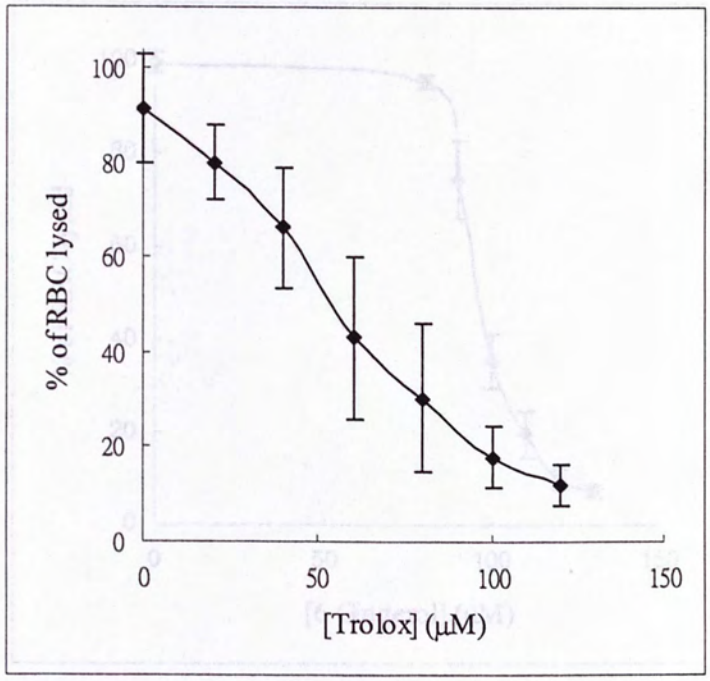

Figure 5.3 The inhibitory effect of trolox on AAPH-induced hemolysis. The assay was conducted with 100mM AAPH, in the absence (control) or presence of various concentrations of trolox. Results are expressed as the percentage of RBC lysed. Data represent mean ± S.D. of duplicate assays in four independent experiments.

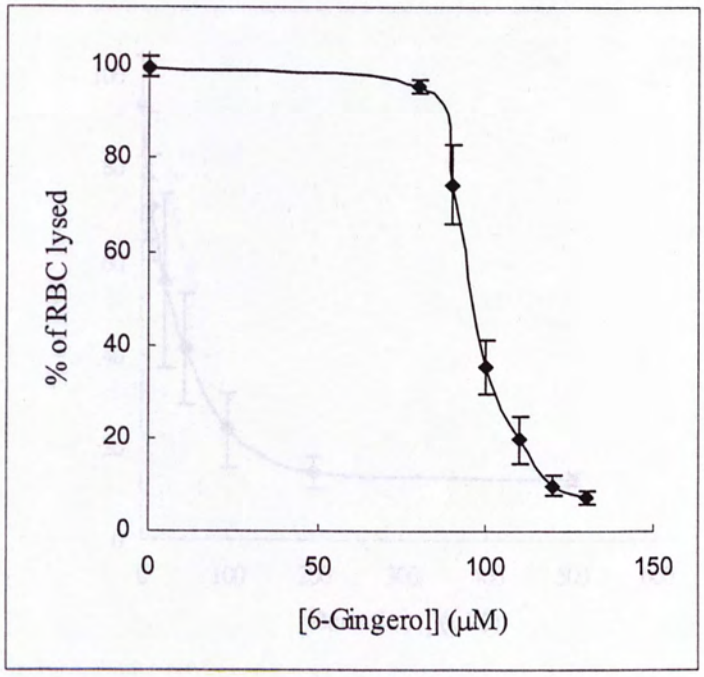

Figure 5.4 The inhibitory effect of 6-gingerol on AAPH-induced hemolysis. The assay was conducted with 100mM AAPH, in the absence (control) or presence of various concentrations of 6-gingerol. Results are expressed as the percentage of RBC lysed. Data represent mean ± S.D. of four independent experiments.

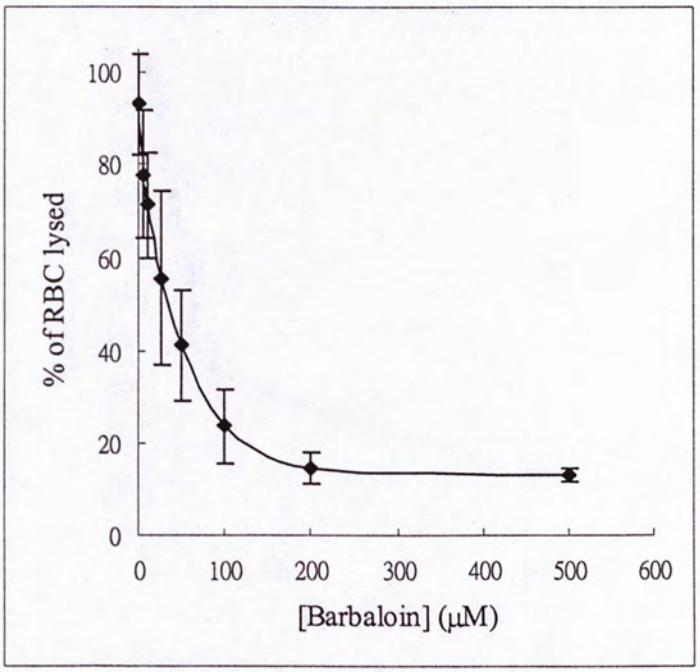

Figure 5.5 The inhibitory effect of barbaloin on AAPH-induced hemolysis. The assay was conducted with 100mM AAPH, in the absence (control) or presence of various concentrations of barbaloin. Results are expressed as the percentage of RBC lysed. Data represent mean ± S.D. of four independent experiments.

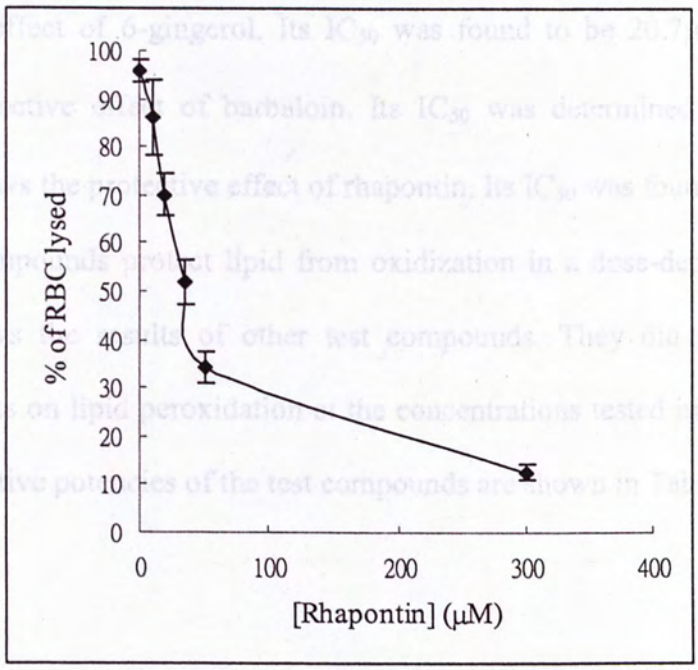

Figure 5.6 The inhibitory effect of rhapontin on AAPH-induced hemolysis. The assay was conducted with 100mM AAPH, in the absence (control) or presence of various concentrations of rhapontin. Results are expressed as the percentage of RBC lysed. Data represent mean ± S.D. of four independent experiments.

5.2.2 Lipid peroxidation inhibition assay of RBC membranes

Figure 5.7 shows the effect of hemin on RBC membrane lipid peroxidation. From the results, the optimal assay condition was determined. Figure 5.8 demonstrates the protective effect of trolox. Its IC_{50} was determined to be 224.4μM. Figure 5.9 shows the protective effect of 6-gingerol. Its IC_{50} was found to be 20.7μM. Figure 5.10 shows the protective effect of barbaloin. Its IC_{50} was determined to be 71.0μM. Figure 5.11 shows the protective effect of rhapontin. Its IC_{50} was found to be 38.3μM. These three compounds protect lipid from oxidization in a dose-dependent manner. Table 5.3 shows the results of other test compounds. They did not exhibit any inhibitory effects on lipid peroxidation at the concentrations tested in the presence of hemin. The relative potencies of the test compounds are shown in Table 5.4.

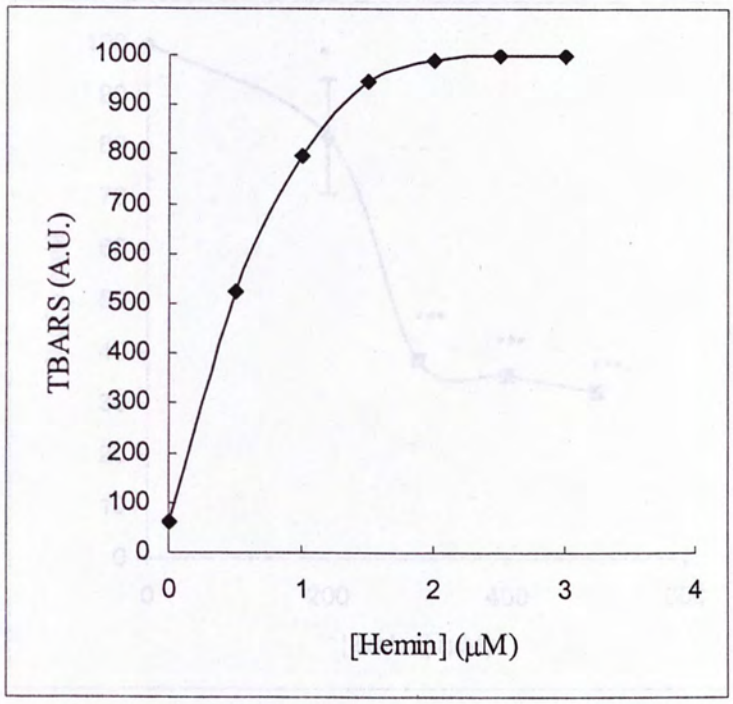

Figure 5.7 The effect of hemin on RBC membrane lipid peroxidation. This is a preliminary experiment for obtaining the appropriate concentration of hemin to be applied in subsequent assays. Various concentrations of hemin were applied in the presence of 0.5mM *t*BHP with 4 h of incubation. Results are expressed as the fluorescent unit of TBARS produced in one experiment. A.U. = arbitary unit.

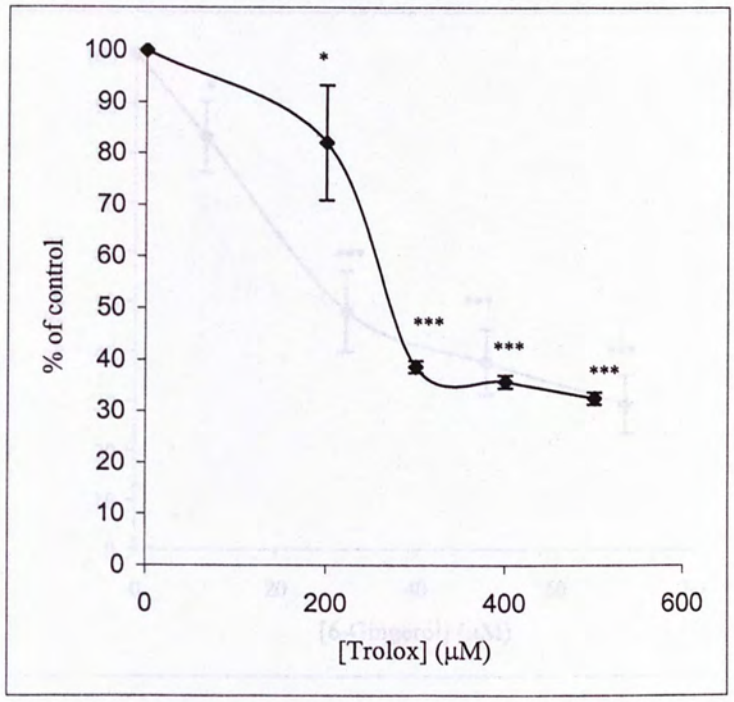

Figure 5.8 The inhibitory effect of trolox on lipid peroxidation of RBC membrane. The assay was conducted with 0.5mM *t*BHP and 1.5μM hemin, in the absence (control) or presence of various concentrations of trolox. Results are expressed as the percentage of control. Data represent mean ± S.D. in three independent experiments. The results were compared to the control with oxidative damage by one-way ANOVA followed by Dunnett's test. *, $p < 0.05$; ***, $p < 0.001$.

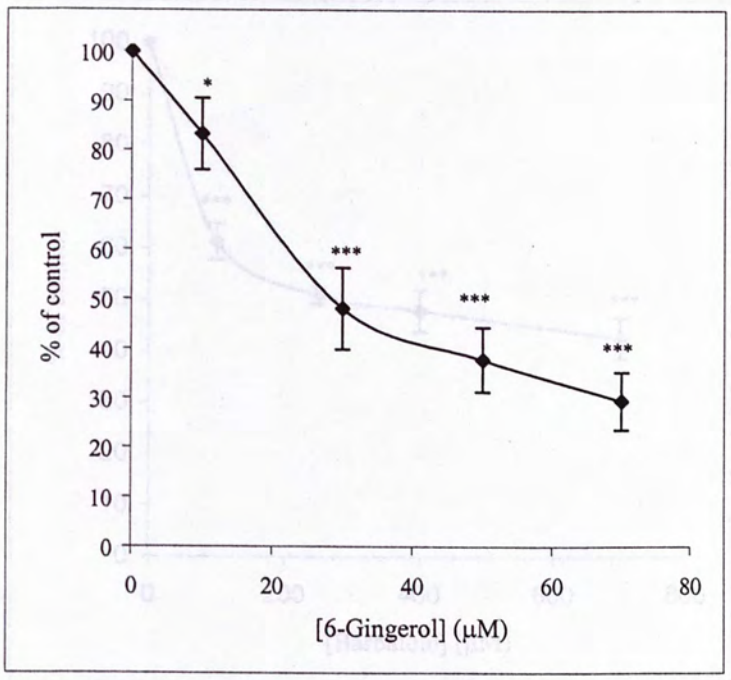

Figure 5.9 The inhibitory effect of 6-gingerol on lipid peroxidation of RBC membrane. The assay was conducted with 0.5mM *t*BHP and 1.5μM hemin, in the absence (control) or presence of various concentrations of 6-gingerol. Results are expressed as the percentage of control. Data represent mean ± S.D. in four independent experiments. The results were compared to the control with oxidative damage by one-way ANOVA followed by Dunnett's test. *, $p < 0.05$; ***, $p < 0.001$.

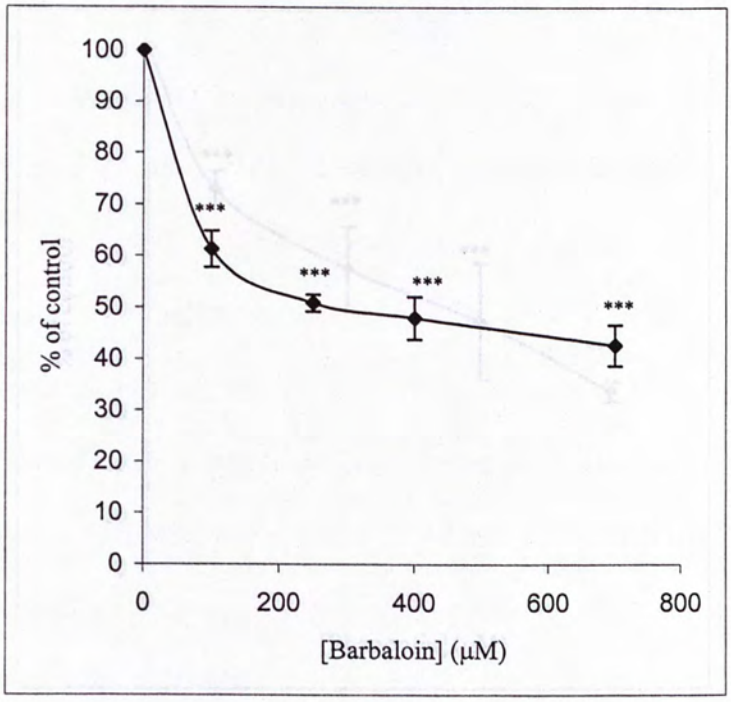

Figure 5.10 The inhibitory effect of barbaloin on lipid peroxidation of RBC membrane. The assay was conducted with 0.5mM *t*BHP and 1.5μM hemin, in the absence (control) or presence of various concentrations of barbaloin. Results are expressed as the percentage of control. Data represent mean ± S.D. in four independent experiments. The results were compared to the control with oxidative damage by one-way ANOVA followed by Dunnett's test. ***, $p < 0.001$.

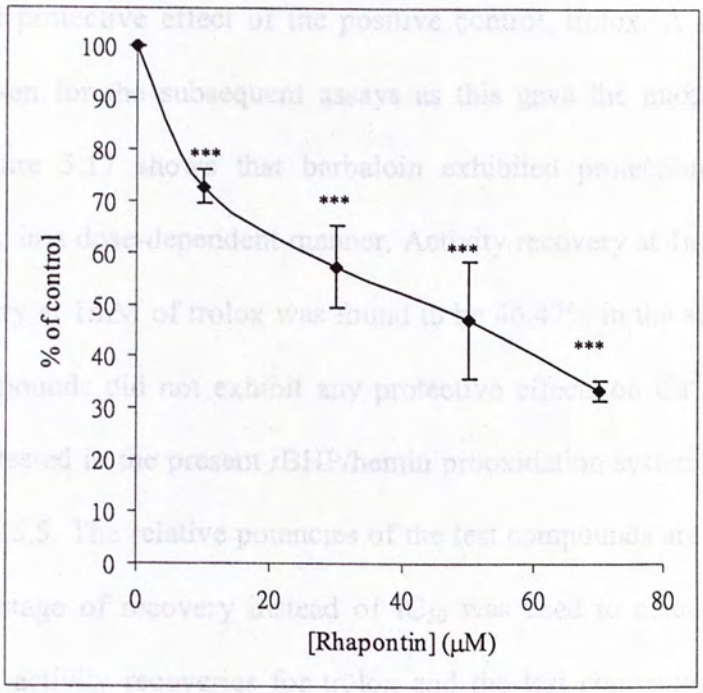

Figure 5.11 The inhibitory effect of rhapontin on lipid peroxidation of RBC membrane. The assay was conducted with 0.5mM *t*BHP and 1.5μM hemin, in the absence (control) or presence of various concentrations of rhapontin. Results are expressed as the percentage of control. Data represent mean ± S.D. in four independent experiments. The results were compared to the control with oxidative damage by one-way ANOVA followed by Dunnett's test. ***, $p < 0.001$.

5.2.3 Ca^{2+}-ATPase protection assay

Figure 5.12 is the standard curve for P_i. Figures 5.13, 5.14, and 5.15 show the effect of Triton X-100, hemin and *t*BHP respectively on Ca^{2+}-ATPase activity of RBC membrane. From these results, the optimal assay conditions were determined. Figure 5.16 shows the protective effect of the positive control, trolox. A concentration of 1mM was chosen for the subsequent assays as this gave the maximum degree of protection. Figure 5.17 shows that barbaloin exhibited protection towards Ca^{2+}-ATPase activity in a dose-dependent manner. Activity recovery at 1mM was 42.30%. Activity recovery at 1mM of trolox was found to be 46.47% in the same experiment. Other test compounds did not exhibit any protective effects on Ca^{2+}-ATPase at the concentrations tested in the present *t*BHP/hemin prooxidation system. The results are shown in Table 5.5. The relative potencies of the test compounds are shown in Table 5.6. The percentage of recovery instead of IC_{50} was used to calculate the relative potencies since activity recoveries for trolox and the test compounds with positive results could hardly reach 50%.

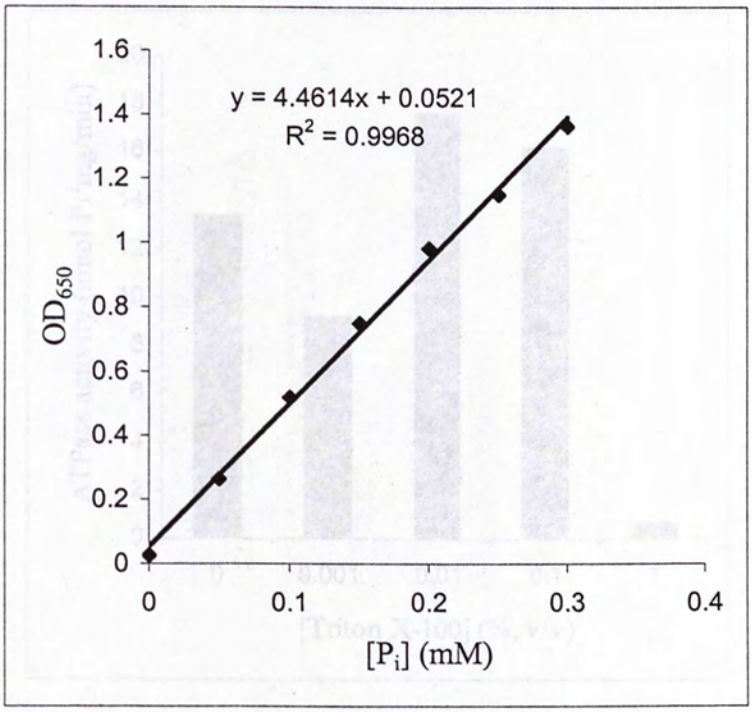

Figure 5.12 Standard curve for inorganic phosphate (P_i) determination. Different concentrations of phosphate vary with absorbance at 650nm in the ATPase assay. OD=optical density.

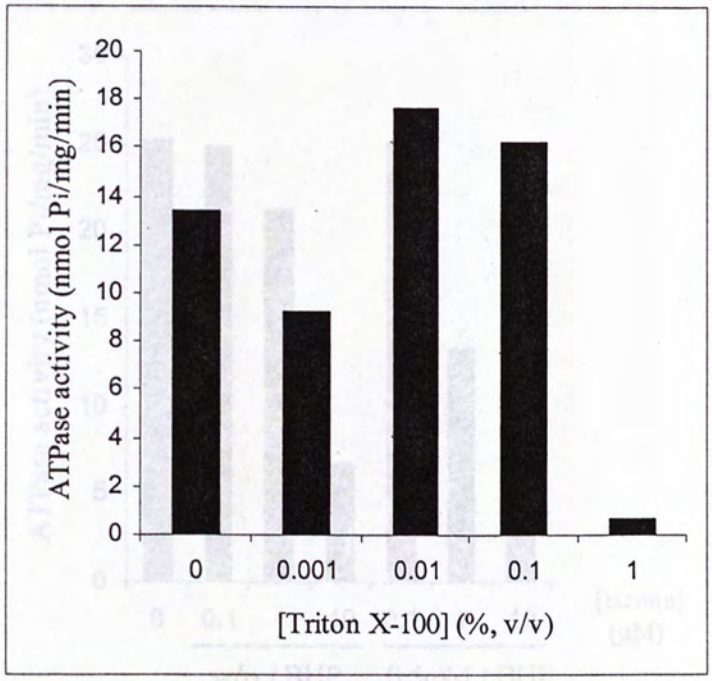

Figure 5.13 The effect of Triton X-100 on Ca^{2+}-ATPase activity of RBC membrane. This is a preliminary experiment for obtaining the appropriate concentration of TritonX-100 to be applied in subsequent assays. Triton X-100 was applied in the resuspension buffer of the assay. Results are expressed as ATPase activity unit in nmol P_i/mg/min in one experiment.

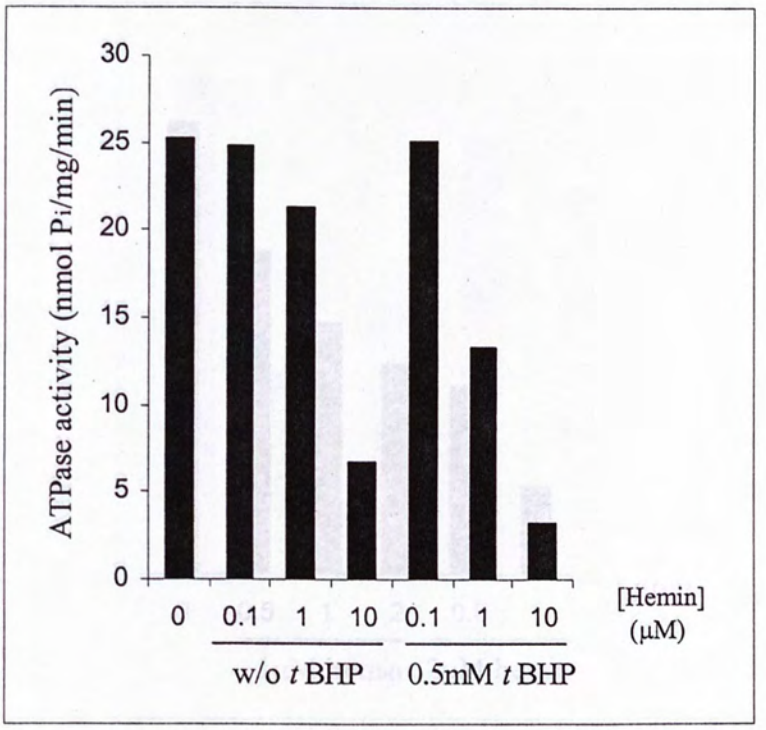

Figure 5.14 The effect of hemin on Ca^{2+}-ATPase activity of RBC membrane. This is a preliminary experiment for obtaining the appropriate concentration of hemin to be applied in subsequent assays. Various concentrations of hemin were applied in the absence or presence of 0.5mM *t*BHP. Results are expressed as ATPase activity unit in nmol P_i/mg/min in one experiment.

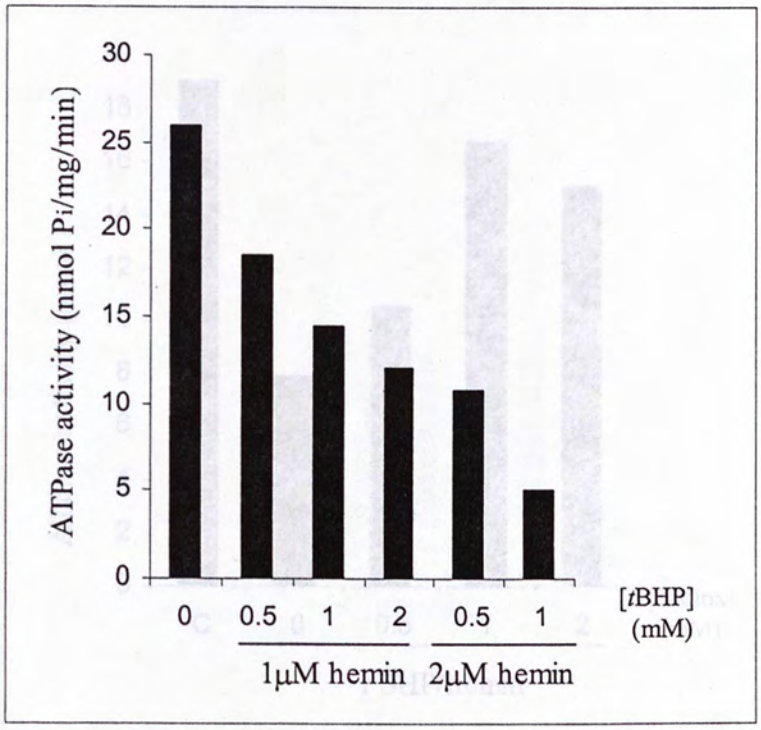

Figure 5.15 The effect of *t*BHP on Ca^{2+}-ATPase activity of RBC membrane. This is a preliminary experiment for obtaining the appropriate concentration of *t*BHP to be applied in subsequent assays. The assay was conducted with 1μM and 2μM hemin, in the absence or presence of various concentrations of *t*BHP. Results are expressed as ATPase activity unit in nmol P_i/mg/min in one experiment.

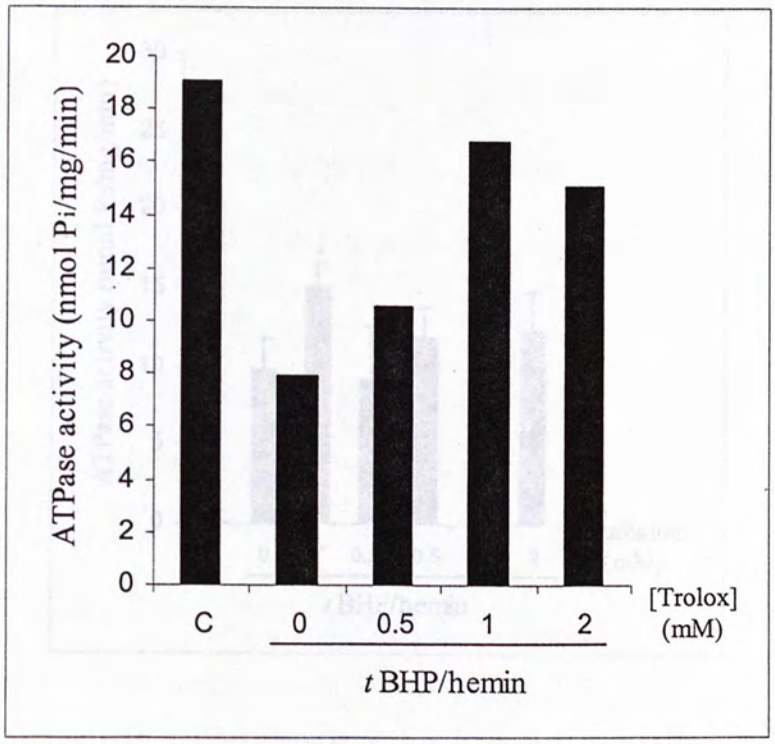

Figure 5.16 The protective effect of trolox on Ca^{2+}-ATPase activity against oxidative damage on RBC membrane. This is a preliminary experiment for obtaining the appropriate concentration of trolox to be applied in subsequent assays. The assay was conducted with 0.5mM *t*BHP and 2μM hemin, in the absence (control) or presence of various concentrations of trolox. Results are expressed as ATPase activity unit in nmol P_i/mg/min in one experiment. C = control without test compound.

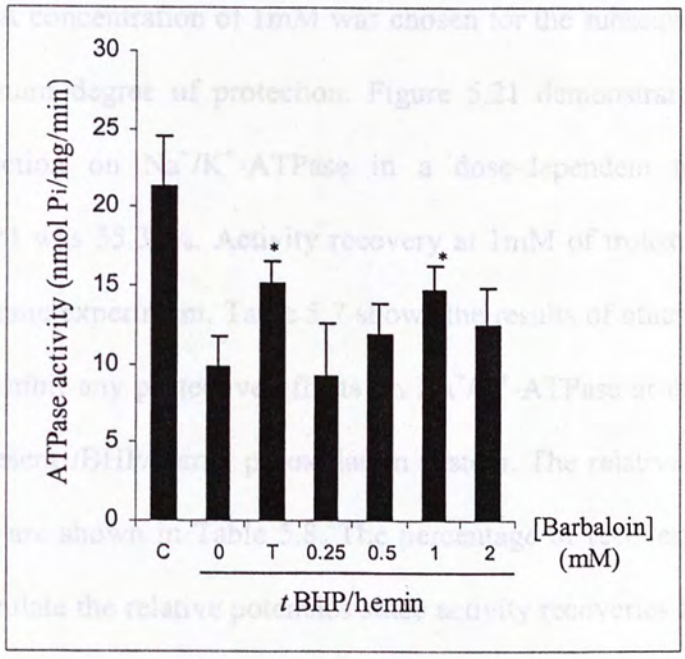

Figure 5.17 The protective effect of barbaloin on Ca^{2+}-ATPase activity against oxidative damage in RBC membrane. The assay was conducted with 0.5mM *t*BHP and 2μM hemin, in the absence (control) or presence of various concentrations of barbaloin. Results are expressed as ATPase activity unit in nmol P_i/mg/min. Data represent mean ± S.D. in four independent experiments. C = control without test compound, T = 1mM trolox. The results were compared to the negative control with oxidative damage by one-way ANOVA followed by Dunnett's test. *, $p < 0.05$.

5.2.4 Na^+/K^+-ATPase protection assay

Figures 5.18 and 5.19 show the effect of Triton X-100 and hemin respectively on Na^+/K^+-ATPase activity of RBC membrane. From these results, the optimal assay conditions were determined. Figure 5.20 shows the protective effect of the positive control, trolox. A concentration of 1mM was chosen for the subsequent assays as this gave the maximum degree of protection. Figure 5.21 demonstrates that rhapontin exhibited protection on Na^+/K^+-ATPase in a dose-dependent manner. Activity recovery at 1mM was 35.37%. Activity recovery at 1mM of trolox was found to be 55.09% in the same experiment. Table 5.7 shows the results of other test compounds. They did not exhibit any protective effects on Na^+/K^+-ATPase at the concentrations tested in the present *t*BHP/hemin prooxidation system. The relative potencies of the test compounds are shown in Table 5.8. The percentage of recovery instead of IC_{50} was used to calculate the relative potencies since activity recoveries for trolox and the test compound with positive effects could hardly reach 50%.

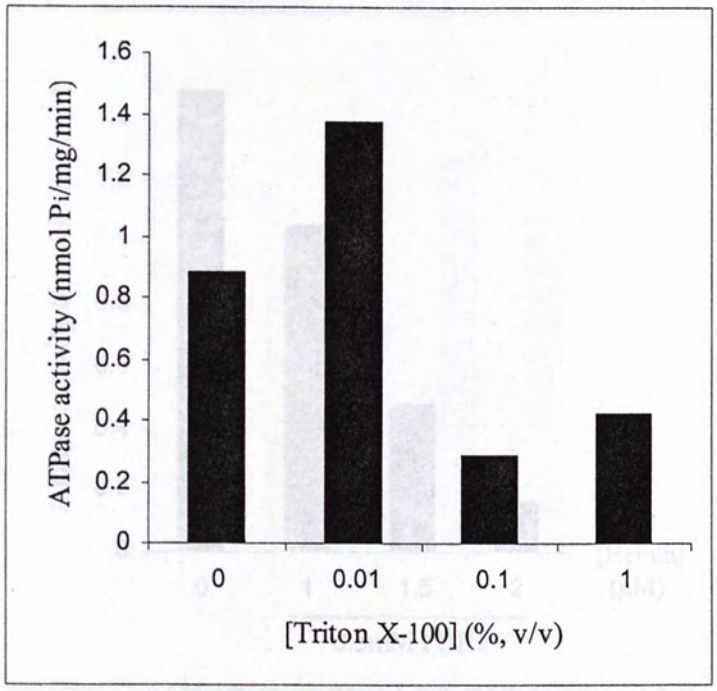

Figure 5.18 The effect of Triton X-100 on Na^+/K^+-ATPase activity of RBC membrane. This is a preliminary experiment for obtaining the appropriate concentration of Triton X-100 to be applied in subsequent assays. Triton X-100 was applied in the resuspension buffer of the assay. Results are expressed as ATPase activity unit in nmol P_i/mg/min in one experiment.

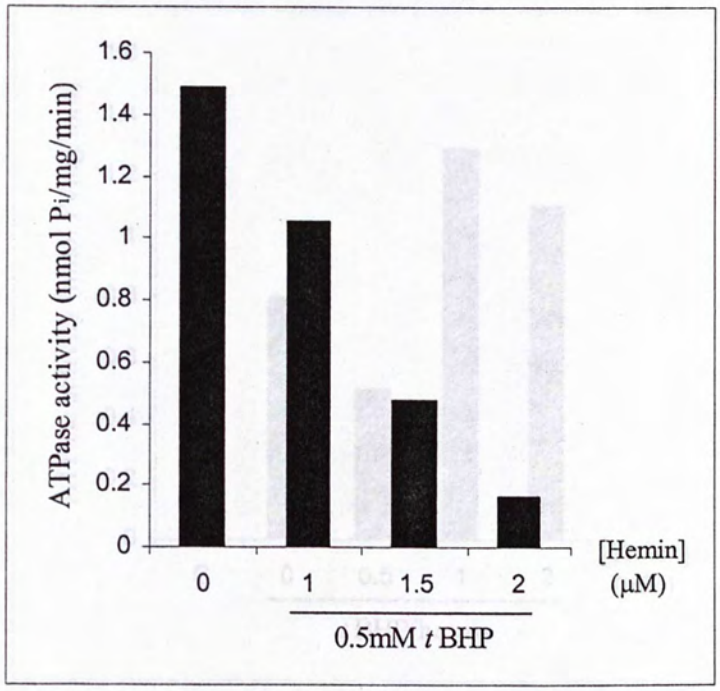

Figure 5.19 The effect of hemin on Na^+/K^+-ATPase activity of RBC membrane. This is a preliminary experiment for obtaining the appropriate concentration of hemin to be applied in subsequent assays. Various concentrations of hemin were applied in the absence or presence of 0.5mM *t*BHP. Results are expressed as ATPase activity unit in nmol P_i/mg/min in one experiment.

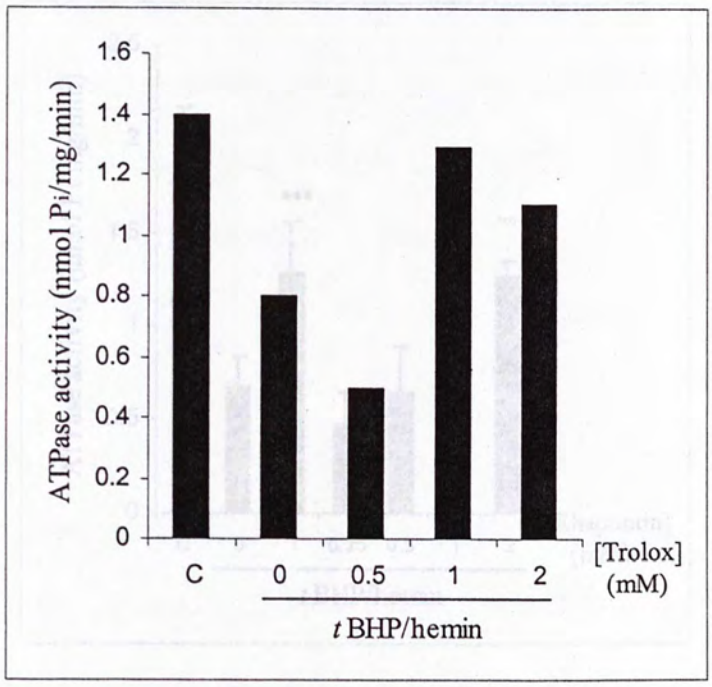

Figure 5.20 The protective effect of trolox on Na^+/K^+-ATPase activity against oxidative damage in RBC membrane. This is a preliminary experiment for obtaining the appropriate concentration of trolox to be applied in subsequent assays. The assay was conducted with 0.5mM *t*BHP and 1.5μM hemin, in the absence (control) or presence of various concentrations of trolox. Results are expressed as ATPase activity unit in nmol P_i/mg/min in one experiment. C= control without test compound.

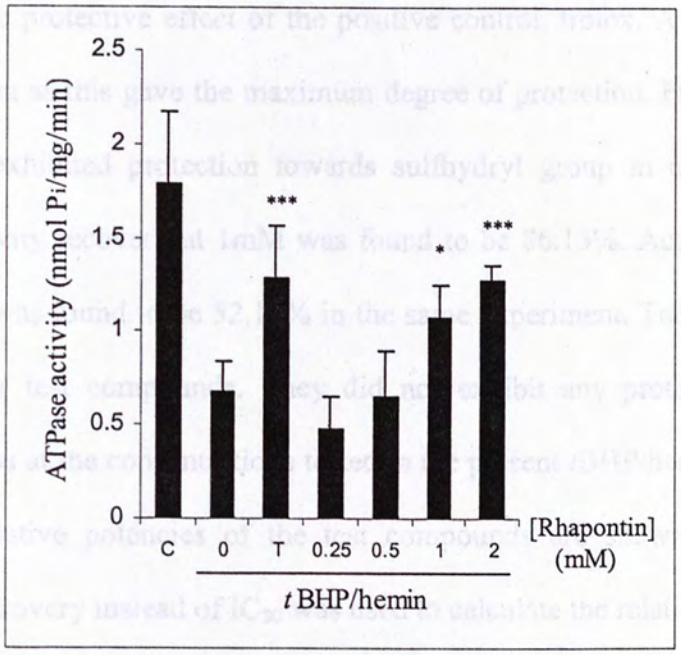

Figure 5.21 The protective effect of rhapontin on Na^+/K^+-ATPase activity against oxidative damage in RBC membrane. The assay was conducted with 0.5mM *t*BHP and 1.5μM hemin, in the absence (control) or presence of various concentrations of rhapontin. Results are expressed as ATPase activity unit in nmol P_i/mg/min. Data represent mean ± S.D. in four independent experiments. C = control without test compound, T = 1mM trolox. The results were compared to the negative control with oxidative damage by one-way ANOVA followed by Dunnett's test. *, $p < 0.05$; ***, $p < 0.001$.

5.2.5 Sulfhydryl group protection assay

Figure 5.22 shows the GSH standard curve. Figure 5.23 shows the loss of RBC membrane sulfhydryl groups in the presence of *t*BHP and varying amounts of hemin. From the results, the optimal assay conditions were determined. Figure 5.24 demonstrates the protective effect of the positive control, trolox. A concentration of 1mM was chosen as this gave the maximum degree of protection. Figure 5.25 shows that barbaloin exhibited protection towards sulfhydryl group in a dose-dependent manner. Its activity recovery at 1mM was found to be 86.13%. Activity recovery at 1mM of trolox was found to be 52.10% in the same experiment. Table 5.9 shows the results for other test compounds. They did not exhibit any protective effects on sulfhydryl groups at the concentrations tested in the present *t*BHP/hemin prooxidation system. The relative potencies of the test compounds are shown in Table 5.10. Percentage of recovery instead of IC_{50} was used to calculate the relative potency.

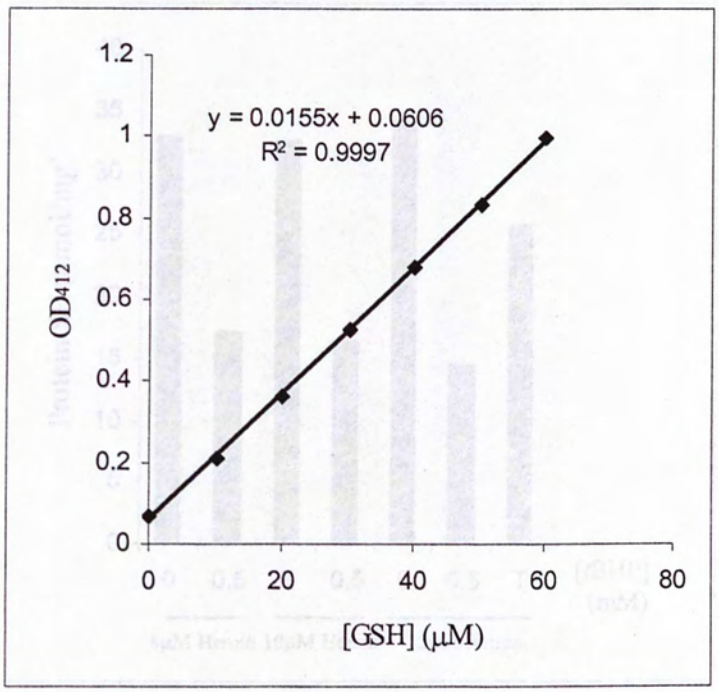

Figure 5.22 Standard curve for GSH. Different concentrations of GSH vary with absorbance at 412nm in the assay. OD = optical density.

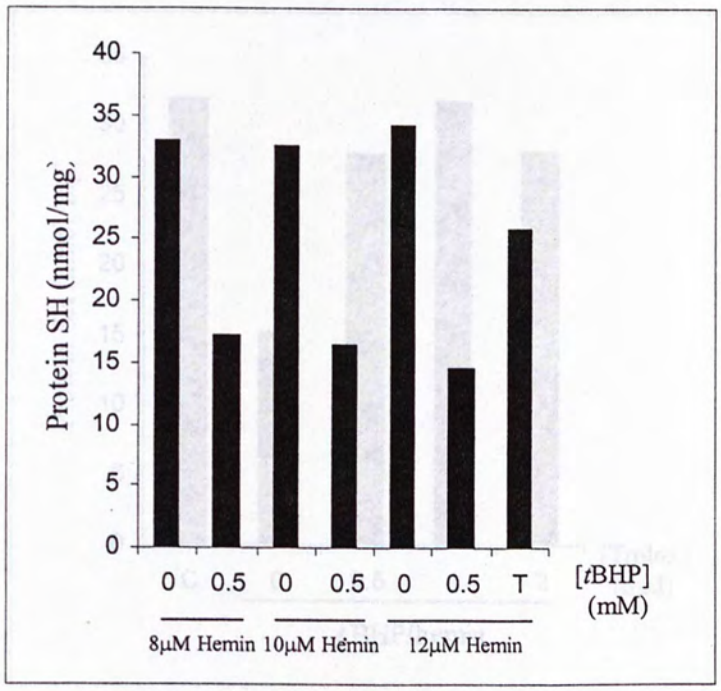

Figure 5.23 The loss of RBC membrane sulfhydryl groups in the presence of *t*BHP and varying amounts of hemin. This is a preliminary experiment for obtaining the appropriate concentration of *t*BHP to be applied in subsequent assays. Various concentrations of hemin were applied in the absence or presence of 0.5mM *t*BHP. Results are expressed as nmol SH/mg protein in one experiment. SH = sulfhydryl group, T = 1mM trolox (with 0.5mM *t*BHP).

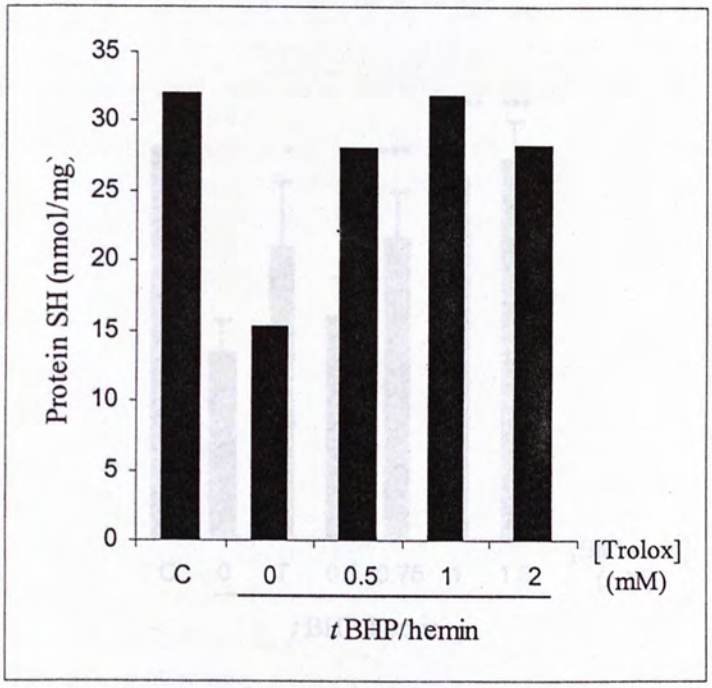

Figure 5.24 The protective effect of trolox on sulfhydryl groups against oxidative damage on RBC membrane. This is a preliminary experiment for obtaining the appropriate concentration of trolox to be applied in subsequent assays. The assay was conducted with 0.5mM *t*BHP and 10μM hemin, in the absence (control) or presence of various concentrations of trolox. Results are expressed as nmol SH/mg protein in one experiment. C= control without test compound, SH = sulfhydryl group.

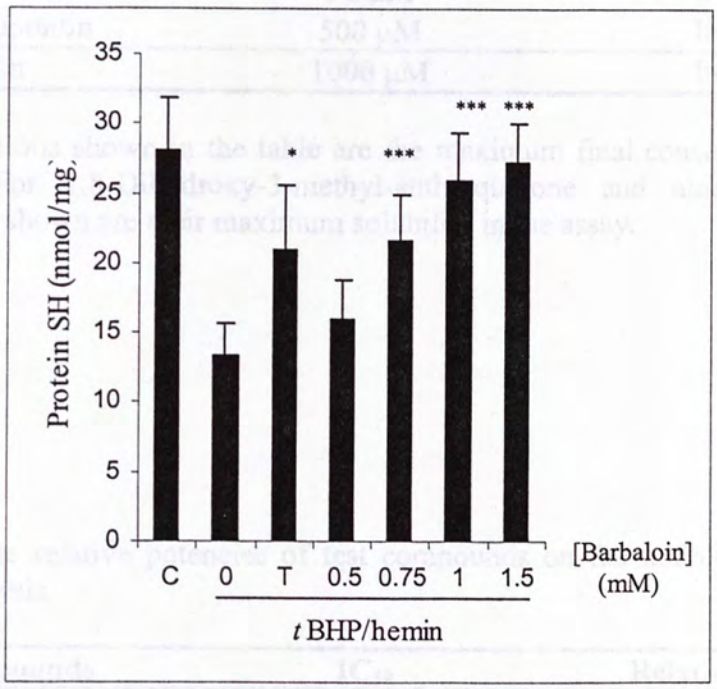

Figure 5.25 The protective effect of barbaloin on sulfhydryl groups against oxidative damage on RBC membrane. The assay was conducted with 0.5mM *t*BHP and 10μM hemin, in the absence (control) or presence of various concentrations of barbaloin. Results are expressed as nmol SH/mg protein. Data represent mean ± S.D. in four independent experiments. C= control without test compound, T = 1mM trolox, SH = sulfhydryl group. The results were compared to the negative control with oxidative damage by one-way ANOVA followed by Dunnett's test. *, $p < 0.05$; ***, $p < 0.001$.

Table 5.1 The inhibitory effects of different compounds on AAPH-induced hemolysis.

Test compounds	Maximum conc. tested	Effect
Aloe-emodin	50 μM	Inactive
Chrysophanol	50 μM	Inactive
Deoxyrhapontin	500 μM	Inactive
Rhein	1000 μM	Inactive

The concentrations shown in the table are the maximum final concentrations of the compounds. For 1,8-Dihydroxy-3-methyl-anthraquinone and aloe-emodine, the concentrations shown are their maximum solubility in the assay.

Table 5.2 The relative potencies of test compounds on the inhibition of AAPH-induced hemolysis.

Test compounds	IC_{50}	Relative potency
Trolox	59.2 μM	1
6-Gingerol	95.3 μM	0.62
Barbaloin	31.7 μM	1.87
Rhapontin	31.9 μM	1.86
Vitamin C	120.3 μM	1
6-Gingerol	95.3 μM	1.26
Barbaloin	31.7 μM	3.79
Rhapontin	31.9 μM	3.77

Their IC_{50} values are compared against trolox and vitamin C which were used as the positive controls. Relative potency = IC_{50} of trolox / IC_{50} of test compound or IC_{50} of vitamin C / IC_{50} of test compound.

Table 5.3 The inhibitory effects of different compounds on lipid peroxidation of RBC membrane.

Test compounds	Maximum conc. tested	Effect
Aloe-emodin	50 μM	Inactive
Chrysophanol	50 μM	Inactive
Deoxyrhapontin	500 μM	Inactive
Rhein	1000 μM	Inactive

The concentrations shown in the table are the maximum final concentrations of the compounds. For 1,8-Dihydroxy-3-methyl-anthraquinone, aloe-emodine, deoxyrhapontin and rhein, the concentrations shown are their maximum solubility in the assay.

Table 5.4 The relative potencies of test compounds on the inhibition of RBC membrane lipid peroxidation.

Test compounds	IC_{50}	Relative potency
Trolox	224.4 μM	1
6-Gingerol	20.7 μM	10.84
Barbaloin	71.0 μM	3.16
Rhapontin	38.3 μM	5.86

Their IC_{50} values are compared against trolox which was used as the positive control. Relative potency = IC_{50} of trolox / IC_{50} of test compound.

Table 5.5 The protective effects of different compounds on Ca^{2+}-ATPase activity of RBC membrane.

Test compounds	Maximum conc. tested	Effect
6-Gingerol	1000 μM	Inactive
Aloe-emodin	50 μM	Inactive
Chrysophanol	50 μM	Inactive
Deoxyrhapontin	500 μM	Inactive
Rhapontin	1000 μM	Inactive
Rhein	1000 μM	Inactive

The concentrations shown in the table are the maximum final concentrations of the compounds.

Table 5.6 The relative potency of babaloin on the protection of Ca^{2+}-ATPase activity.

Test compounds	% Recovery	Relative potency
Trolox	46.47%	1
Barbaloin	42.30%	0.91

The percentages of ATPase activity recovered by 1mM trolox and 1mM barbaloin were compared. Relative potency = % recovery by test compound / % recovery by trolox.

Table 5.7 The protective effects of different compounds on Na^+/K^+-ATPase activity of RBC membrane.

Test compounds	Maximum conc. tested	Effect
6-Gingerol	1000 μM	Inactive
Aloe-emodin	50 μM	Inactive
Barbaloin	1000 μM	Inactive
Chrysophanol	50 μM	Inactive
Deoxyrhapontin	500 μM	Inactive
Rhein	1000 μM	Inactive

The concentrations shown in the table are the maximum final concentrations of the compounds.

Table 5.8 The relative potency of rhapontin on the protection of Na^+/K^+-ATPase.

Test compounds	% Recovery	Relative potency
Trolox	55.09%	1
Rhapontin	35.37%	0.64

The percentages of ATPase activity recovered by 1mM trolox and 1mM rhapontin were compared. Relative potency = % recovery by test compound / % recovery by trolox.

Table 5.9 The protective effects of different compounds on the sulfhydryl groups of RBC membrane.

Test compounds	Maximum conc. tested	Effect
6-Gingerol	1000 μM	Inactive
Aloe-emodin	50 μM	Inactive
Chrysophanol	50 μM	Inactive
Deoxyrhapontin	500 μM	Inactive
Rhapontin	1000 μM	Inactive
Rhein	1000 μM	Inactive

The concentrations shown in the table are the maximum final concentrations of the compounds.

Table 5.10 The relative potency of barbaloin on the protection of sulfhydryl groups of RBC membrane.

Test compounds	% Recovery	Relative potency
Trolox	52.10%	1
Barbaloin	86.13%	1.65

The percentages of sulfhydryl groups recovered by 1mM trolox and 1mM barbaloin were compared. Relative potency = % recovery by test compound / % recovery by trolox.

5.3 Discussion

5.3.1 AAPH-induced hemolysis inhibition assay

The inhibition of AAPH-induced hemolysis assay addresses a more physiological parameter for studying the mechanisms of free radical-derived diseases *in vitro*. The compounds are tested for their abilities to protect RBC from lysis. From the results, 6-gingerol, barbaloin and rhapontin possess such protective abilities. The IC_{50} in ascending order is barbaloin, rhapontin and 6-gingerol. Barbaloin has the smallest IC_{50} value, meaning that it has the strongest antioxidant effect among them. The results were compared against the positive controls vitamin C and trolox, the common natural antioxidants. 6-Gingerol, barbaloin and rhapontin possess IC_{50} values smaller than vitamin C. In other words, they all exhibit higher protective abilities on RBC than vitamin C. Barbaloin and rhapontin possess smaller IC_{50} values than trolox, whereas 6-gingerol has a larger one. This means barbaloin and rhapontin are more potent than trolox and 6-gingerol in this case.

Among the compounds with positive effects in this assay, barbaloin has the lowest IC_{50} value, followed by rhapontin, then 6-gingerol. The other compounds were inactive in this assay. This might be due to their poor solubility except deoxyrhapontin. The absence of hydroxyl group renders the formation of phenoxyl radical impossible in deoxyrhapontin (Nakao *et al.*, 1998).

Therefore, compounds with positive results were able to protect RBC from lysis due to either one or both of the following aspects. They include the ability to scavenge

AAPH-derived radicals to inhibit their attack on RBC membranes and the ability to terminate the propagation of chain reactions after the commencement of lipid peroxidation which might lead to the disintegration of RBC membranes. In fact, cellular membrane damage could be caused by peroxidation of membrane lipids, cross-linkage of membrane proteins or influx of ions. Upon the completion of RBC hemolysis assay, it is necessary to examine whether lipid peroxidation is the main reason for hemolysis on the exposure of RBC to oxidative stress. Therefore, the lipid peroxidation assay for RBC membrane was subsequently performed.

5.3.2 Lipid peroxidation inhibition assay of RBC membranes

After the hemolysis assay, it is necessary to observe the ability of the test compounds to inhibit RBC membrane lipid from oxidization. Lipid peroxidation consists of the lag phase, the propagation phase and the degradation phase. In this assay, the *t*BHP/hemin system was employed to initiate free radical production. Lipid peroxides and lipid peroxyl radicals were then formed (Marks *et al.*, 1996). The chain reaction propagates unless it is stopped by an antioxidant. This *in vitro* reaction may represent certain pathophysiological conditions, as hemin was released into human blood during hemoglobin degradation. Excess hemin might cause oxidation to blood components due to the metal ion it possesses.

MDA is produced as the product of lipid degradation and it forms complex with TBA. Fluorescence intensity of the adduct could thus reflect the amount of MDA. Results in this assay could explain whether the protective mechanisms of the test compounds involved lipid peroxidation inhibition. If the test compounds could exhibit positive

results in the lipid peroxidation inhibition assay of RBC membranes, it might protect RBC from lysis by inhibiting membrane lipid peroxidation. Regarding the results of hemolysis assay and RBC membrane lipid peroxidation assay, the test compounds which exhibited positive effects in the hemolysis assay also exhibited positive results in the RBC membrane lipid peroxidation assay. The results show that 6-gingerol, barbaloin and rhapontin protected RBC from lysis through inhibition of lipid peroxidation. The antioxidative effect of barbaloin, rhapontin and 6-gingerol, might probably be due to their abilities to form stable phenoxyl radicals ($ArO^{\bullet}$) (Ar = aromatic), enabling them to react with the AAPH-derived radicals or lipid peroxyl radicals, thus terminating the chain reaction (Ou *et al.*, 2002).

$$ArOH + ROO^{\bullet} \longrightarrow ArO^{\bullet} + ROOH$$

$$ArO^{\bullet} + R^{\bullet} \longrightarrow ArOR$$

Comparing their IC_{50} values, 6-gingerol has the smallest, followed by rhapontin then barbaloin. They possess stronger antioxidative abilities than trolox. 6-Gingerol and rhapontin are able to scavenge free radicals. The phenol groups in their structures can form stable phenoxyl radicals by delocalization of electrons (Cao *et al.*, 2003).

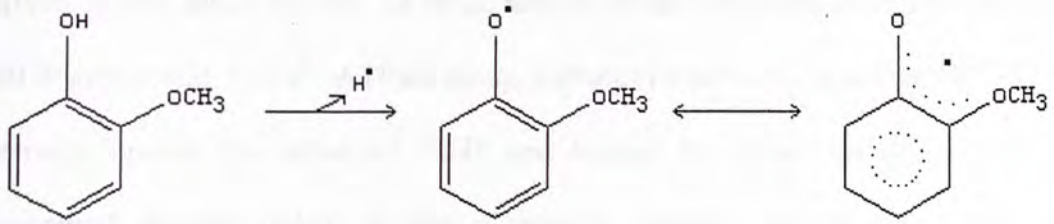

The phenoxyl radicals terminate chain propagation by reacting with the lipid radicals. 6-Gingerol has the smallest IC_{50} value since it does not have a glycoside moiety to reduce its potency as in the case of rhapontin and barbaloin (Matsuda *et al.*, 2000). Rhapontin has a larger IC_{50} value than 6-gingerol. The phenolic hydroxyl group of

rhapontin is located at the *m* position (Nakao *et al.*, 1998). The resonance effect in this case is comparatively weaker than in a situation when the hydroxyl group is at the *p* position. Thus, phenoxyl radical may form less readily in rhapontin compared with 6-gingerol. Although the phenol groups in the anthraquinone structure of barbaloin may be more difficult to become phenoxyl radicals due to the formation of intramolecular hydrogen bonds with the carbonyl oxygen, phenoxyl radical may form since the glucosyl group provides an attacking point for ROS. Other test compounds show negative results. It may be due to their poor solubilities. In order to understand whether the test compounds protect other membrane components apart from membrane lipid, the ATPase protection assays on RBC were subsequently performed.

5.3.3 Ca^{2+}-ATPase protection assay

After performing the RBC membrane lipid peroxidation assay, compounds were assessed for their protective abilities towards ATPases, which are RBC membrane components. *t*BHP and hemin could generate free radicals that cross-link proteins thus inactivating RBC membrane Ca^{2+}-ATPases. If the test compounds possess positive effects in this assay, the Ca^{2+}-ATPase activity would be spared after incubation with *t*BHP and hemin. In Ca^{2+}-ATPase assay, barbaloin was found to protect Ca^{2+}-ATPase activity against the action of *t*BHP and hemin. Its percentage of recovery was compared against trolox. It has a weaker potency than trolox at the same concentration.

Although 6-gingerol and rhapontin also inhibited hemolysis as barbaloin did (Figures 5.4, 5.5 and 5.6), they did not protect Ca^{2+}-ATPase activity. The present results

suggest that the protective mechanism of barbaloin against membrane damage might be due to its protective actions on membrane proteins as revealed in the recovery of the ATPase activity.

5.3.4 Na^+/K^+-ATPase protection assay

Apart from Ca^{2+}-ATPase assay, Na^+/K^+-ATPase assay was also performed. In the Na^+/K^+-ATPase assay, *t*BHP and hemin generate free radicals that cross-link proteins and inactivate RBC membrane Na^+/K^+-ATPase. The test compounds with antioxidant effects would be able to protect the activity of Na^+/K^+-ATPase.

In this assay, rhapontin showed positive effect. It has a weaker potency than trolox in recovering the ATPase activity (Table 5.8). Rhapontin is capable of forming stable phenoxyl radicals due to delocalization of electrons into the benzene ring structure (Cao *et al.*, 2003), so it may neutralize free radicals and protect Na^+/K^+-ATPase from free radical attack. Results in hemolysis assay and Na^+/K^+-ATPase assay revealed that rhapontin possessed both radical scavenging and ATPase protection abilities. Although 6-gingerol and barbaloin inhibited hemolysis as rhapontin did (Figures 5.4, 5.5 and 5.6), they did not protect Na^+/K^+-ATPase activity.

Since the reduced state of sulfhydryl groups on ATPase is involved in the activity of the enzyme and sulfhydryl groups are prone to free radical attack, it is necessary to find out whether the test compounds inhibit ROS attack on protein sulfhydryl groups. Sulfhydryl group protection assay was thus performed after the ATPase protection

assay to determine whether sulfhydryl group protection contributes to the antioxidant effects of the test compounds.

5.3.5 Sulfhydryl group protection assay

After ATPase protection assays, sulfhydryl group assay was performed to study the protective mechanism of the test compounds at a greater depth. *t*BHP and hemin served as the oxidants in this assay. They generated free radicals to oxidize the RBC membrane. The sulfhydryl groups on the membrane proteins would thus be subjected to oxidation or cross-linkage (Marks *et al.*, 1996). Although sulfhydryl group oxidation could take place in the presence of high concentration of *t*BHP alone, both *t*BHP and hemin were applied in this assay. This was to keep the consistency of oxidation system used, so that the action mechanisms of the test compounds could be made comprehensible. If the test compounds possess positive effect in this assay, sulfhydryl groups could be preserved in the reduced state and could react with DTNB to produce a colored compound. Barbaloin showed positive results in this sulhydryl group protection assay (Figure 5.25) suggesting that it can protect sulfhydryl groups of RBC membrane against free radical attack. The percentage of protein sulfhydryl group recovery was compared against trolox, the positive control. Barbaloin was determined to have a stronger potency than trolox (Table 5.10).

It was found that rhapontin was effective in protecting Na^+/K^+-ATPase but not Ca^{2+}-ATPase, whereas barbaloin was effective in protecting Ca^{2+}-ATPase but not Na^+/K^+-ATPase. However, it is still uncertain about the cause of different protective effects of rhapontin and barbaloin towards the two ATPases at this stage. A possible

explanation is that Ca^{2+}-ATPase is more sensitive to sulfhydryl group oxidation than Na^{+}/K^{+}-ATPase, so a sulfhydryl group protector such as barbaloin could protect Ca^{2+}-ATPase from oxidative stress. One of the studies has shown that a sulfhydryl group modifying reagent N-ethylmaleimide (NEM) is able to inhibit Ca^{2+}-ATPase, as sulfhydryl group is essential to the activity of Ca^{2+}-ATPase (Takahashi and Yamaguchi, 1994). Therefore, inactivation of Na^{+}/K^{+}-ATPase by *t*BHP/hemin may be caused by mechanisms other than sulfhydryl group oxidation and rhapontin is probably matched to provoke this effect. This showed that antioxidants have different specific antioxidant properties.

Results in hemolysis assay and Ca^{2+}-ATPase assay reveal that barbaloin possesses both radical scavenging and Ca^{2+}-ATPase protective effects. Together with the results in the sulfhydryl group assay, it may be concluded that protection of the protein sulfhydryl group by barbaloin might lead to the preservation of the Ca^{2+}-ATPase activity and the RBC membrane integrity. Although rhapontin possesses similar antioxidative characteristics as barbaloin, it has no effect in the sulfhydryl group protection assay, suggesting that rhapontin does not inhibit hemolysis through sulfhydryl group protection. Moreover, 6-gingerol does not show protection to either ATPases or protein sulfhydryl groups. Therefore, its protective effects on hemolysis cannot be attributed to these mechanisms. This indicates that 6-gingerol might not be able to inhibit protein cross-linkage. In summary, barbaloin has a wider aspect of antioxidant abilities than rhapontin and 6-gingerol. After the assays related to the RBC were performed, the test compounds' actions on another important blood component, LDL, were investigated.

5.3.6 Chapter summary

6-Gingerol, barbaloin and rhapontin possess antioxidative effects, but their protective mechanisms vary. 6-Gingerol inhibited hemolysis and RBC membrane lipid peroxidation (Figure 5.4 and 5.9), but it could neither reduce ATPase inhibition nor protect protein sulfhydryl groups in RBC membranes (Tables 5.5, 5.7 and 5.9). This indicates that it may inhibit free radical propagation after free radical attack. Rhapontin protects RBC from lysis (Figure 5.6), protects RBC membrane against lipid peroxidation (Figure 5.11) and protects Na^+/K^+-ATPase from inhibition (Figure 5.21), but it neither reduces Ca^{2+}-ATPase inhibition (Table 5.5) nor protects protein sulfhydryl group in the membrane (Table 5.9). When compared to 6-gingerol, it possesses a wider scope of protection. Barbaloin inhibited hemolysis and RBC membrane lipid peroxidation (Figure 5.5 and 5.10). It also reduced Ca^{2+}-ATPase inhibition (Figure 5.17) and protected protein sulfhydryl group in membrane (Figure 5.25), but it did not reduce Na^+/K^+-ATPase inhibition (Table 5.7). Thus, it has the widest range of antioxidant abilities among the compounds tested.

Chapter 6 Lipid peroxidation inhibition assay of LDL: results and discussion

6.1 Introduction

Apart from RBC, LDL is another blood component prone to oxidant attack. LDL oxidation is the basis of some free radical-derived diseases. Under oxidative stress, oxidized LDL accumulates causing inflammation of arterial wall. This eventually leads to atherosclerosis. Protection of LDL from oxidation delays the progress of atherosclerosis. Therefore, the antioxidative effects of the test compounds on LDL were evaluated through lipid peroxidation inhibition assays. Two oxidants, AAPH and hemin, were applied. The assays were carried out according to the protocols described in the Materials and methods chapter.

6.2 Results

The results for the AAPH-induced lipid peroxidation inhibition assay of LDL are summarized in Figures 6.1 to 6.6, and Tables 6.1 to 6.2. Figure 6.1 and 6.2 show the effect of variation in incubation time and different concentrations of AAPH on AAPH-induced lipid peroxidation of LDL respectively. From the results, the optimal assay conditions were determined. Figure 6.3 demonstrates the effects of the positive control, trolox. Its IC_{50} was determined to be 40.9μM. Figure 6.4 shows the effects of 6-gingerol. Its IC_{50} was found to be 19.1μM. Figure 6.5 shows the effects of barbaloin.

Its IC_{50} was determined to be 142.4μM. Figure 6.6 demonstrates the effects of rhapontin. Its IC_{50} was found to be 14.1μM. The three compounds were able to protect LDL from lipid peroxidation in a dose-dependent manner. Table 6.1 displays the results of the other test compounds. They did not exhibit any inhibitory effects on LDL lipid peroxidation at the concentrations tested in the presence of AAPH. The relative potencies of the test compounds with positive effects in this assay are shown in Table 6.2.

The results for the hemin-induced lipid peroxidation inhibition assay of LDL are summarized in Figures 6.7 to 6.12, and Tables 6.3 to 6.4. Figure 6.7 and 6.8 show the effect of variation in incubation time and different concentrations of hemin on hemin-induced lipid peroxidation of LDL respectively. From the results, the optimal assay conditions were determined. Figure 6.9 demonstrates the effects of the positive control, trolox. Its IC_{50} was determined to be 0.195μM. Figure 6.10 shows the effects of 6-gingerol. Its IC_{50} was found to be 0.054μM. Figure 6.11 demonstrates the effects of barbaloin. Its IC_{50} was determined to be 2.845μM. Figure 6.12 shows the effects of rhapontin. Its IC_{50} was found to be 0.104μM. These three compounds exhibited positive effects towards LDL oxidation produced by hemin in a dose dependent manner. Table 6.3 displays the results of the other test compounds. They did not exhibit any inhibitory effects on LDL lipid peroxidation at the concentrations tested in the presence of hemin. The relative potencies of the test compounds with positive effects in this assay are shown in Table 6.4.

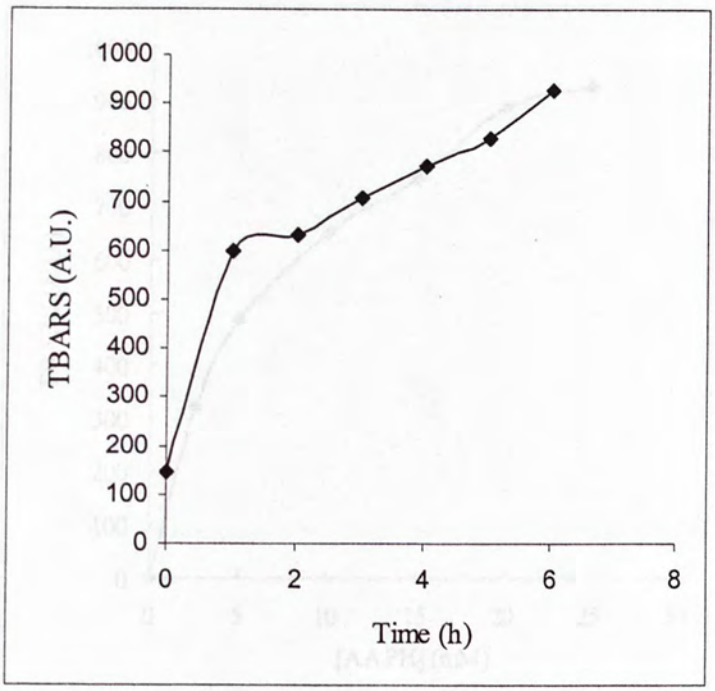

Figure 6.1 The time-dependent AAPH-induced lipid peroxidation of LDL. This is a preliminary experiment for obtaining the appropriate incubation time to be applied in subsequent assays. The assay was conducted with 10mM AAPH. Results are expressed as the fluorescent unit of TBARS produced in one experiment. A.U. = arbitary unit.

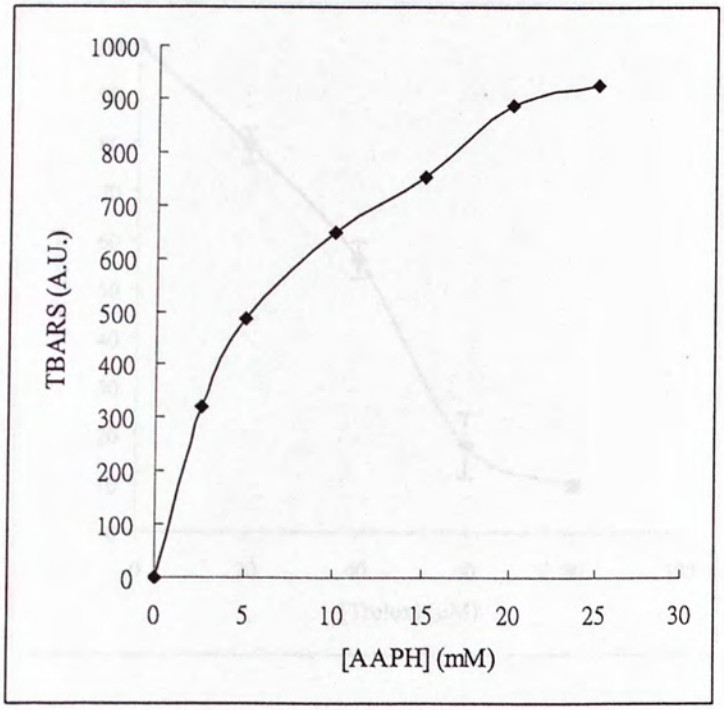

Figure 6.2 The dose-dependent AAPH-induced lipid peroxidation of LDL. This is a preliminary experiment for obtaining the appropriate concentration of AAPH to be applied in subsequent assays. LDL was incubated with AAPH for 2 h. Results are expressed as the fluorescent unit of TBARS produced in one experiment. A.U. = arbitary unit.

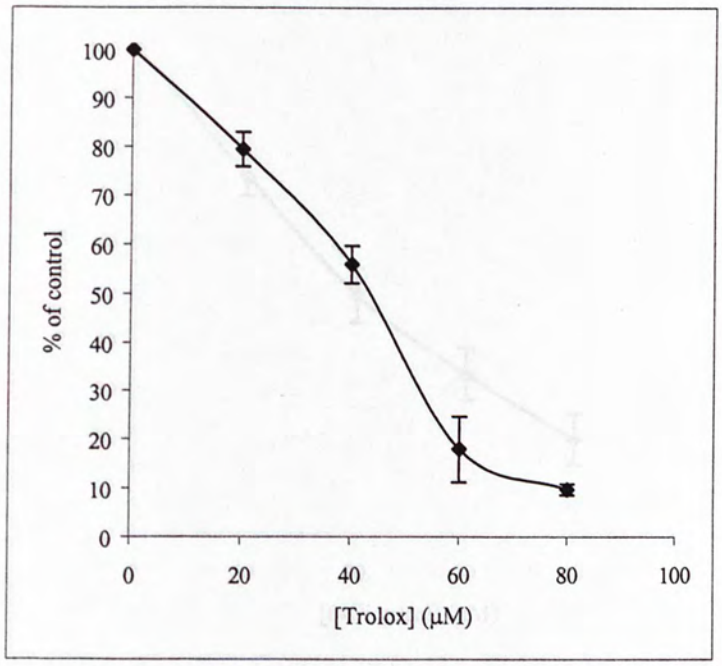

Figure 6.3 The inhibitory effect of trolox on AAPH-induced lipid peroxidation of LDL. The assay was conducted with 20mM AAPH, in the absence (control) or presence of various concentrations of trolox. Degree of lipid peroxidation inhibition is expressed as percentage of control. Data represent mean ± S.D. in four independent experiments.

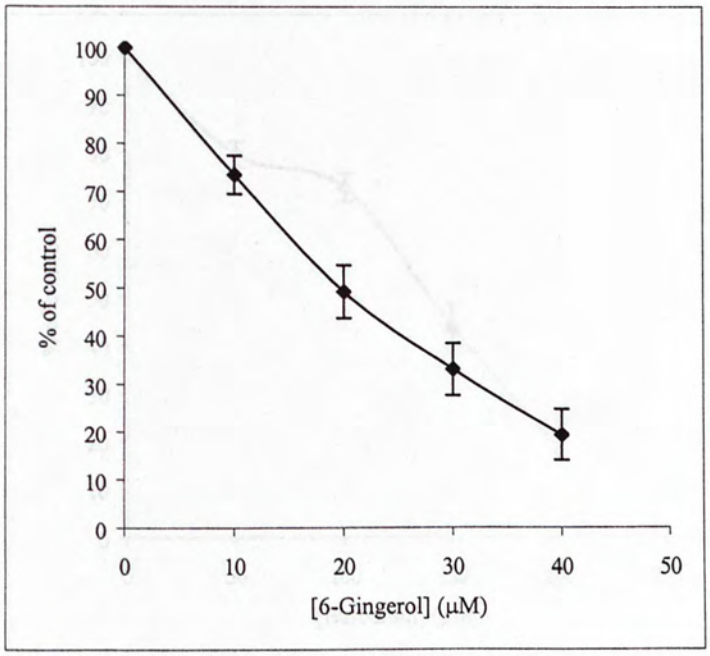

Figure 6.4 The inhibitory effect of 6-gingerol on AAPH-induced lipid peroxidation of LDL. The assay was conducted with 20mM AAPH, in the absence (control) or presence of various concentrations of 6-gingerol. Degree of lipid peroxidation inhibition is expressed as percentage of control. Data represent mean ± S.D. in four independent experiments.

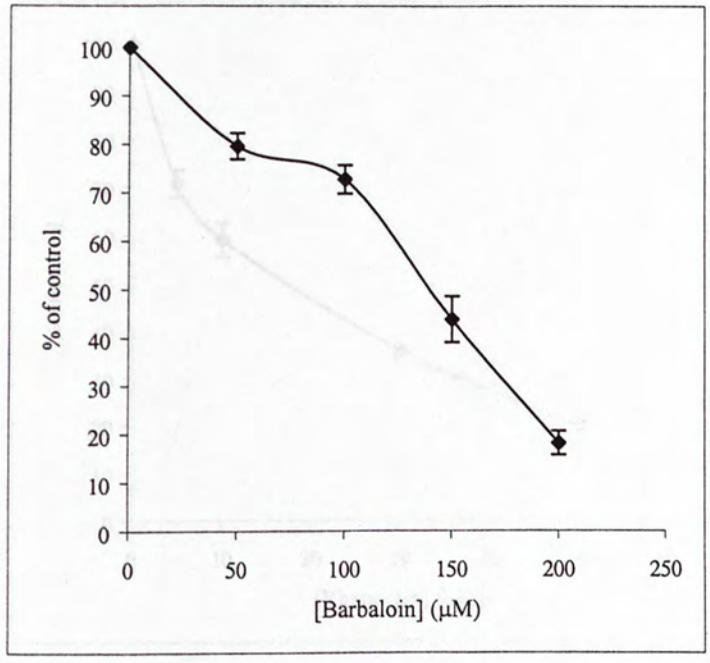

Figure 6.5 The inhibitory effect of barbaloin on AAPH-induced lipid peroxidation of LDL. The assay was conducted with 20mM AAPH, in the absence (control) or presence of various concentrations of barbaloin. Degree of lipid peroxidation inhibition is expressed as percentage of control. Data represent mean ± S.D. in four independent experiments.

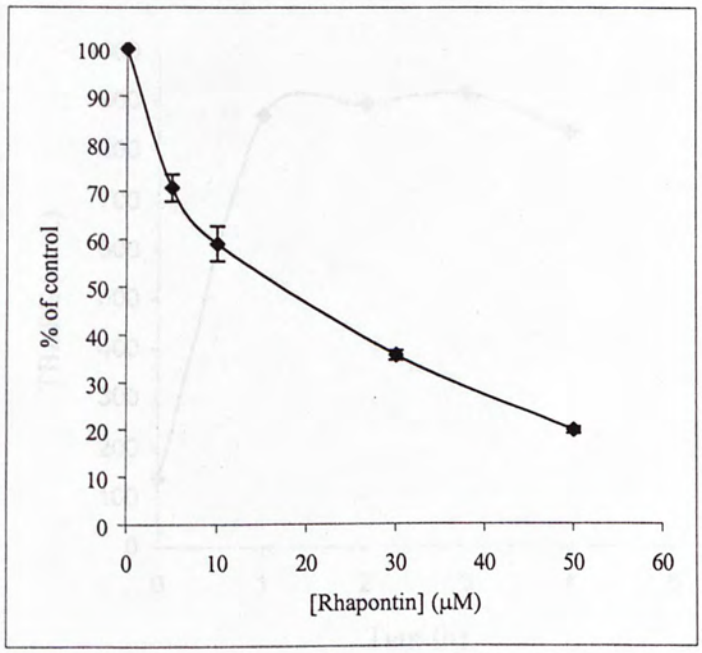

Figure 6.6 The inhibitory effect of rhapontin on AAPH-induced lipid peroxidation of LDL. The assay was conducted with 20mM AAPH, in the absence (control) or presence of various concentrations of rhapontin. Degree of lipid peroxidation inhibition is expressed as percentage of control. Data represent mean ± S.D. in four independent experiments.

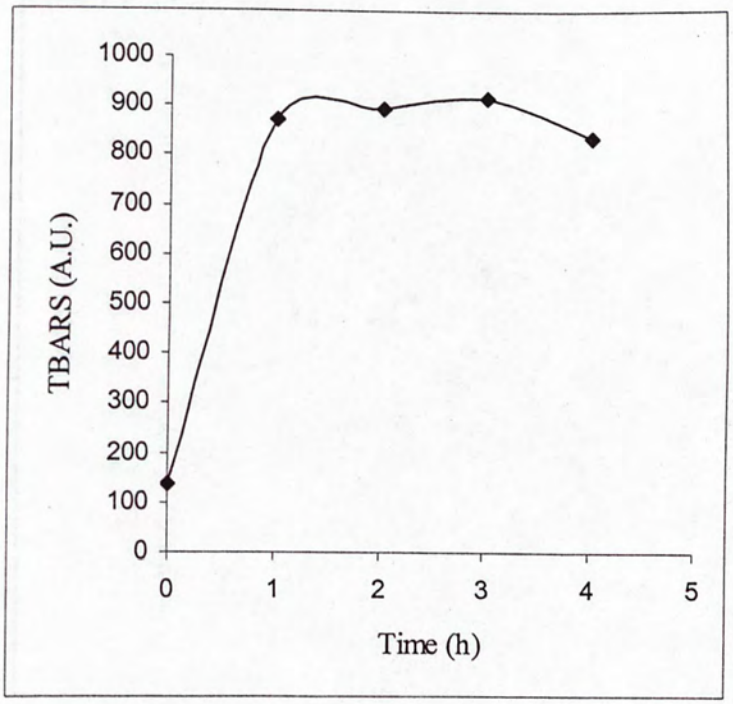

Figure 6.7 The time-dependent hemin-induced lipid peroxidation of LDL. This is a preliminary experiment for obtaining the appropriate incubation time to be applied in subsequent assays. The assay was conducted with 1μM hemin. Results are expressed as the fluorescent unit of TBARS produced in one experiment. A.U. = arbitary unit.

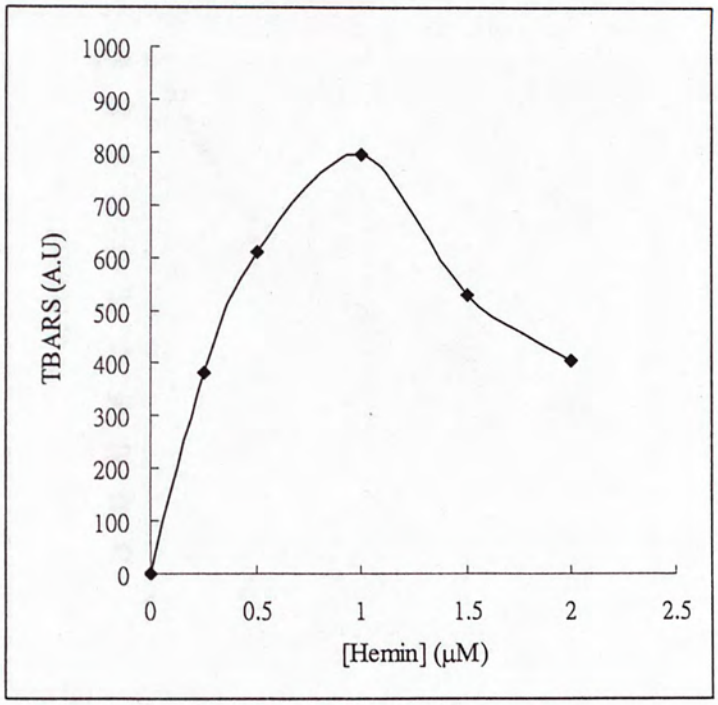

Figure 6.8 The dose-dependent hemin-induced lipid peroxidation of LDL. This is a preliminary experiment for obtaining the appropriate concentration of hemin to be applied in subsequent assays. LDL was incubated with hemin for 2 h. Results are expressed as the fluorescent unit of TBARS produced in one experiment. A.U. = arbitary unit.

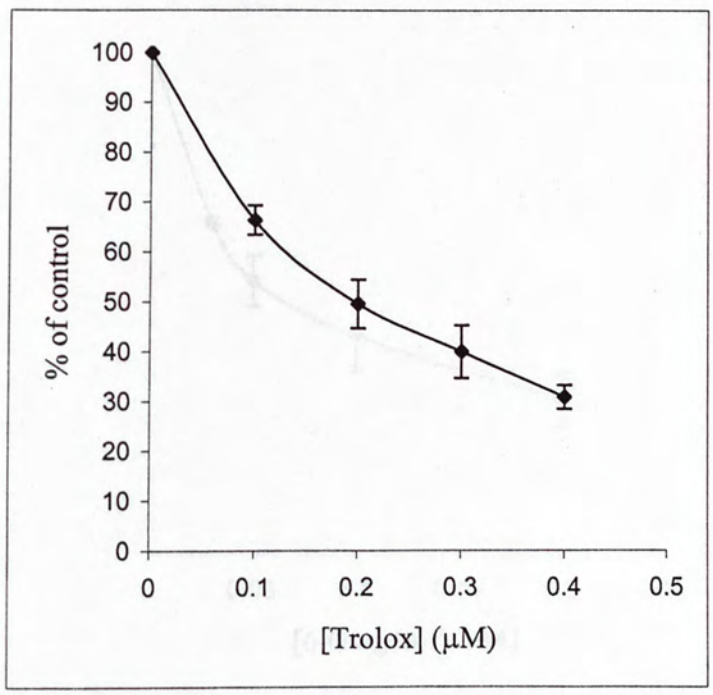

Figure 6.9 The inhibitory effect of trolox on hemin-induced lipid peroxidation of LDL. The assay was conducted with 1μM hemin, in the absence (control) or presence of various concentrations of trolox. Degree of lipid peroxidation inhibition is expressed as percentage of control. Data represent mean ± S.D. in four independent experiments.

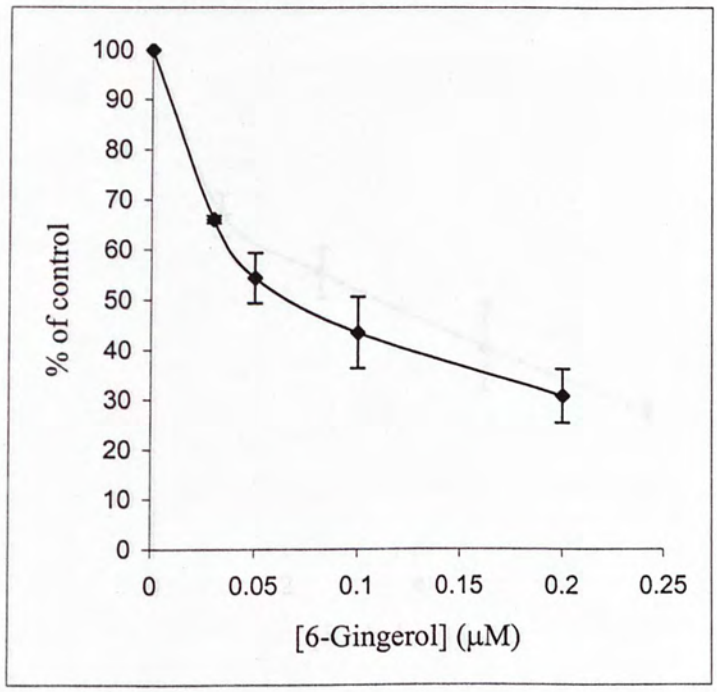

Figure 6.10 The inhibitory effect of 6-gingerol on hemin-induced lipid peroxidation of LDL. The assay was conducted with 1μM hemin, in the absence (control) or presence of various concentrations of 6-gingerol. Degree of lipid peroxidation inhibition is expressed as percentage of control. Data represent mean ± S.D. in four independent experiments.

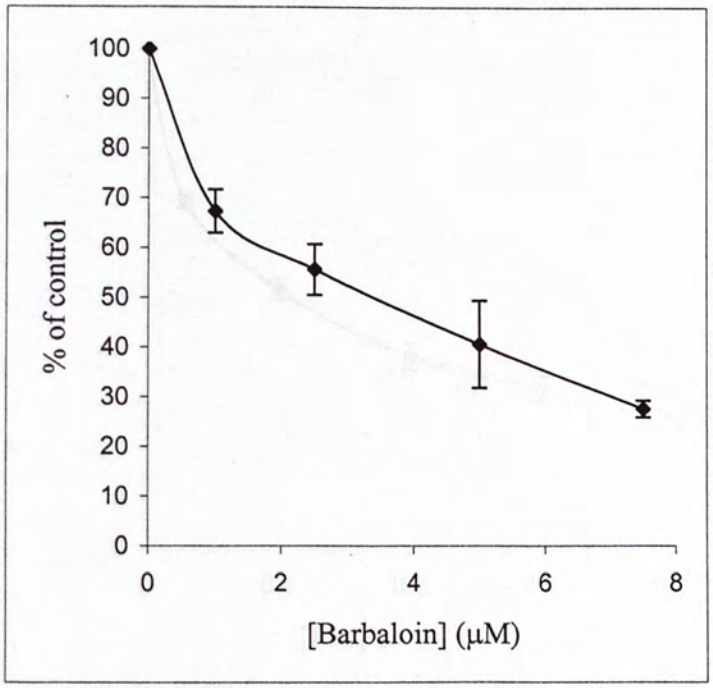

Figure 6.11 The inhibitory effect of barbaloin on hemin-induced lipid peroxidation of LDL. The assay was conducted with 1μM hemin, in the absence (control) or presence of various concentrations of barbaloin. Degree of lipid peroxidation inhibition is expressed as percentage of control. Data represent mean ± S.D. in four independent experiments.

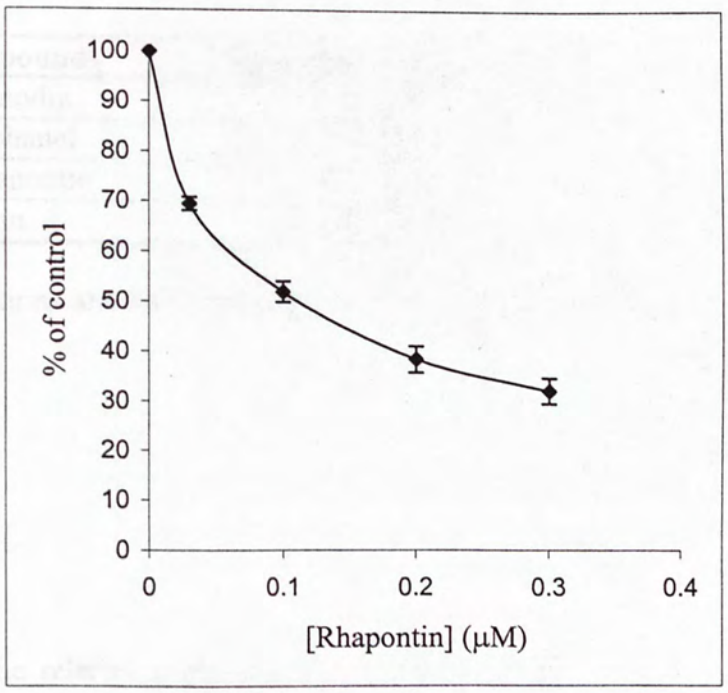

Figure 6.12 The inhibitory effect of rhapontin on hemin-induced lipid peroxidation of LDL. The assay was conducted with 1μM hemin, in the absence (control) or presence of various concentrations of rhapontin. Degree of lipid peroxidation inhibition is expressed as percentage of control. Data represent mean ± S.D. in four independent experiments.

Table 6.1 The inhibitory effects of different compounds on AAPH-induced lipid peroxidation of LDL.

Test compounds	Maximum conc. tested	Effect
Aloe-emodin	50 μM	Inactive
Chrysophanol	50 μM	Inactive
Deoxyrhapontin	500 μM	Inactive
Rhein	1000 μM	Inactive

The concentrations shown in the table are the maximum final concentrations of the compounds.

Table 6.2 The relative potencies of test compounds on the inhibition of AAPH-induced lipid peroxidation of LDL.

Test compounds	IC_{50}	Relative potency
Trolox	40.9 μM	1
6-Gingerol	19.1 μM	2.14
Barbaloin	142.4 μM	0.29
Rhapontin	14.1 μM	2.90

Their IC_{50} values are compared against trolox, which is the positive control. Relative potency = IC_{50} of trolox / IC_{50} of compound.

Table 6.3 The inhibitory effects of different compounds on hemin-induced lipid peroxidation of LDL.

Test compounds	Maximum conc. tested	Effect
Aloe-emodin	50 μM	Inactive
Chrysophanol	50 μM	Inactive
Deoxyrhapontin	500 μM	Inactive
Rhein	1000 μM	Inactive

The concentrations shown in the table are the maximum final concentrations of the compounds.

Table 6.4 The relative potencies of test compounds on the inhibition of hemin-induced lipid peroxidation of LDL.

Test compounds	IC_{50}	Relative potency
Trolox	0.195 μM	1
6-Gingerol	0.054 μM	3.611
Barbaloin	2.845 μM	0.069
Rhapontin	0.104 μM	1.875

Their IC_{50} values are compared against trolox, which is the positive control. Relative potency = IC_{50} of trolox / IC_{50} of test compounds.

6.3 Discussion

After studying the compounds' abilities to protect RBC and its components against oxidative stress, the abilities of these compounds to inhibit LDL oxidation were also investigated to evaluate their potentials in preventing diseases linked to the oxidation of LDL. AAPH and hemin were applied as the oxidants in these assays.

In order to understand the reason for performing AAPH-induced and hemin-induced lipid peroxidation inhibition assay of LDL, it is necessary to observe the difference between the two oxidants used in these two assays. RBC could be lysed when extreme oxidative stress arises and hemoglobin will be released. Hemoglobin is also released from RBC as a natural process during RBC degradation. Hemoglobin releases heme during degradation (Marks *et al.*, 1996). Heme could be oxidized to form hemin. Hemin is an oxidant that may appear in blood. Therefore, the LDL assay using hemin as the oxidant was performed. On the other hand, AAPH is an artificial oxidant. It is applied in the present study since it is a reliable radical source, such that an effective radical scavenger can be identified in the assay.

Both hemin and AAPH were used as oxidants in the assay in order to investigate the two possible protective mechanisms of the test compounds. AAPH initiates chain reaction of lipid peroxidation as it can become radical itself or form peroxyl radical in the presence of oxygen, whereas hemin propagates chain reaction by catalyzing the formation of lipid peroxyl radicals from the existing lipid hydroperoxides in LDL. Existing peroxide in LDL (LOOH) is converted by hemin to peroxyl radical ($LOO^{\bullet}$) which propagates lipid peroxidation.

$$LOOH \xrightarrow{\text{hemin}} LOO^{\bullet}$$

If the test compounds exhibit protection of LDL against AAPH-induced lipid peroxidation, they might either scavenge AAPH radicals or scavenge lipid peroxyl radicals to terminate the chain reaction. In the case of hemin-catalyzed lipid peroxidation, the compounds could only act as chain-breaking antioxidant by scavenging lipid peroxyl radicals. The effects of the test compounds were studied under both oxidation systems to evaluate their antioxidative mechanisms, whether they serve as chain-breaking antioxidants, or as free radical scavengers, or both.

Regarding the AAPH-induced lipid peroxidation of LDL, peroxyl radicals were generated. The resulting peroxides started to propagate the chain reaction. MDA produced by lipid peroxidation formed colored complex with TBA, and fluorescence was measured. 6-Gingerol, barbaloin and rhapontin were demonstrated to exhibit inhibitory actions in this assay. When compared to trolox, 6-gingerol and rhapontin had a smaller IC_{50} values, whereas barbaloin had a higher one. This means that 6-gingerol and rhapontin are more effective in protecting LDL from lipid peroxidation. These compounds are able to inhibit LDL oxidation and may have potential applications in atherosclerosis and other related diseases. This awaits further *in vivo* studies.

6-Gingerol, barbaloin and rhapontin were demonstrated to exhibit positive results in the hemin-induced lipid peroxidation inhibition assay of LDL. Their results were compared against the positive control, trolox. The IC_{50} values of 6-gingerol and rhapontin were smaller than that of trolox, whereas barbaloin was larger. When comparing 6-gingerol and rhapontin, the former had a smaller IC_{50} values. In other

words, 6-gingerol has the strongest lipid peroxidation inhibitory effect, followed by rhapontin, and then barbaloin. These compounds might possess the ability to scavenge lipid peroxyl radicals and reduce the degree of LDL oxidation. Although 6-gingerol has previously been reported to possess antioxidative activity (Kikuzaki *et al.*, 1993; Aeschbach *et al.*, 1994), to my knowledge the present study is the first report to demonstrate its antioxidative effects in more physiological systems on human blood components, RBC and LDL, and the results may have clinical implications on free radical-derived diseases.

From the results of these two assays, it was found that 6-gingerol and rhapontin scavenge lipid peroxyl radicals, and they have stronger potencies than trolox. They are chain-breaking antioxidants. Barbaloin also possesses antioxidative abilities but it has weaker potency than trolox. Its radical scavenging ability is better than its chain-breaking ability, since its potency in comparison to trolox is comparatively higher in the assay with AAPH.

When the active compounds are compared between the AAPH-induced and the hemin-induced lipid peroxidation of LDL, it is found that the IC_{50} values of the test compounds are much smaller in the hemin-induced assay. This may be due to the low level of lipid peroxides exists in the LDL for the chain reaction initiation. Nevertheless, the test compounds with positive effects possess significant antioxidant properties towards lipids.

Chapter 7 General discussion

XOD plays a significant role in hyperuricemia and ischemia-reperfusion injury. Compounds with inhibitory actions on XOD would contribute towards the alleviation of one or both of these conditions. Deoxyrhapontin, a compound isolated from rhubarb root, was found to have the ability in inhibiting XOD activity. From our results, the mode of inhibition of deoxyrhapontin was of mixed type and its inhibitory effect was reversible in nature. The present results therefore suggest that the traditional use of *Rheum* species in the treatment of gout and other related clinical syndromes may have its scientific basis on the XOD inhibitory compounds they contain. More studies are required before it could be applied clinically, such as *in vivo* data and toxicity profile. It was also found that deoxyrhapontin did not possess antioxidant effect.

The lipid peroxidation inhibition assay using mouse liver microsomes was performed to study the compounds regarding their antioxidative strength. As RBC are exposed to oxidative stress constantly, therefore AAPH-induced hemolysis assay was performed to evaluate the compounds' antioxidative ability. It was found that 6-gingerol, barbaloin and rhapontin possessed positive effects, meaning that they are able to scavenge radicals and inhibit hemolysis. The positive effects of the test compounds in the AAPH-induced hemolysis assay prompted the development of other assays related to the components of RBC for detailed studies of the compounds' antioxidant effects on the RBC.

Factors contributing to hemolysis include membrane lipid peroxidation, protein oxidation, ion influx and depletion of antioxidants. Therefore, assays relating to these aspects were performed to evaluate the test compounds' antioxidative ability on hemolysis. The assays include lipid peroxidation inhibition assay, protein sulfhydryl group protection assay and ATPase protection assays. They aim at investigating whether the test compounds could inhibit hemolysis through inhibition of lipid peroxidation, inhibition of protein oxidation or protection of ion transport vehicles. Results in these assays implied the antioxidant mechanisms of the test compounds and are summarized as follows. In RBC membrane lipid peroxidation assay, 6-gingerol, barbaloin and rhapontin exhibited positive effects (Figures 5.9, 5.10 and 5.11). This indicates that these compounds might possess the ability to scavenge lipid peroxyl radicals and reduce the degree of RBC membrane disintegration through lipid peroxidation inhibition. The results of protein sulfhydryl group protection assay and ATPase assays (Figures 5.17 and 5.25) indicate that barbaloin was able to protect membrane protein and Ca^{2+}-ATPase through protein sulfhydryl group protection. Rhapontin showed positive results in Na^{+}/K^{+}-ATPase assay (Figure 5.21) but not sulfhydryl group protection assay (Table 5.9), meaning it probably protects Na^{+}/K^{+}-ATPase through other mechanisms instead of protein sulfhydryl group protection.

Taking all the results regarding RBC into consideration, it could be concluded that prevention of membrane lipid peroxidation is important to protect RBC against hemolysis. This is due to the fact that peroxidation of membrane does not only distort the lipid bilayer array, the resulting peroxyl radicals also cross-linked transmembrane proteins and intracellular proteins, thus destroying the complete cellular structure eventually (Marks *et al.*, 1996). Although 6-gingerol and rhapontin have more

restricted aspects in their protection mechanisms as compared to barbaloin, they could still demonstrate significant protective effects against hemolysis through lipid peroxidation inhibition. This indicates the significance of lipid peroxidation inhibition.

For LDL lipid peroxidation assay, the potency of 6-gingerol, barbaloin and rhapontin were directly proportional to their protective effects towards LDL and their capability to act against atherosclerosis. In view of the results of antioxidant assays, the three compounds might possess the potential to offer protection against ROS-derived diseases. Among the test compounds in the present study, none of them possess both XOD inhibitory and antioxidant activities. Some of them were found to possess either one of the activities and some of them possess neither one of the activities.

With reference to the compounds' relative potency against trolox in all assays, the antioxidative characteristics of barbaloin, 6-gingerol and rhapontin are identified as follows. Barbaloin has a lower potency than trolox in hemin-induced lipid peroxidation of LDL (Table 6.4) and it has no effect in mouse liver microsome lipid peroxidation (Table 4.1), meaning that barbaloin is a poor chain-breaking antioxidant. Barbaloin has greater protective effect than trolox in AAPH-induced hemolysis assay (Table 5.2), lipid peroxidation inhibition assay of RBC membrane (Table 5.4) and sulfhydryl group protection assay (Table 5.10). This indicates that barbaloin is able to scavenge AAPH and *t*BHP radicals to inhibit lipid peroxidation and protein degradation. Moreover, 6-gingerol is unable to protect protein sulfhydryl groups and ATPases from *t*BHP radical attack (Table 5.5, 5.7 and 5.9), suggesting that it is a poor *t*BHP radical scavenger. It has low activity in AAPH-induced hemolysis assay (Table 5.2), meaning that it has low ability in scavenging AAPH-derived radicals. 6-Gingerol

has higher potency than trolox in all lipid peroxidation assays (Tables 4.2, 5.4, 6.2 and 6.4), meaning that it is a strong chain-breaking antioxidant. Furthermore, rhapontin has higher potency then trolox in all lipid peroxidation assays, but it is a less potent chain-breaking antioxidant when compared to 6-gingerol. Rhapontin is more potent than 6-gingerol in all AAPH-induced reactions (Tables 5.2 and 6.2), which means that it is a better AAPH-derived radical scavenger.

Most of the compounds showing negative effects on XOD inhibition and antioxidant assays are the anthraquinones. However, it should be noted that one of the factors which contributes to their negative effects in these assays is their poor solubility. Barbaloin is an exception. Apart from the anthraquinone structure, barbaloin also contains a glycosidic moiety which increases its solubility in water. Therefore solutions with higher concentrations of the compound could be prepared. Solubility is a factor that might contribute to the detection of activity among the anthraquinones. This example illustrates the importance of solubility of the test compounds in determining their usefulness, so the solubility issue should be considered in any drug screening exercise.

From the results of this study, it is found that each active component of CMM has a unique biological significance. As an extract of CMM is usually composed of a number of active components, it may have a number of therapeutic actions. Therefore, CMM are sometimes suggested to possess bidirectional regulatory effects, which is an advantage over western drugs. This is due to the fact that effects exerted by two compounds are able to complement each other to give a greater combined effect. For example, the stilbene components in rhubarb can act together in a complementary

manner with deoxyrhapontin inhibiting XOD on the one hand and rhapontin attenuating oxidative stress on the other, thus achieving both ends of urate-lowering and antioxidant supplementation. Another synthesis from the present study is the possible combined usage of ginger and aloe. 6-Gingerol from ginger and barbaloin from aloe were demonstrated to preferentially protect lipids and proteins respectively. Their combination provides a wider scope of antioxidative effects which might increase their abilities in the protection against ROS-derived diseases such as aging and atherosclerosis. They may find potential applications in health products such as cosmetics and drinks – "ginger juice aloe drinks".

In this project, the XOD inhibitory and antioxidant effects of a number of CMM-derived compounds and their mechanisms of action were evaluated. The results may provide some information on the structure-activity relationship for these compounds, which could be useful for future drug development for diseases involving abnormal antioxidant and pro-oxidant conditions. Since the results obtained are limited to *in vitro* conditions, further studies are required to examine the safety and efficacy of these compounds. *In vivo* experiments, toxicity determination, and finally clinical trials have to be performed to substantiate the clinical potentials of these compounds.

References

Aeschbach R., Loliger J., Scott B.C., Murcia A., Butler J., Halliwell B., Aruoma O.I. (1994) Antioxidant actions of thymol, carvacrol, 6-gingerol, zingerone and hydroxytyrosol. Food Chem Toxicol 32: 31-36

Alberts B., Bray D., Lewis J., Raff M., Roberts K., Watson J. (1994) Molecular biology of the cell, 3rd ed. New York: Garland Publishing.

Al-Jobore A., Roufogalis B.D. (1981) Influence of EGTA on the apparent Ca^{2+} affinity of Mg^{2+}-dependent, Ca^{2+}-stimulated ATPase in the human erythrocyte membrane. Biochim Biophys Acta 645: 1-9

Ames B.N., Cathcart R., Schwiers E., Hochstein P. (1981) Uric acid provides an antioxidant defense in humans against oxidant- and radical-caused aging and cancer: a hypothesis. Proc Natl Acad Sci USA 78: 6858-6862

Aucamp J., Gaspar A., Hara Y., Apostolides Z. (1997) Inhibition of xanthine oxidase by catechins from tea (*Camellia sinensis*). Anticancer Res 17: 4381-4385

Basaga H., Poli G., Tekkaya C., Aras I. (1997) Free radical scavenging and antioxidative properties of 'silibin' complexes on microsomal lipid peroxidation. Cell Biochem Funct 15: 27-33

Bowler R.P., Nicks M., Olsen D.A., Thogersen I.B., Valnickova Z., Hojrup P., Franzusoff A., Enghild J.J., Crapo J.D. (2002) Furin proteolytically processes the heparin-binding region of extracellular superoxide dismutase. J Biol Chem 277: 16505-16511

Camejo G., Halberg C., Manschik-Lundin A., Hurt-Camejo E., Rosengren B., Olsson H., Hansson G.I., Forsberg G.B., Ylhen B. (1998) Hemin binding and oxidation of lipoproteins in serum: mechanisms and effect on the interaction of LDL with human macrophages. J Lipid Res 39: 755-766

Canas P.E. (1999) The role of xanthine oxidase and the effects of antioxidants in ischemia reperfusion cell injury. Acta Physiol Pharmacol Ther Latinoam 49: 13-20

Cao H., Pan X., Li C., Zhou C., Deng F., Li T. (2003) Density functional theory calculations for resveratrol. Bioorg Med Chem Lett 13: 1869-1871

Chan W.S., Wen P.C., Chiang H.C. (1995) Structure-activity relationship of caffeic acid analogues on xanthine oxidase inhibition. Anticancer Res 15: 703-708

Chang H.Y., Pan W.H., Yeh W.T., Tsai K.S. (2001) Hyperuricemia and gout in Taiwan: results from the Nutritional and Health Survey in Taiwan (1993-96). J Rheumatol 28: 1640-1646

Chang W.S., Chang Y.H., Lu F.J., Chiang H.C. (1994) Inhibitory effects of phenolics on xanthine oxidase. Anticancer Res 14: 501-506

Engerson T.D., McKelvey T.G., Rhyne D.B., Boggio E.B., Snyder S.J., Jones H.P. (1987) Conversion of xanthine dehydrogenase to oxidase in ischemic rat tissues. J Clin Invest 79: 1564-1570

Fernández L., Carrasco-Chaumel E., Serafín A., Xaus C., Grande L., Rimola A., Roselló-Catafau J., Peralta C. (2004) Is ischemic preconditioning a useful strategy in steatotic liver transplantation? Am J Transplant 4: 888-899

Haest C.W.M., Plasa G., Kamp D., Deuticke B. (1978) Spectrin as a stabilizer of the phospholipid asymmetry in the human erythrocyte membrane. Biochim Biophys Acta 509: 21-32.

Harris M.D., Siegel L.B., Alloway J.A. (1999) Gout and hyperuricemia. Am Fam Physician 59: 925-934

Higuchi A., Yonemitsu K., Koreeda A., Tsunenari S. (2003) Inhibitory activity of epigallocatechin gallate (EGCg) in paraquat-induced microsomal lipid peroxidation--a mechanism of protective effects of EGCg against paraquat toxicity. Toxicology 183: 143-149

Horiuchi H., Ota M., Nishimura S., Kaneko H., Kasahara Y., Ohta T., Komoriya K. (2000) Allopurinol induces renal toxicity by impairing pyrimidine metabolism in mice. Life Sci 66: 2051-2070

Hotter G., Closa D., Pi F., Rosello-Catafau J., Bulbena O., Badosa F., Fernandez-Cruz L., Gelpi E. (1994) Arachidonate metabolism in ischemia-reperfusion associated with pancreas transplantation. J Lipid Mediat Cell Signal 9: 135-143

Jansson P.J., Asplund K.U., Makela J.C., Lindqvist C., Nordstrom T. (2003) Vitamin C (ascorbic acid) induced hydroxyl radical formation in copper contaminated household drinking water: role of bicarbonate concentration. Free Radic Res 37: 901-905

Jimenez I., Garrido A., Bannach R., Gotteland M., Speisky H. (2000) Protective effects of boldine against free radical-induced erythrocyte lysis. Phytother Res 14: 339-343

Jorgensen P.L., Hakansson K.O., Karlish S.J.D. (2003) Structure and mechanism of Na,K-ATPase: functional sites and their interactions. Annu Rev Physiol 65: 817-849

Kallner A. (1975) Determination of phosphate in serum and urine by a single step malachite-green method. Clin Chim Acta 59: 35-39

Kenney I.J. (1991) Renal sonography in long standing Lesch-Nyhan syndrome. Clin Radiol 43: 39-41

Kikuzaki H., Nakatani N. (1993) Antioxidant effects of some ginger constituents. J Food Sci 58: 1407-1410

Kim D.H., Park E.K., Bae E.A., Han M.J. (2000) Metabolism of rhaponticin and chrysophanol 8-O-beta-D-glucopyranoside from the rhizome of *Rheum Undulatum* by human intestinal bacteria and their anti-allergic actions. Biol Pharm Bull 23: 830-833

Kim Y.M., Yun J., Lee C.K., Lee H., Min K.R., Kim Y. (2002) Oxyresveratrol and hydroxystilbene compounds. Inhibitory effect on tyrosinase and mechanism of action. J Biol Chem 277:16340-16344

Kirschbaum B. (2001) Renal regulation of plasma total antioxidant capacity. Med Hypotheses 56: 625-629

Knight J.A. (2000) The biochemistry of aging. Adv Clin Chem 35: 1-62

Kong L.D., Cai Y., Huang W.W., Cheng C.H., Tan R.X. (2000) Inhibition of xanthine oxidase by some Chinese medicinal plants used to treat gout. J Ethnopharmacol 73: 199-207

Kong L.D., Zhang Y., Pan X., Tan R.X., Cheng C.H. (2000) Inhibition of xanthine oxidase by liquiritigenin and isoliquiritigenin isolated from *Sinofranchetia chinensis*. Cell Mol Life Sci 57: 500-505

Larson R.A. (1997) Naturally occurring antioxidants. Boca Raton: Lewis Publishers.

Lee K.H. (2000) Research and future trends in the pharmaceutical development of medicinal herbs from Chinese medicine. Public Health Nutr 3: 515-522

Lehninger A.L., Nelson D.L., Cox M.M. (2000) Lehninger principles of biochemistry, 3rd ed. New York: Worth Publishers.

Li C.L., Ye Y.W. (1981) Effects of rhapontin of *Rheum hotaoense* on serum lipid and lipoprotein levels (serum). Yao Xue Xue Bao 16: 699-702

Li H., Meng J.C., Cheng C.H., Higa T., Tanaka J., Tan R.X. (1999) New guaianolides and xanthine oxidase inhibitory flavonols from *Ajania fruticulosa*. J Nat Prod 62: 1053-1055

Lin K.C., Tsao H.M., Chen C.H., Chou P. (2004) Hypertension was the major risk factor leading to development of cardiovascular diseases among men with hyperuricemia. J Rheumatol 31: 1152-1158

Liu G.T., Zhang T.M., Wang B.E., Wang, Y.W. (1992) Protective action of seven natural phenolic compounds against peroxidative damage to biomembranes. Biochem Pharmacol 43: 147-152.

Lowry O.H., Rosebrough N.J., Farr A.L., Randall R.J. (1951) Protein measurement with the Folin phenol reagent. J Biol Chem 193: 265-275

Marks D.B., Marks A.D., Smith C.M. (1996) Basic medical biochemistry: a clinical approach. Baltimore: Williams and Wilkins.

Matsuda H., Kageura T., Morikawa T., Toguchida I., Harima S., Yoshikawa M. (2000) Effects of stilbene constituents from rhubarb on nitric oxide production in lipopolysaccharide-activated macrophages. Bioorg Med Chem Lett 10: 323-327

Matsuda H., Morikawa T., Toguchida I., Park J.Y., Harima S., Yoshikawa M. (2001) Antioxidant constituents from rhubarb: structural requirements of stilbenes for the activity and structures of two new anthraquinone glucosides. Bioorg Med Chem 9: 41-50

Matteucci E., Cocci F., Pellegrim L., Gregori G., Giampietro O. (1995) Measurement of ATPase in red cells: setting up and validation of a highly reproducible method. Enzyme Protein 48:105-119

Medvedev A.E., Ivanov A.S., Kamyshanskaya N.S., Kirkel A.Z., Moskvitina T.A., Gorkin V.Z., Li N.Y., Marshakov V.Y. (1995) Interaction of indole derivatives with monoamine oxidase A and B. Studies on the structure-inhibitory activity relationship. Biochem Mol Biol Int 36: 113-122

Messina M.J. (1991) Oxidative stress and cancer: methodology application for human studies. Free Radic Biol Med 10: 177-184

Miller Y.I., Felikman Y., Shaklai N. (1995) The involvement of low-density lipoprotein in hemin transport potentiates peroxidative damage. Biochim Biophys Acta 1272: 119-127

Miller Y.I., Smith A., Morgan W.T., Shaklai N. (1996) Role of hemopexin in protection of low-density lipoprotein against hemoglobin-induced oxidation. Biochemistry 35: 13112-13117

Mireles L.C., Lum M.A., Dennery P.A. (1999) Antioxidant and cytotoxic effects of bilirubin on neonatal erythrocytes. Pediatr Res 45: 355-362

Moriwaki Y., Yamamoto T., Higashino K. (1999) Enzymes involved in purine metabolism. Histol Histopathol 14: 1321-1340

Nakao K., Shimizu R., Kubota H., Yasuhara M., Hashimura Y., Suzuki T., Fujita T., Ohmizu H. (1998) Quantitative structure-activity analyses of novel hydroxyphenylurea derivatives as antioxidants. Bioorg Med Chem 6: 849-868

Nieto F.J., Iribarren C., Gross M.D., Comstock G.W., Cutler R.G. (2000) Uric acid and serum antioxidant capacity: a reaction to atherosclerosis? Atherosclerosis 148: 131-139

Olinescu R., Smith T. (2002) Free radicals in medicine. Hungtington, New York: Nova Science Publishers, Inc.

Osada Y., Tsuchimoto M., Fukushima H., Takahashi K., Kondo S., Hasegawa M., Komoriya K. (1993) Hypouricemic effect of the novel xanthine oxidase inhibitor, TEI-6720, in rodents. Eur J Pharmacol 241: 183-188

Ou B., Huang D., Hampsch-Woodill M., Flanagan J.A., Deemer E.K. (2002) Analysis of antioxidant activities of common vegetables employing Oxygen Radical Absorbance Capacity (ORAC) and Ferric Reducing Antioxidant Power (FRAP) assays: a comparative study. J Agric Food Chem 50: 3122-3128

Owen P.L., Johns T. (1999) Xanthine oxidase inhibitory activity of northeastern North American plant remedies used for gout. J Ethnopharmacol 64: 149-160

Reinila M., MacDonald E., Salem N., Linnoila M., Trams E.G. (1982) Standardized method for the determination of human erythrocyte membrane adenosine triphosphatases. Anal Biochem 124: 19-26

Rice-Evans C., Halliwell B., Lunt G.G. (1995) Free radicals and oxidative stress: environment, drugs and food additives. London: Portland Press.

Rice-Evans C.A., Diplock A.T., Symons M.C. (1991) Techniques in free radical research. Amsterdam: Elsevier.

Roberfroid M., Calderon P.B. (1995) Free radicals and oxidation phenomena in biological systems. New York: Marcel Dekker.

Sato S., Tatsumi K., Nishino T. (1991) A novel xanthine dehydrogenase inhibitor (BOF-4272). Adv Exp Med Biol 309A: 135-138

Sheu S.Y., Chiang H.C. (1997) Inhibition of xanthine oxidase by hydroxylated anthraquinones and related compounds. Anticancer Res 17: 3293-3297

Shigematsu S., Ishida S., Hara M., Takahashi N., Yoshimatsu H., Sakata T., Korthuis R.J. (2003) Resveratrol, a red wine constituent polyphenol, prevents superoxide-dependent inflammatory responses induced by ischemia/reperfusion, platelet-activating factor, or oxidants. Free Radic Biol Med 34: 810-817

Shin N.H., Ryu S.Y., Choi E.J., Kang S.H., Chang I.M., Min K.R., Kim Y. (1998) Oxyresveratrol as the potent inhibitor on dopa oxidase activity of mushroom tyrosinase. Biochem Biophys Res Commun 243: 801-803

Shviro Y., Shaklai N. (1987) Glutathione as a scavenger of free hemin. A mechanism of preventing red cell membrane damage. Biochem Pharmacol 36: 3801-3807

Silverman R.B. (2000) The organic chemistry of enzyme-catalyzed reactions. San Diego: Academic Press.

Soszynski M., Bartosz G. (1997) Decrease in accessible thiols as an index of oxidative damage to membrane proteins. Free Radic Biol Med 23: 463-469.

Stocker R. (1993) Natural antioxidants and atherosclerosis. Asia Pacific J Clin Nutr 2: 15-20

Stryer L. (1995) Biochemistry, 4th ed. New York: W.H. Freeman.

Stupans I., Ryan A.J. (1984) *In vitro* inhibition of 3-methylcholanthrene-induced rat hepatic aryl hydrocarbon hydroxylase by 8-acyl-7-hydroxycoumarins. Structure-activity relationships and metabolite profiles. Biochem Pharmacol 33: 131-139

Surgenor D.M. (1974) The red blood cell, Volume I, 2nd ed. New York: Academic Press.

Suzumura K., Yasuhara M., Narita H. (1999) Superoxide anion scavenging properties of fluvastatin and its metabolites. Chem Pharm Bull (Tokyo) 47: 1477-1480

Takahashi H., Yamaguchi M. (1994) Activating effect of regucalcin on (Ca^{2+}-Mg^{2+})-ATPase in rat liver plasma membranes: relation to sulfhydryl group. Mol Cell Biochem 136: 71-76

Takahashi T., Morita K., Akagi R., Sassa S. (2004) Heme oxygenase-1: a novel therapeutic target in oxidative tissue injuries. Curr Med Chem 11: 1545-1561

Tsutsumi Z., Moriwaki Y., Takahashi S., Ka T., Yamamoto T. (2004) Oxidized low-density lipoprotein autoantibodies in patients with primary gout: effect of urate-lowering therapy. Clin Chim Acta 339: 117-122

Waring W.S., Webb D.J., Maxwell S.R. (2001) Systemic uric acid administration increases serum antioxidant capacity in healthy volunteers. J Cardiovasc Pharmacol 38: 365-371

Watanabe T., Tawada Y., Shigekawa M. (1988) Purification of cardiac (Na^+,K^+)-activated adenosine triphosphatase from rat. Anal Biochem 175: 284-288

World Health Organization (WHO). (1999) WHO monographs on selected medicinal plants, Volume I. Geneva: WHO.

Wortmann R.L. (2002) Gout and hyperuricemia. Curr Opin Rheumatol 14: 281-286

Wu Y., Fisher W. (1944) *Bi* patterns. In Fratkin J. (Ed.). Practical therapeutics of traditional Chinese medicine: 254-264. Massachusetts: Paradigm Publications.

Xia J., Browning J.D., O'Dell B.L. (1999) Decreased plasma membrane thiol concentration is associated with increased osmotic fragility of erythrocytes in zinc-deficient rats. J Nutr 129: 814-819

Xiao P., He L.Y., Wang L.W. (1984) Ethnopharmacologic study of Chinese rhubarb. J Ethnopharmacol 10: 275-293

Yagi A., Kabash A., Okamura N., Haraguchi H., Moustafa S.M., Khalifa T.I. (2002) Antioxidant, free radical scavenging and anti-inflammatory effects of aloesin derivatives in *Aloe vera*. Planta Med 68: 957-960

Yen G.C., Duh P.D., Chuang D.Y. (2000) Antioxidant activity of anthraquinones and anthrone. Food Chem 70: 437-441

Yokode M., Kita T. (1988) LDL isolation and copper-catalysed oxidation. In Taniguchi N., Gutteridge J.M. (Ed.). Experimental protocols for reactive oxygen and nitrogen species: 149-151. New York: Oxford University Press.

Yuan Z., Gao R. (1997) Anti-oxidant actions of anthraquinolines contained in *Rheum*. Pharm Pharmacol Lett 7: 9-12

Zheng R.L., Zheng T.S. (1992) Retardation of cell aging by lipid peroxidation. Mol Cell Biochem 115: 59-62

Zhou C.X., Kong L.D., Ye W.C., Cheng C.H., Tan R.X. (2001) Inhibition of xanthine and monoamine oxidases by stilbenoids from *Veratrum taliense*. Planta Med 67: 158-161

Zhou C.X., Tanaka J., Cheng C.H., Higa T., Tan R.X. (1999) Steroidal alkaloids and stilbenoids from *Veratrum taliense*. Planta Med 65: 480-482

Zuckerman S.H., Bryan N. (1996) Inhibition of LDL oxidation and myeloperoxide dependent tyrosyl radical formation by the selective estrogen receptor modulator raloxifene (LY139481 HCL). Atherosclerosis 126: 65-75